UNIVERSITY OF BELGRADE

FACULTY OF MECHANICAL ENGINEERING

ABDO-ALMONAIM A. M. ALGHLAM

NUMERICAL SIMULATION OF NATURAL GAS PIPELINE TRANSIENTS

DOCTORAL DISSERTATION

BELGRADE, 2020

УНИВЕРЗИТЕТ У БЕОГРАДУ

МАШИНСКИ ФАКУЛТЕТ

ABDO-ALMONAIM S. M. ALGHLAM

НУМЕРИЧКА СИМУЛАЦИЈА ПРЕЛАЗНИХ ПРОЦЕСА У ГАСОВОДИМА

Докторска дисертација

Београд, 2020

Mentor of Doctoral Dissertation

Dr. Vladimir Stevanovic, full professor

University of Belgrade, Faculty of Mechanical Engineering

Members of the Committee

Dr. Milos Banjac, full professor

University of Belgrade, Faculty of Mechanical Engineering

Dr. Aleksandar Cocic, associate professor

University of Belgrade, Faculty of Mechanical Engineering

Dr. Sanja Milivojevic, assistant professor

University of Belgrade, Faculty of Mechanical Engineering

Dr. Milica Ilic, research associate

University of Belgrade, Innovation Center of the Faculty of Mechanical Engineering

Date of Defence:

Ментор докторске дисертације

др Владимир Стевановић, редовни професор

Универзитет у Београду, Машински факултет

Članovi komisije

др Милош Бањац, редовни професор

Универзитет у Београду, Машински факултет

др Александар Ћоћић, ванредни професор

Универзитет у Београду, Машински факултет

др Сања Миливојевић, доцент

Универзитет у Београду, Машински факултет

др Милица Илић, научни сарадник

Универзитет у Београду, Иновациони центар Машинског факултета у Београду

Датум одбране:

Dedication

This thesis is dedicated to who taught me that it is never too late to change careers to pursue your true passion and that context is everything

To my beloved, mother, wife, children, brothers, and sisters

Also in memory of my father

all with love and appreciation

To whom I respect, my supervisor Prof. Vladimir Stevanovic,

with sincere appreciation and thankful

ACKNWLEDGEMENT

First and foremost, I would like to deeply thank my dissertation supervisor Prof. Vladimir Stevanovic for his invaluable guidance, encouragement and endless support through my Ph.D. study.

My sincere appreciations also extend to all my colleagues and others who have provided assistance on various occasions. Their views and tips are useful indeed. I also wish to express my warm and sincere thanks and appreciation to all staff of the Faculty of Mechanical Engineering – University of Belgrade for their continuous help during the completion of this dissertation.

I give my deepest gratitude to my beloved mother, wife, brothers, and sisters, for their supporting.

Above all praise and thank “Allah” who helped me to perform this work, and I hope to be satisfied with me.

ABSTRACT

Simulations and analyses of natural gas pipeline transients provide insights into behavior of natural gas pipeline network and transmission pipelines during the action of various disturbances, as well as control and safety systems. The results of these simulations are a support to the design of safe, reliable and efficient natural gas systems operation. knowing all deviations of operational parameters from the prescribed values are very essential in order to control these parameter changes within acceptable spans that are determined by upper and lower setpoints, as well as to plan and schedule a maintenance with the aim of sustaining a gas supply to consumers in cases of various disturbances. Therefore, a numerical model and a computer code have been developed for the simulation and analyses of natural gas pipeline transients, as those that typically occur in high-pressure gas transmission pipelines. The developed model is based on the mass and momentum balance equations that describe one-dimensional, compressible, frictional natural gas transient flow, as well as on boundary conditions that enable simulation of gas flows in complex pipeline networks. The developed model is solved with the numerical procedures of the method of characteristics and implemented into the Gas Transient Analysis (GTA) computer code.

The developed model and the GTA code are validated by simulations of several test cases which are available in open literature. The simulated transients are caused by variable gas consumptions from gas pipelines of different lengths and networks, as well as by a pressure pulse at the pipeline inlet. The comparison between the obtained numerical results and the previously measured or calculated data from the literature, shows a good agreement. Afterwards, the code is applied to the simulation and analyses of transients in a real natural gas transmission pipeline in Libya with the length of over 500 km. The simulated scenarios cover common operating conditions, as well as abrupt disturbances of the gas parameters at the inlet gas manifold in the gas source fields and trips of gas delivery to consumers, with the aim of getting insight into the supply capacity of the gas transmission pipeline under abnormal conditions. The comparison between results obtained with the GTA code and measured data for normal real conditions shows good agreement as well, while the calculated results for the abnormal conditions show a significant accumulation and inertia of the gas within the long distance transmission pipeline, which allow gas accumulation and consumers supply during a half-day time period. Since the GTA code results are obtained under isothermal gas transient conditions, an analytical method is derived for the evaluation of differences between isothermal and non-isothermal transient flow predictions of pressure and non-isothermal temperature change. It is shown that non-isothermal transient effects can be neglected in engineering predictions of natural gas packing and discharging transient in long distance transmission pipelines during hourly time periods.

In addition, the prescribed isothermal temperature should be a few degrees K higher than the soil temperature as a result of the heat generation by friction on the pipelines wall and heat transfer from the gas to the surrounding soil. The GTA code simulations are robust and numerically stable, while the gas network and boundary conditions can be simply defined by specification of code input parameters.

Key words: natural gas, pipelines, transients, numerical simulations, non-isothermal flow, heat transfer, wall friction.

Scientific field: Mechanical engineering

Scientific subfield: Thermal power engineering

UCD number: 622.691-021.388]:004.942(043.3)

АПСТРАКТ

Симулације и анализе прелазних процеса у гасоводима омогућавају увид у понашање гасних мрежа и магистралних гасовода током деловања различитих поремећаја, као и током деловања управљачких и сигурносних система. Резултати ових симулација су подршка пројектовању сигурног, поузданог и ефикасног погона система са природним гасом. Познавање свих одступања погонских параметара од прописаних вредности је веома битно за управљање и одржавање ових параметара у прописаним границама дефинисаним доњим и горњим граничним вредностима, као и за планирање и временско усклађивање одржавања са циљем обезбеђења снабдевања потрошача гасом током дејства различитих поремећаја. Узимајући у обзир значај ових резултата, развијени су нумерички модел и компјутерски програм за симулације и анализе прелазних процеса у гасоводима са природним гасом, као што су типични прелазни процеси у магистралним гасоводима на великим притисцима. Развијени модел је заснован на билансним једначинама масе и количине кретања које описују једнодимензијско, стишљиво, нестационарно струјање природног гаса са трењем, као и на граничним условима који омогућавају симулацију струјања у сложеним гасним мрежама. Развијени модел се решава нумеричким поступком методе карактеристика и примењен је у комјутерском програму за анализе прелазних процеса у гасоводима („Gas Transient Analysis – GTA“ програм).

Развијени модел и GTA програм су валидирани симулацијама неколико тест примера који су расположиви у литератури. Симулирани прелазни услови су изазвани промењљивом потрошњом гаса из гасовода са различитим мрежама и дужинама цевовода, као и импулсом притиска на улазу у гасовод. Поређење добијених нумеричких резултата са претходним измереним или срачунатим вредностима из литературе даје добро слагање. Након тога програм је примењен за симулације и анализе прелазних процеса у реалном магистралном гасоводу у Либији дужине преко 500 km. Симулирани сценарији обухватају уобичајене погонске услове, као и нагле поремећаје у извору напајања гасом и престанак испоруке потрошачима, са циљем одређивања капацитета испоруке и акумулације гаса у овим поремећеним условима. Поређење резултата добијених GTA програмом и измерених вредности током нормалних стварних услова погона показује добро слагање. Резултати добијени за поремећене услове рада показују значајну акумулациону способност магистралног гасовода велике дужине и инерцију масе гаса, што омогућава акумулацију гаса и снабдевање потрошача у периодима од око 12 часова. Пошто су резултати са GTA програмом добијени за изотермске услове, развијен је аналитички поступак за одређивање разлике у резултатима који се добијају изотермским и неизотермским моделом. Показује се да се неизотермски ефекти прелазних процеса могу занемарити током вишечасовних процеса акумулације и пражњења магистралних гасовода велике дужине. Такође, вредност изотермске температуре гаса треба да буде пар степени K виша од температуре околине услед генерације топлоте услед трења на зидовима гасовода и пролаза топлоте са гаса на околину. Програм GTA је поздан и нумерички стабилан, при чему се гасоводна мрежа и гранични услови једноставно задају преко улазних параметара.

Кључне речи: природни гас, гасоводи, прелазни процеси, нумеричке симулације.
Научна област: Машинство
Ужа научна област: Термоенергетика
УДК број: 622.691-021.388]:004.942(043.3)

TABLE OF CONTENTS

LIST OF FIGURES

LIST OF TABLES

NOMENCLATURE

A	indicator of the pipe inlet (A = 1) or outlet (A=2)
C_1, C_2	imperial constants.
C^+, C^-	corresponding characteristics paths
c	sonic velocity, m/s
c_p	specific heat capacity at constant pressure, J/kgK
D	diameter, m or mm
e	absolute or internal pipe wall roughness, mm
	internal energy per unit mass, J/kg. Eq. (A-5)
E	pipeline efficiency
f	friction coefficient
$G=\rho_g/\rho_a$	specific gravity (gas and air densities under standard conditions)
G(A,J)	indicator of the pipe boundary type
g	acceleration of gravity, m/s^2
H	total enthalpy, J
h	specific enthalpy, J/kg
k	heat transfer coefficient, W/m^2K
L	length, m
M_g	Molecular weight of gas, g/mole
M_{air}	Molecular weight of air, g/mole
M_i	Molecular weight of natural gas component i, g/mole
m	mass, kg
$\dot{m}$	mass flow rate, kg/s
n	maximum number of nodes,
	number of moles in Eq. (3-7)
p	pressure, Pa
p_{ave}	average pressure, Pa
p_c	gas critical pressure, Pa
p_{pc}	pseudo-critical pressure, Pa

p_{pr}	pseudo-reduced pressure of gas mixture
p_r	reduced pressure of gas (dimensionless)
Δp	pressure change, Pa
$\dot{Q}$	heat power, W
$\dot{q}_L$	heat power per unit length of pipe, W/m
Re	Reynolds number, $\left(\frac{u\rho D}{\mu}\right)$
R_g	gas constant, J/mol K
T	temperature, K
T_c	gas critical temperature, K
T_{pc}	pseudo-critical temperature, K
T_{pr}	pseudo-reduced temperature of gas mixture
T_r	reduced temperature of gas
T_s	The temperature of pipeline surrounding (soil), K
Δt	time step of integration, s
u	velocity, m/s
V	volume, m^3
$\dot{V}$	Volume flow rate, m^3/s
x	spatial coordinate, depth, m
Δx	spatial step of integration, m
w	frictional force per unit length of pipe, N/m
y_i	Mole fraction or percent of natural gas component i, %
z	compressibility factor of natural gas

Greek symbols

λ	thermal conductivity, W/mK
μ	dynamic viscosity, kg/ms
μ_i	dynamic viscosity of natural gas component i, kg/ms
θ	pipeline angle of upward inclination from the horizontal, rad
τ	shear stress between the fluid and pipe wall, Pa

ρ	density, kg/m^3

Indices

0	initial value
H	hydraulic parameter
I_j	pipe that transports gas from the junction, Eq. (20)
in	inlet
J	counter of pipes
J_i	pipe that transports gas towards the junction, Eq. (19)
out	outlet
s	soil

Abbreviation

GTA	Gas Transients Analysis
MASL	meters above sea level
TPP	thermal power plant

CHAPTER 1

INTRODUCTION

1.1 General

Over the past couple of centuries, fossil fuels, as primary energy sources, have been essential for global economic growth. During the industrial revolution in Europe in the 19th century, coal played a key role in supporting technological progress in agriculture, manufacturing and transport. Since then, petroleum has superseded the position of coal, and is an essential factor in sustaining our very expensive and 'dangerous' lifestyle.

Nowadays, however, the need for the cleaner fuels usage with lower content of carbon, as well as proven sufficient reserves and more stable prices than in case of oil market prices lead to the strong increase of the natural gas usage. The exploitable reserves of the natural gas are enough for the consumption in longer future time period, the carbon emission during the combustion of natural gas is approximately half of the emission by coal combustion and its price is more stable than in case of oil [1].

The natural gas is used in various sectors of industry, both as a fuel and as a raw material. As a fuel it is used in boilers and furnaces to generate steam, heat water or to provide heat for technological purposes. It is a raw material in petrochemical manufacturing, in polymer manufacturing and used to produce hydrogen, sulphur, carbon black, ammonia, and ethylene. In domestic sector natural gas is a fuel for district and individual building heating, for cooking and sanitary water preparation.

In contrast to petroleum or coal, natural gas can be used directly as a source of primary energy that causes less carbon dioxide and nitrogen oxide emissions (greenhouse gases). Besides substantially lower carbon dioxide emissions in comparison to usage of coal and oil, the combustion of natural gas leads to negligible emissions of sulfur dioxide, as well as lower nitrous oxide emissions. All these characteristics provide benefits such as elimination of acid rains, and reduced ozone layer depletion and effects of the greenhouse gasses in the atmosphere. In addition, it can be safely transported, stored and used [2].

Hence, the current position of natural gas as a primary non-renewable energy source (second to oil in OECD[1] countries) leads to the conclusion that the analysis, design and improvement of its processes, including transportation, play a significant role for both private and public sectors while offering a number of challenges to the scientific research community [1].

1.2 Natural gas and its transmission: history and present

The natural gas is known to humans since ancient times in the Middle East. At the beginning people had been aware of burning springs of natural gas. In Persia, Greece, or India, temples were built around these eternal flames for religious practices [2]. There is also historical evidence from the ancient times that people had started to harness natural gas springs with the aim of providing their living needs. Some 900 years B.C. the drilling of the ground was applied in China with the aim of obtaining springs of gas and that gas was used as a fuel for efficient provision of their living needs. Namely, the seawater was evaporated by natural gas combustion in order to obtain salt and drinkable water. In addition, by the first century, the Chinese had developed “an advanced techniques for tapping underground reservoirs of natural gas, which allowed them to drill wells as deep as 1,460 m in soft soil; they used metal drilling bits inserted through sections of hollowed-out bamboo pipes to reach the gas and bring it to the surface” [2].

The Romans were also aware about natural gas existence. It is supposed that Julius Caesar saw a "burning spring" near Grenoble in France. Also, there is evidence that religious temples in early Russia were built around burning sources of natural gas in the ground, which represented some kind of "eternal flames" [3].

The natural gas was discovered in Great Britain in 1659, but its commercial usage started more than a century later in 1790. A source of natural gas was discovered in Fredonia in United States US in 1821, as bubbles that rose to the surface from a creek. The first natural gas well in North America was dug by William Hart, who is called as “America’s father of natural gas” [2]. He applied hollowed logs for the transport of gas from the well to a nearby building and the gas was burned for illumination. In 1865, the Fredonia Gas, Light, and Waterworks Company became the first natural gas company in the United States. The first transmission natural gas pipeline was built in 1872. It was some 40 km long and it supplied gas from the wells to the city of Rochester in New York. This

[1] Organization for Economic Cooperation and Development

pipeline was also built of hollowed logs. In 1885 Robert Bunsen developed so called “Bunsen burner”, which enabled the usage of natural gas for heating and cooking, besides its use for lighting. Certainly, at the beginning of these commercial natural gas consumptions, an obstacle of its wider usage was the lack of pipeline infrastructure for natural gas transport and distribution. In addition, a need for facilities for gas storage was encountered [2].

Further development of technology related to natural gas usage led to the exploitation of a high-pressure gas deposit in central Indiana, which started in 1891. This gas was transported for consumption to Chicago in Illinois and a 192 km long pipeline was built for that purpose. Natural gas is also extracted together with oil from the oil wells, but during the early period of oil exploitation it was observed as burden. Hence, natural gas was leaked directly to the atmosphere at the oil fields or it was burnt and the flame illuminated the oil fields day and night. Oil companies realized that this is an unreasonable practice and they started to develop gas transmission pipelines and pipeline networks for gas distribution to the consumers in large cities. This activity was an additional source of profit for them. The technological progress after the World War II boosted the natural gas consumption, for example in pipeline manufacturing, metallurgy and welding. Gas transport companies started building and expanding their pipeline systems. The fast and steady growth of gas industry finally entailed the construction of various gas facilities, including processing and storage plants, as well as a number of sustainable projects around the world since the late 20th century. In this way natural gas became an attractive alternative to electricity and coal [1].

Despite periodic economic and international crises, new oil and gas pipelines are being planned and built. Pipeline and Gas Journal’s worldwide survey (January 2017) [4] figures indicate 134866 kilometres of pipelines are planned and under construction. Of these, 61783 kilometres represent projects in the engineering and design phase (planned) while 73083 kilometres reflect pipelines in various stages of construction. Next figure 1.1 identifies regions by levels of new and planned pipeline kilometres in seven basic country groupings in the report: North America 51200 kilometres; South/Central America and Caribbean 7532 kilometres; Africa 6412 kilometres; Asia Pacific Region 31926 kilometres; Former Soviet Union and Eastern Europe 20448 kilometres; Middle East 14833 kilometres; and Western Europe and European Union 2515 kilometres [4].

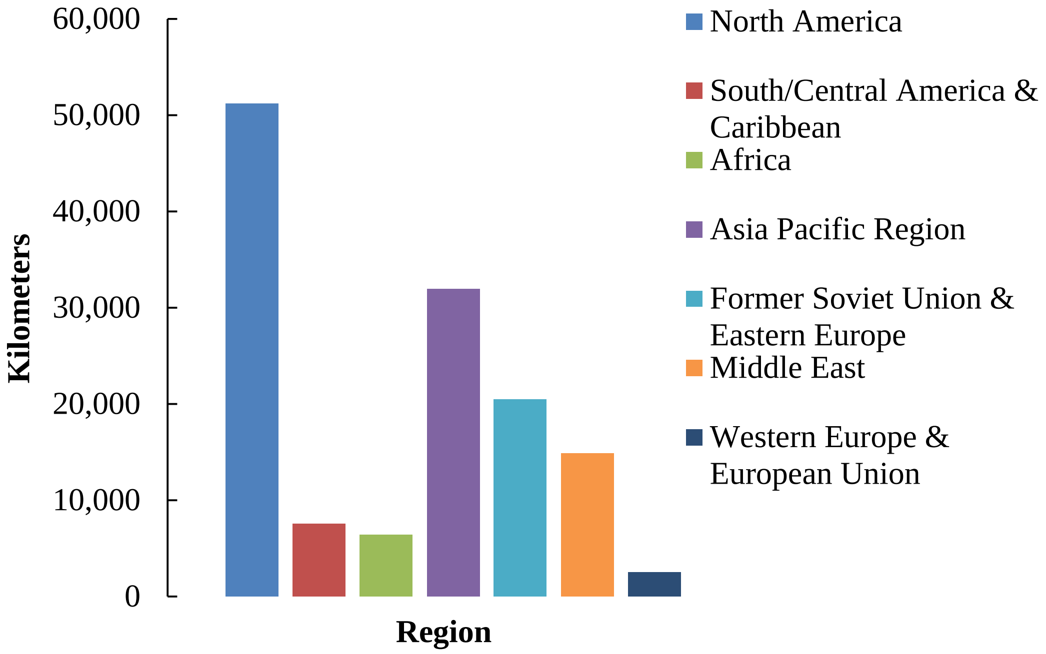

Figure 1.1: Planned and under construction pipelines worldwide, 2017 [4]

"Primary energy consumption growth averaged 2.2% in 2017, up from 1.2% in 2016 and the fastest since 2013. This compares with the 10-year average of 1.7% per year. By fuel, natural gas accounted for the largest increment in energy consumption, followed by renewables and then oil. Natural gas consumption rose by 96 billion cubic metres (bcm), or 3%, the fastest since 2010. This consumption growth was driven by China (31 bcm), the Middle East (28 bcm) and Europe (26 bcm)" [5].

"Global natural gas production increased by 131 bcm, or 4%, almost double the 10-year average growth rate. Russian growth was the largest at 46 bcm, followed by Iran (21 bcm). Gas trade expanded by 63 bcm, or 6.2%, with growth in LNG outpacing growth in pipeline trade. The increase in gas exports was driven largely by Australian and US LNG (up by 17 and 13 bcm respectively), and Russian pipeline exports (15 bcm)" [5].

"2017 was a bumper year for natural gas, with consumption (3.0%, 96 bcm) and production (4.0%, 131 bcm) both increasing at their fastest rates since the immediate aftermath of the financial crises. The growth in consumption was led by Asia, with particularly strong growth in China (15.1%, 31 bcm), supported by increases in the Middle East (Iran 6.8%, 13 bcm) and Europe. The growth in consumption was more than matched by increasing production, particularly in Russia (8.2%, 46 bcm), supported by Iran (10.5%, 21 bcm), Australia (18%, 17 bcm) and China (8.5%, 11 bcm)" [5].

Natural gas is foreseen as the fuel source with the highest increase in consumption in the near future. Huge projects of transmission pipelines are planned and conducted with the aim of transporting gas from distant gas fields with great reserves to industrial areas and big cities. Natural gas is transported through long distance pipelines by work of a series of compressor stations.

1.3 Natural gas origin and composition

"Natural gas exists in nature under pressure in rock reservoirs in the Earth's crust, either in conjunction with and dissolved in heavier hydrocarbons and water or by itself" [2]. It is exploited alone from the natural cavities or porous sediments or together with crude oil. "Natural gas has been formed by the degradation of organic matter accumulate in the past millions of years. Two mechanisms (biogenic and thermogenic) are responsible for this degradation" [2].

Natural gas is composed mainly of methane. Other ingredients are paraffinic hydrocarbons such as ethane, propane, and butane. Natural gas contains nitrogen as well as carbon dioxide and hydrogen sulfide [2]. A minor amount of argon, hydrogen, and helium may exist in it. Natural gas from geographically separated areas can have substantially different composition. Table (1.1) illustrates the typical composition of natural gas. Hydrocarbons C5+ can be also included and it can be separated as a light gasoline. Some toxic substances might be present in small quantities, such as benzene, toluene, and xylenes, as well as some acid contaminants like mercaptans R-SH, carbonyl sulfide (COS), and carbon disulfide (CS2). Mercury can also be present either as a metal in vapor phase or as an organometallic compound in liquid fractions [2].

Typical composition of natural gas is presented in Table 1.1. It should be emphasise that the gas composition can vary substantially from the values presented in Table 1.1. Standard test methods were developed for the determination of the natural gas composition and description of these methods is available elsewhere [2].

1.4 Demand for natural gas

The demand for natural gas has been steadily increasing over the last several years as shown in figure (1.2). The world consumption of natural gas in the year 2018 was 3.85 trillion cubic meters (Tm^3) (on the left vertical axis the consumption is presented in trillion cubic feets - TCF) [6, 7]. The projected demand up to 2030 is also illustrated in the same figure.

It is difficult to predict the increase in natural gas demand in the future since it depends on several socioeconomic factors. Starting with worldwide energy demand, figure (1.3), the energy demand is expected to grow from 5.71×10^5 PJ (petajoule (PJ) = 10^{15} J) in 2010 to 9.54×10^5 PJ in 2050 for about 67% total increasing.

Table 1.1: Typical Composition of Natural Gas [2]

Name	Formula	Volume (%)
Methane	CH_4	>85
Ethane	C_2H_6	3-8
Propane	C_3H_8	1-2
Butane	C_4H_{10}	<1
Pentane	C_5H_{12}	<1
Carbon dioxide	CO_2	1-2
Hydrogen sulfide	H_2S	<1
Nitrogen	N_2	1-5
Helium	He	<0.5

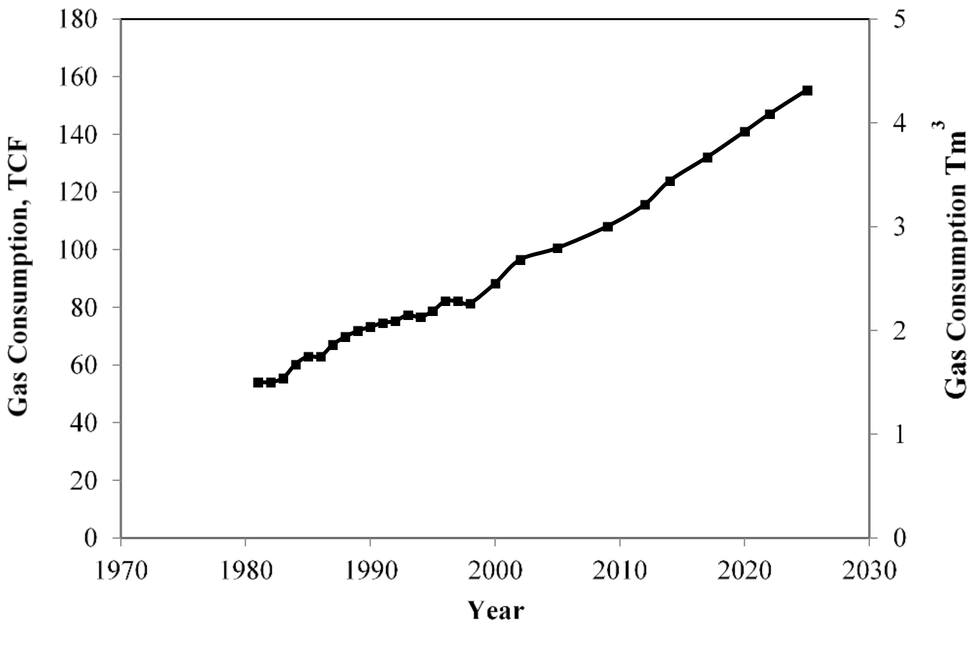

Figure 1.2: Historic demand for natural gas [6]

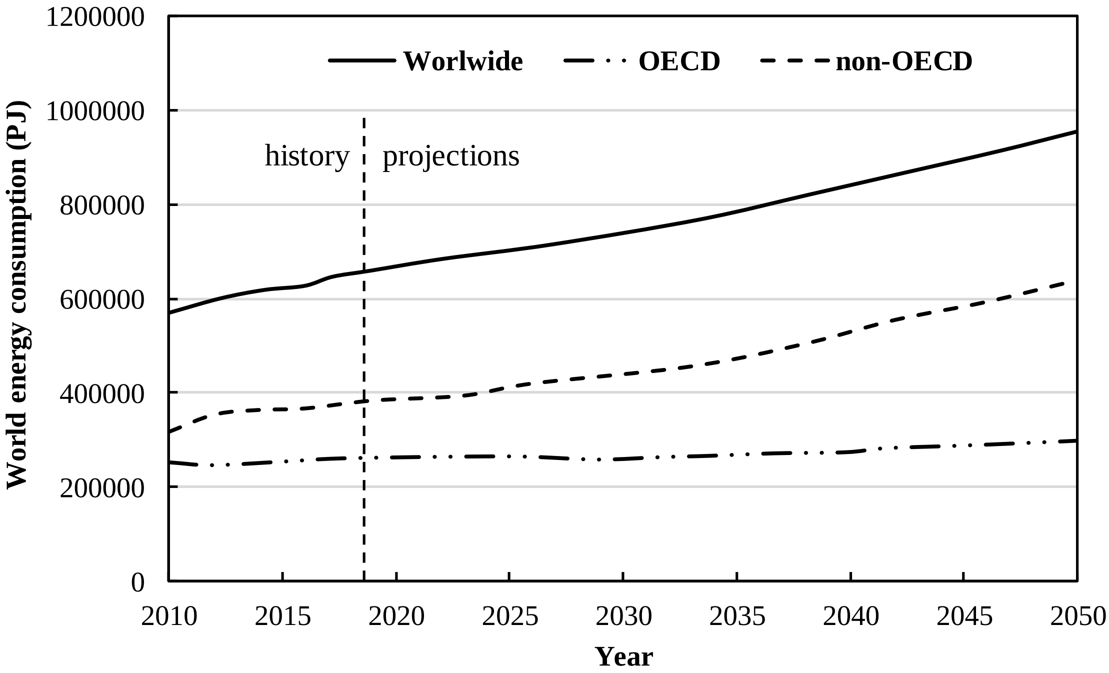

Figure 1.3: World-wide energy consumption with projections to 2050 [8]

Figure 1.3 shows that the greatest increase in energy consumption occurs in non-OECD countries, "where strong economic growth, increased access to marketed energy, and rapid population growth lead to rising energy consumption. On the other hand, in OECD countries, growth in energy consumption is slower as a result of relatively slower population and economic growth, improvements in energy efficiency, and less growth in energy-intensive industries. Energy consumption in non-OECD countries increases nearly 70% between 2018 and 2050 in contrast to about 15% increase in OECD countries" [8].

In figure (1.3), the energy demand increase is uneven across the world. In developing countries, the increase in demand is a lot higher (22% over last eight years), whereas, for industrialized countries the increase is slower (4% over last ten years). The shift in demand can have significant consequences on the demand for natural gas since transportation of gas is an important bottleneck in satisfying the demand for natural gas [8].

According to the U.S. Energy Information Administration (EIA) report (September 2019) [8] the world natural gas consumption demand will increase more than 60% from 2010 to 2050, from about 1.3×10^5 PJ to 2.1×10^5 PJ over forty years. "Natural gas use accelerates the most in countries outside of the Organization of Economic Cooperation and Development (OECD) to meet demand from increased industrial activity, natural gas-fired electricity generation, and transportation fueled by liquefied natural gas (LNG)."

Natural gas consumption in non-OECD countries will grow from about 74×10^3 PJ in 2018 to around 126.5×10^3 PJ in 2050, a 71% increase. It is projected that the natural gas consumption during this time in the OECD countries will increase 17% between 2018 and 2050.

Also, the projected demand of natural gas is shown in figure (1.4). This is the most likely demand based on an assumption that fuel cell technology will not have significant contribution to transportation power. If fuel cell technology indeed becomes viable, the demand for natural gas can be even higher than predicted in figure.

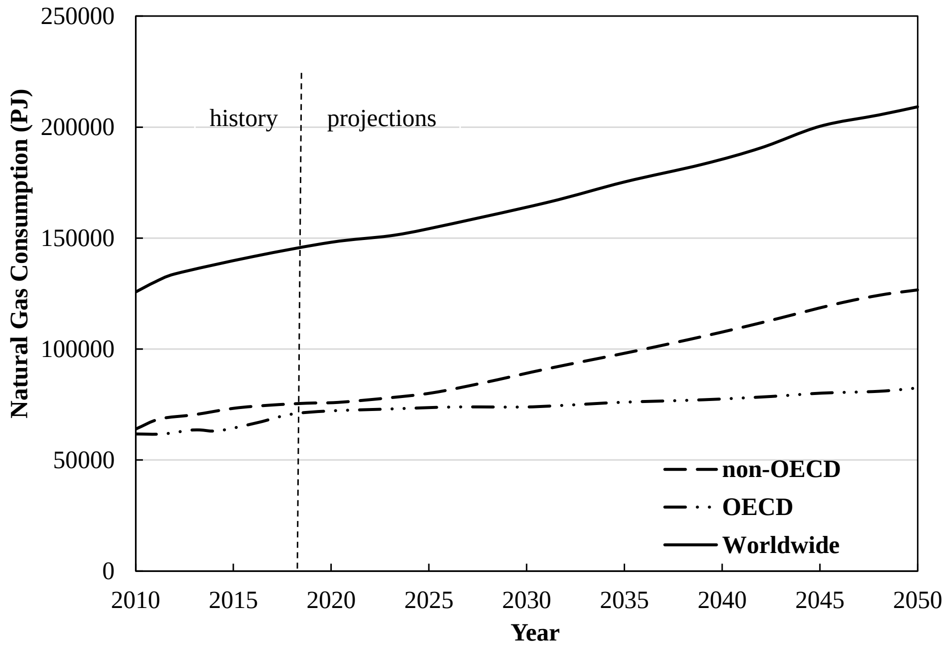

Figure 1.4: World natural gas consumption with projections to 2050 [8]

Even more interesting to examine is the percentage of world energy provided by natural gas compared with the other sources of energy. As in figure (1.5), the primary energy consumption by different types of fuel (sources) in the year of 2018 is illustrated where the natural gas occupies the third place preceded by oil and coal. In this review, primary energy comprises commercially-traded fuels, including modern renewables used to generate electricity [7].

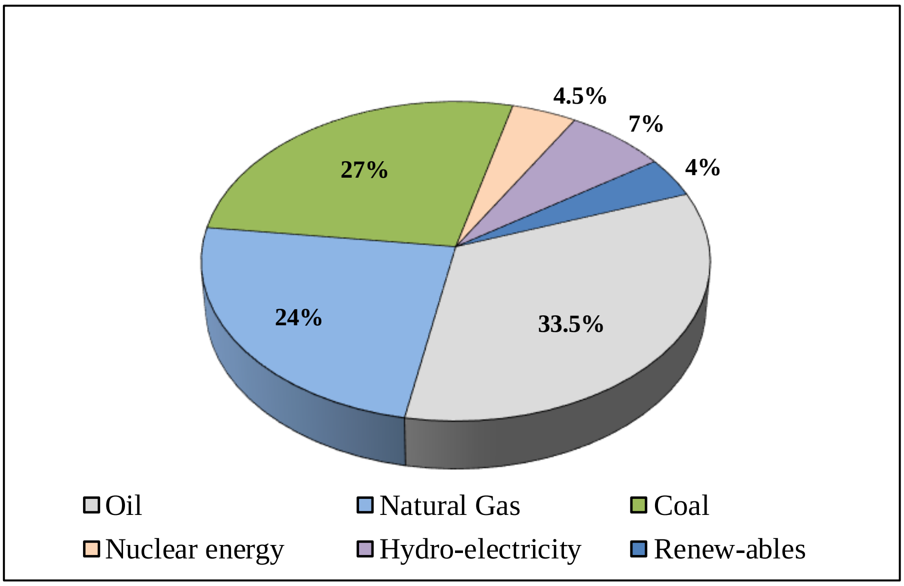

Figure 1.5: World-wide primary energy consumption by fuel (sources), 2018

In figure (1.6), energy produced from the natural gas and its projected demand is show and compared with the energy provided from coal for the period of forty years. In 2010, the energy produced from coal was more than the energy from natural gas by about 3.6×10^3 PJ. For three years after, both fuels keep to increase. In 2013 coal shows decline in energy production and the production of natural gas continues to increase. The 2028 is the year where both coal and natural gas production is about 1.5×10^5 PJ. After this, the energy provided by natural gas will be more than the energy produced by coal. For about five years after 2028 the energy provided by coal is expected to remain constant and then start to slightly increase up to 2050. The energy produced from natural gas is expected to show a gradual increase and reach 2.1×10^5 PJ in 2050 that is about 0.2×10^5 PJ more than the energy provided by coal [8]. Hence, it is concluded that the outlook of the future natural gas roll in the primary energy mix in the World shows that its consumption, production and reserves will continue to increase for the foreseeable future [8].

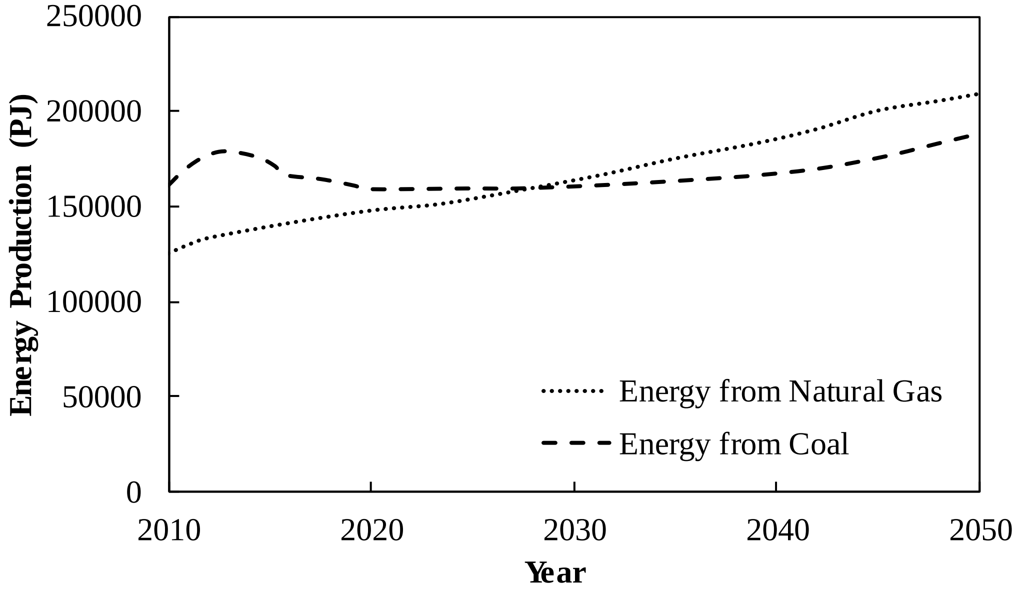

Figure 1.6: World energy production demand by natural gas and coal [6]

The natural gas supply to the consumers is based on the following chain of technical and technological processes and activities [9].

- “Exploration: In this stage, the issue of how natural gas is found and how companies decide where to drill wells for it is addressed.
- Extraction: This stage deals with the drilling process, and how natural gas is brought from its underground reservoirs to the surface.
- Production: In this stage the processing of natural gas once is brought out from the underground takes place.
- Transport: The natural gas is transported from the processing plant to local distribution companies across a pipeline network in this stage.
- Storage: This stage accounts for the storage of natural gas.
- Distribution: In this stage, natural gas is delivered from the major pipelines to the end users.
- Marketing: This stage involves the buying/selling activity from the natural gas marketeers.”

The reliable and efficient transportation of natural gas from production to consumption areas needs a developed transportation system. In the majority of cases the distance between the natural gas wells and consumers in industry or domestic sector is long over thousands of kilometres. Therefore, long distance transmission pipelines are being built, accompanied with the development of complex distribution systems in urban and industrial areas with the aim of gas supply to final consumers. The supply of the natural gas is closely linked with its storage. The roll of the gas storage is to adjust mainly constant gas extraction from the natural wells with variable seasonal or daily gas consumption by the final consumers. In winter periods natural gas consumption increases due to heating. Hence, the gas is accumulated in summer period usually in huge natural underground cavities, and discharged from them and consumed in winter period. On the daily level, during the reduced consumption periods, natural gas can be packed in long transmission pipelines, distribution networks and built gas storage facilities, while in later periods the gas is discharged from these storage units in order to cover peaks of increased consumption.

The whole transportation path, from the gas wells to the final consumers consists of three major types of pipelines: “the gathering system, the interstate pipeline system, and the distribution system. The gathering system consists of low pressure, small diameter pipelines that transport raw natural gas from the wellhead to the processing plant. Natural gas from a particular well might have high sulfur and carbon dioxide contents (sour gas), a specialized sour gas gathering pipe must be installed. Sour gas is corrosive, thus its transportation from the wellhead to the sweetening plant must be done carefully” [9].

1.5 Transportation of natural gas

Natural gas is often found in places where there is no local market, such as in the many offshore fields or onshore fields in the deserts around the world. For natural gas to be available to the market it must be collected, processed, and transported.

Natural gas, as a result of the storage difficulties, needs to be transported immediately to its destination after production and processing from a reservoir. There are a number of options for transporting natural gas energy from oil and gas fields to market. These include pipelines, LNG (liquefied natural gas), MLG (medium conditioned liquefied gas), or CNG (compressed natural gas) [2].

1.5.1 Liquefied natural gas (LNG)

Liquefied natural gas (LNG) technology has proven to be effective over the last 30 years. In 2005, about 0.2 Tm^3 or 5.6% of natural gas was transported using LNG technology. By 2020, the worldwide demand for gas transported through LNG is expected to be 0.49 Tm^3. The LNG was exported from eight countries (Indonesia, Malaysia, Algeria, Australia, Brunei, United Arab

Emirates, United States, and Libya) and was imported by eight countries (United States, Japan, South Korea, Taiwan, Belgium, France, Spain, and Turkey).

1.5.2 Gas to liquid products

Gas to liquid (GTL) technology refers to the conversion of natural gas into synthetic hydrocarbon liquids, particularly middle distillates. By some estimates, 25.5 Tm^3 of natural gas are stranded too far from markets to be produced or transported profitably. This is sufficient to justify about 200 gas-to-liquid plants.

The technology of converting natural gas to liquids is not new. In the first step, natural gas is reformed and converted to hydrogen and CO. The mixture is called synthetic gas or syngas. This is the same process for converting natural gas to hydrogen, which can be used as a fuel in a fuel cell. This step is the most expensive and consumes about 50% of the total GTL costs. In the second step, in a slurry reactor the syngas is blown over a catalyst at about 232°C and is converted to liquids. This is called Fischer-Tropsch synthesis. These liquids can be converted to other desirable products, such as synthetic fuels, using the cracking process.

1.5.3 Natural gas transportation via pipelines

Transportation of natural gas from gas fields with wells to consumers' areas is very important and crucial activity regarding reliability and economics of gas supply to the consumers. Natural gas can be transported by different technological solutions, but the most economically acceptable method to transport large quantities of natural gas is by pipelines. This method of gas transport by pipelines has been boosted by metallurgical and welding techniques improvements. Hence, there is a fast increase of pipeline networks deployment during the last decades all over the world, which enables economic gas transportation.

Pipelines can be installed both offshore and onshore, but there is a substantial difference in terms of security and construction prices. "Building pipeline systems under the sea is highly costly and technically demanding, a lot more than onshore" [9].

Transportation pipelines can be divided into three types: gathering pipelines, transmission pipelines, and distribution pipelines. Raw natural gas is transported from the production wells to the gas processing plant by gathering pipelines. Transmission pipelines transport natural gas from the gas processing plants towards storage facilities and distribution systems, while these distances can be of the order of hundred or even thousands of kilometres. The transmission pipelines are under high pressure and the pressure is reduced at connections with the distribution network pipeline systems. Distribution pipeline systems can be found in communities and distribute natural gas to homes and businesses.

At the end, the natural gas pressure is further reduced in devices called regulators, which decrease the pressure to a level that is safe to enter homes or other facilities [10].

The main differences among these systems are the physical properties of the pipelines used, such as diameter, stiffness, material, etc., and the specifications of the maximum and minimum upstream and downstream pressures.

The major transportation of natural gas is carried through cross-border pipelines. Throughout the world, major efforts are under way to increase the gathering, transmission, and distribution capacity in order to promote and support projected growth of natural gas demand [6].

The natural gas cross-border transmission pipeline infrastructure in the U.S. represents one of the largest and most complex mechanical systems in the world. This system of natural gas pipeline network is a highly integrated network that moves natural gas throughout the continental United States. More than 210 natural gas pipeline systems have about 490850 kilometres of interstate and intrastate transmission pipelines that link natural gas production areas and storage facilities with consumers. In 2017, this natural gas transportation network delivered about 0.708 trillion cubic meter (Tm^3) of natural gas to 75 million customers. These pipelines systems are driven by more than 1,400 compressor stations that maintain pressure on the natural gas pipeline network and assure continuous forward movement of supplies.

This system has been developed over the last 60 years, and is controlled at a very low level of sophistication [6]. Quite often, collected natural gas (raw gas) must be transported over a substantial distance in pipelines of different sizes. These pipelines vary in length between hundreds of meters to hundreds of kilometres, across undulating terrain commonly occurs because of the multicomponent nature of transmitted natural gas and its associated phase behaviour to the inevitable temperature and pressure changes that occur along the pipeline [2].

1.6 Mathematical flow modelling of gas pipelines

Optimal design of the gas transmission pipeline diameter for steady-state operational conditions is determined by the minimal overall exploitation costs. The major parts of these costs are investment cost in the pipeline and operational cost of fuel that energizes compressors. The greater pipe diameter means higher investment costs, but lower gas velocity, lower pressure drop and lower compressors' power and fuel consumption, and vice versa, the lower diameter reduces investments but increases fuel expenditures. But, the gas consumption has transient character and it also influence the optimal design of gas pipeline diameter. A design according to the maximum gas flow rate, without taking into account the possibility of gas accumulation, would lead to an uneconomical solution. Hence, there is a need for accurate prediction of operational parameters (mainly flow rates, velocities and pressure drops) of natural gas transmission pipelines both in steady-state and transient conditions. Such an engineering need has led to the development of various types of mathematical models for the prediction of gas transport. "Isothermal steady-state and transient pressure drop or flow rate calculation methods for single-phase dry gas pipelines are the most widely used and the most basic relationships in the engineering of gas delivery systems. They also form the basis of other more complex transient flow calculations and network designs" [2].

There are several purposes that shape the demand of having precise and accurate pipeline mathematical flow models, mainly serving for pipeline balance, pressure monitoring, and deliverability. There are two types of mathematical models for lengthy pipeline flow; the steady-state and the transient models. The core difference between the two types of flow models lies in the equation of motion. In the transient flow models, there are terms that represent the change of transport parameters with time. When these terms are set to zero, the steady- state representation of the flow equation is obtained. Consequently, and due to this fundamental difference between the two types of models, the functionality of each of them differs. For purposes such as pressure monitoring and leak localization, in which the change of transport parameters with time is vital, transient flow models become a necessity. For other purposes such as pipeline design, sizing, line capacity estimations and line packing, where the changes of transport parameters with time are of no significance, steady-state models become ideal. Both of the two types are approximations of the actual conditions of the pipeline.

The prediction of the pressure drop due to gas friction on the inner pipeline wall is one of the most important tasks in the design of the gas transmission and network distribution systems. On the basis of this prediction the capacity and operational characteristics of compressor stations should be determined [11].

A mathematical modelling for the simulation of gas transport parameters is especially important for the transmission systems of large capacity due to its overall influence on the whole energy systems of regions and countries. Researchers have simulated and optimized gas pipeline networks and equipment for both steady-state and transient conditions with varying degrees of success. In Chapter 2 of this dissertation a literature review of previous research results are presented. “Historically, most of the efforts have been focused on steady-state flow conditions, but researchers have also identified the need for transient flow simulation” [12].

Fluid dynamicists and mechanical engineers are devising robust mathematical and numerical models to serve the gas transmission related purposes. Material engineers and scientists are developing advanced materials for the pipeline insulation and protection. Electric, control, and telecommunications engineers are developing sophisticated SCADA (Supervisory Control and Data Acquisition) systems in order to gain full control over the millions kilometres of gas pipelines worldwide.

A range of numerical schemes have been applied for the simulation of natural gas flow in pipelines, such as the method of characteristics, finite element methods, and explicit and implicit finite difference methods. The choice of the method is influenced more or less on the individual requirements of the system under investigation.

1.7 Problem background

In general, a mathematical model to simulate pipeline system operation, as well as the impact of design changes and equipment enhancements is urgently needed for this huge system to adjust the operation conditions. Simulation allows us to predict the behaviour of natural gas pipelines under different conditions.

Such predictions can then be used to guide decisions regarding the design and operation of the real system. The control of natural gas pipelines system also requires simulation in order to obtain information about the pressure and flow rates at given points of the pipeline [13].

Natural gas driven by pressure is transported through pipeline for a hundreds or thousands of kilometres or miles (cross-border). As it flows over long distances through pipelines, energy and so pressure is lost due to both the friction of pipelines and heat transfer between the natural gas and its environment [14]. This lost pressure of the natural gas is added or recovered at the compressor stations which are installed along the route of the natural gas pipelines which consume un-neglected amount of money.

Many pipelines systems use online pressure and flow monitoring to detect leaks. In these systems, a computer algorithm compares actual pipeline operating conditions to calculated conditions. Discrepancies beyond a certain threshold are potential leaks. Numerical simulations have been used for solving these problems; these simulations are based on either transient or steady-state models of pipelines [14].

1.8 Problem statement

Simulations and analyses of natural gas pipeline transients provide an insight into flow parameters changes and a pipeline capacity to deliver gas to consumers or accumulate gas from the source wells under various abnormal conditions. This information is important in order to control gas pressure changes within acceptable minimum and maximum setpoints and to plan repairs in timely manner with the aim of sustaining gas accumulation and supply to consumers in cases of various disturbances.

The major concern of the present thesis is to devise a mathematical model and a proper solution algorithm for modelling compressible, frictional natural gas transient flow in complex pipelines to predict natural gas flow properties. The considered area of application of such model is natural gas flow in cross-border and network pipelines.

Therefore, a numerical model and a computer code have been developed for the simulation and analyses of natural gas transients, such as those typically found in high-pressure gas transmission pipelines. The model is based on the mass and momentum balance equations that describe one-dimensional, compressible, frictional natural gas transient flow, as well as on boundary conditions that enable simulation of gas flows in complex pipeline networks. The developed model is solved with the numerical procedure of the method of characteristics and implemented into the gas transient analysis (GTA) computer code.

1.9 Objective

The objective of this study is to develop a numerical model and a computer code for the simulation and analyses of one-dimensional, compressible, frictional natural gas transient flow in lengthy and shortened pipelines that are able to predict natural gas flow properties in normal and abnormal operation conditions under isothermal or non-isothermal conditions.

1.10 Scope of research

This research involves both mathematical modelling and numerical simulation of one-dimensional, compressible, frictional natural gas transient flow, such as those typically found in high-pressure gas transmission pipelines to predict the behaviour of flow under different operation conditions.

The developed model and the Gas Transient Analysis - GTA code are validated by simulations of several test cases that are available in open literature. Afterwards, the code is applied to the simulation and analyses of transients in a real, several hundred kilometres long natural gas pipeline in Libya.

1.11 Thesis organization

The present thesis proposes a novel mathematical model and a computational algorithm to model the transmission of natural gas in (length/short) pipelines. A predictive numerical scheme is proposed to encapsulate the model equations and solve them consecutively to provide flow rate, pressure, temperature, density, and other profiles for such class of pipelines. The thesis comprises seven chapters; the second and third chapters respectively deal with the literature and discus the properties and flow dynamics of natural gas, as well as the mathematical modelling of natural gas flow in pipeline systems is highlighted in these chapters. Also, methods of computing natural gas properties and flow field variables (density, velocity, mass flow rate, and etc.) are briefly described in chapter three. The model development, the applied numerical procedure and the outline of the GTA (Gas Transient Analysis) code are presented in Chapter 4. In the fifth chapter, the developed model and the corresponding GTA code for the simulation and analyses of gas pipeline transients are validated by simulation of several test cases that are available in the open literature. Numerical results of gas pipeline transient simulations are also illustrated in this chapter.

The natural gas transients in the long gas pipeline of the Western Libya Gas Project are presented and discussed in Chapter 6 for three scenarios related to (i) disruption of gas supply from the gas source wells to the pipeline inlet point and (ii) stopping of gas delivery to a thermal power plant and a terminal for further off-shore gas transport at transmission pipeline outlet points. The method for the evaluation of thermal effects during these gas accumulation and discharging transients are presented in this chapter, together with the comparison of pressure changes obtained with isothermal and non-isothermal model evaluations.

Chapter seven provides detailed conclusions for this thesis. The appendix section contains the derivation of formulas for mathematical modelling of natural gas one-dimensional unsteady compressible flow in pipelines based on the governing equations of one-dimensional, compressible, frictional natural gas transient flow in pipelines.

1.12 Major contribution

The major contributions of this thesis are as following:

1. Presenting chronological and technical reviews of the mathematical modelling of natural gas in pipelines.
2. Devising a novel algorithm based on numerical model and a computer code for the simulation and analyses of natural gas transients, such as those typically found in high-pressure gas transmission pipelines. The developed model is solved with the numerical procedure of the method of characteristics and implemented into the gas transient analysis (GTA) computer code.
3. Providing evidences of code validation and stability using several case studies.
4. Contributes to observed deviations between modelled and measured flow parameters in the natural gas transmission.
5. Analysis of long transmission gas pipeline transients caused by disturbances of gas supply and delivery. The main aim of the performed simulations is to show the pipeline gas accumulation capacity, i.e. to accumulate gas during the disturbance at the gas delivery to consumers and to supply the consumers during disturbance in gas supply at the source.

CHAPTER 2

LITERATURE REVIEW

2.1 Introduction

Natural gas pipelines systems are becoming more complex as the use of this energy source increases. Mathematical modelling is one of the most important tools used in both design and operation of natural gas pipelines. Plentiful efforts have been spent and continue to be spent on steady-state and transient mathematical models.

In recent decades, world consumption of natural gas has grown and it is now one of the most commonly used primary energy source worldwide, accounting for 24% of total primary energy supply, behind coal and oil (33.5% and 27%) respectively [7], and it is the second energy source in power generation by 23.2%, behind coal (IEA, 2019) [15]. Natural gas is becoming a larger portion of the petroleum sector and is considered to play a more important role in the future of environmental friendly energy supply. Transmission pipelines have been developed in order to supply natural gas from source wells to power stations, distribution networks and industries. Numerical simulations of transmission pipeline transients are applied with the aim of predicting their capacity and dynamic behaviour under various normal operational conditions, such as pipeline start-ups and shut-downs, variations of gas consumption, etc., as well as under abnormal conditions caused by various equipment failures and disturbances. Results of the gas pipeline transient simulations are a support to the design of pipelines and its safety and control systems, as well as to the specifications of operational procedures and guidelines.

Numerous researches are available in the open literature on numerical simulations of natural gas pipeline transients. A brief overview of some results is presented in order to illustrate the variety of engineering applications

Simulations and analyses of natural gas pipeline transients provide an insight into flow parameters changes and a pipeline capacity to deliver gas to consumers or accumulate gas from the source wells under various abnormal conditions. This information is important in order to control gas pressure changes within acceptable minimum and maximum setpoints and to plan repairs in timely manner with the aim of sustaining gas accumulation and supply to consumers in cases of various disturbances. Therefore, a numerical models and a computer codes have been developed for the simulation and analyses of natural gas transients, such as those typically found in high-pressure gas transmission pipelines. It is noteworthy to mention that many operation conditions problems can be solved by transient flow modelling.

The most notable efforts dealing with the problem of mathematical modelling of natural gas pipelines are reported in this chapter.

2.2 Steady-state models

Steady-state gas flows have been studied in numerous research papers and theses. Steady-state flows of natural gas through pipelines are simulated in order to investigate and analyse the behaviour of gas flow in both operational and design conditions. In some researches, the investigators as Stoner [16], Mohitpour et al [17], Costa et al [18], etc., developed models which describe isothermal gas flow, and some others applied models that analyse non-isothermal gas flow as what Borujerdi and Rad [19] have done - they analysed the gas flow in pipelines subjected to wall friction and heat transfer. A few researchers presented comparisons between isothermal and non-isothermal pipelines gas flow models, as it was done by Alghlam [20]. On the other hand, some models are developed analytically such as those solved by Cameron [21], Szoplik [22], and Zhou and Adewumi [23] and the others are solved numerically as done by Mohitpour et al. [17] and some other investigators by using a various of numerical methods such as the method of characteristics, the implicit finite difference method, the explicit finite difference method, the finite elements method; the choice depends upon the particular requirements of the system under studying.

In addition, in this subsection, in order to provide some reading structure, it would be useful to find some other common characteristics among these research papers and thesis, such as solving the gas flow models with taking into account or neglecting the term of kinetic energy in the energy equation, studying the gas flow in pipelines systems as a single-phase flow and two-phase flow, and investigate the non-isothermal gas flow with and without consideration of gas wall friction, etc.

The most commonly used equations for the prediction of pressure drop due to wall friction in natural gas pipelines under steady-state calculations are the Weymouth equation, the Panhandle equations, Colebrook-White equation and AGA equation. Governing equations of the compressible fluids flow through the pipes were described by some researcher as Ouyang and Aziz [24], Rhoads [25] and Schroeder [26].

Abbaspour establishes general flow equations of simple form as a principle of the pressure loss calculations due to friction, elevation and kinetic energy [13]. Stoner had developed a new methodology for getting a steady-state solution of an integrated gas system model comprising of pipelines, compressors, control valves and storage fields. He utilized Newton-Raphson method for solving nonlinear algebraic equations [16, 27].

Berard et al. developed a simulation based on computer software to perform a steady-state gas transmission network utilizing the Newton-Raphson method for solving nonlinear equations. The simulated computer software has several features that facilitate efficient, accurate simulation of large nodal systems, including 1) optimal number of nodes, 2) implicit compressor fuel gas consumption calculation, 3) the ability to prorate gas volumes entering the network system, and 4) gas temperature distribution calculation [28].

Hoeven and Gasunie[29] used a linearization method to describe some mathematical aspects of gas network simulation. Tian and Adewumi [30] used a one-dimensional compressible fluid flow equation without neglecting the kinetic energy term to evaluate the flow of natural gas through a pipeline network. This equation includes a functional relationship between the gas flow levels along with a given segment of the pipe's inlet and outlet pressure. This then defines the steady-state compressible gas flow, assuming constant temperature and compressibility factor.

Costa et al. [18] presented a simulation of a steady – state gas pipeline. This simulation selects the pipeline and the compressors as the building components of a compressible flow network. However, this model uses the one-dimensional compressible flow equation to describe the relationship between the pressure and temperature along the pipe, as well as the flow rate through the pipe. To explore the variations between isothermal, adiabatic and polytropic flow conditions, the flow equation and the conservation of energy equation are both solved in a coupled way. The compressors are modelled simply by using a functional relationship between the increase in pressure and the rate of gas mass flow through the compressor.

A hybrid network model (HY-PIPENET) that uses a minimum cost spanning tree was presented by Sung et al. [31]. In their simulation a parametric study was achieved to comprehend the role of each individual parameter such as the source of pressure, flow rate and pipeline diameter on the optimized pipeline network. The authors distinguish that there is an optimal relationship between pipe diameter and the source pressure.

Rios-Mercado et al. [32] proposed a reduction strategy to solve problems related to the optimization of the natural gas transmission pipeline network. Such findings are valid for compressible steady state flow through a pipeline network. The decision variables are the rate of the mass flow through each arc (segment of the pipeline), and the degree of the gas pressure at each node.

Martinez-Romero et al. [33] have defined the compressible steady-state flow through a pipeline. For the most appropriate flow equations, they provided a sensitivity analysis describing the main parameters in the optimization process. The software package "Gas Net" has been used by them based on Stoner's method with some enhancements to solve the system equations. The essential mathematical model assumed a two element gas network: nodes and connectors of nodes. The connectors are components with different inlet and outlet pressures, such as pipes compressors, valves, and regulators.

Cameron [21] introduced TFlow using a steady-state and transient simulation model based on Excel. TFlow contains a user interface written in Microsoft Excel's Visual Basic for Applications (VBA) and a dynamic linked library (DLL) written in C++. All information required to model a pipeline system is contained in an Excel workbook, which also displays the simulation result. The robustness for general applications, however, is not readily apparent.

Doonan et al. [34] simulated a pipeline network using SimulinkTM. The simulation was used to analyse the safety parameters of an alternate control a considerable distance downstream from the main pressure regulating station. The elements that were used in this model were extremely limited. SimulinkTM has very limited knowledge on operation and reliability of pipelines. Fauer [35] proposed a general equation and contributed to making precise predictions for every variable. In order to provide reliable predictions the model must include many descriptions explaining not only the pipeline network but also the fluid it carries and the environment in which it operates. He used two steps to reach a useful model, 1) getting the appropriate level of detail in the model and 2) tuning the model to real world results that include steady-state tuning, steady-state tuning with transient factors, transient tuning and on-line tuning.

The well-known Patankar process "SIMPLE algorithm" (Patankar, 1980), known in Computational Fluid Dynamics (CFD), was used by Greyvenstein and Laurie to solve pipe network problems. The solution of the pressure correction equation, the consistency of the algorithm, the sensitivity to initial conditions and the convergence parameters are given particular attention [36].

Mohitpour et al. [17] addressed the significance of a dynamic simulation on pipeline transmission systems design and optimisation. The authors demonstrate in this paper that steady-state simulations are enough to optimize a pipeline when supply / demand conditions are relatively stable. In general, steady-state simulations should give a reasonable degree of confidence to the designer when the system is not subject to radical changes in mass flow rates on operating conditions. The mass flow rate varies in practice, so the most practical and general simulation is one that allows for transient behaviour.

Zhou and Adewumi [23] presented a new analytical equation which was derived based on the continuity and momentum equation for gas flow in pipelines, without neglecting any terms in the momentum equation. The equation provides a functional relationship among inlet and outlet gas density, gas mass flux, length, internal diameter and wall friction. It can handle any pipeline configuration, including horizontal, vertical and inclined pipelines. Ouyang and Aziz [24] developed a new flow equation to compensate for the drop in pressure due to changes in friction, elevation and kinetic energy. Simplified forms are also provided for new gas flow equations in pipelines or wells in which the term of kinetic energy can be ignored. Such new general flow equations and their simplified forms are compared to the previously used AGA equations and evaluated using field data. Results show that the new equations make excellent estimates of flow rates or drops in pressure, and are valid over a much wider range of gas types and gas flow rates than the AGA equation and old simplified flow equations. Furthermore, various empirical explicit correlations for the Fanning friction factor are compared.

Schroeder outlined equations that control compressible fluid flow through pipes. Particular emphasis has been placed on those used in the natural gas industry, in the hope that engineers in that industry will make informed decisions on how to model pipes. All practical equations were developed to solve extreme numerical problems, and the development in computing technology had made them absolute. It discussed further a new flow formula proposed by the research project GERG * [26].

Borujerdi and Rad [19] analysed the gas flow in high pressure buried pipelines treated with wall friction and heat transfer. The governing equations for one-dimensional compressible pipe flow are derived and solved numerically. This examines the effects of friction, heat transfer from the pipeline wall and inlet temperature on several parameters such as gas pressure, temperature and mass flow rate. By using some previous numerical experiments and available experimental data, the numerical scheme and numerical solution was verified.

Zhou and Adewumi [37] presented a mathematical model describing steady-state gas flow in pipeline. The model was reduced to a second-order ODE (Ordinary Differential equations) system of first order initial-value problem with gas pressure and temperature as the two dependent variables. The fourth-order Runge-Kutta method was used to solve this ODE system.

2.3 Transient models

Some researchers developed or presented natural gas models for prediction of pressure transients, temperature transients, leakages, etc. Numerical simulations of gas pipeline network of transient flow were conducted by Osiadacz [38] to predict the gas pressure and flow rate distribution and time change within the network, with the aim of minimization of compressors' operational costs. Osiadacz used the theory of hierarchical systems to explain the dynamic optimisation of high-pressure gas networks. The author explains that mathematically the transient optimization is more complicated than the steady state simulation, but the advantage of using a dynamic simulation is that the operator can achieve greater savings. He further states that it is of great importance to be able to optimize large-scale systems represented by partial differential equations as fast as possible in order to achieve real time optimization.

Gas pressure and flow rate changes in the long transmission pipeline network under the partial reduction of the gas supply at the inlet point were predicted by Pambour et al. [39]. They applied the approach with the isothermal gas flow model, also in an investigation of long transmission pipeline transients. According to these authors, a prediction of the influence of thermal effects on the gas flow would require a good knowledge of the thermal resistance of the ground and the distribution of ground temperature, which is typically difficult to estimate. Moreover, due to the slow dynamics in transport pipelines (with gas velocity lower than 15 m/s) the flowing gas typically has sufficient time to exchange heat with the ground and adapt its temperature to ground temperature. Thus, it is reasonable to neglect the temperature changes and assume a constant temperature equal to the ground temperature, as it is done by many authors in the literature.

Also, Mohitpour et al. [17] showed that the natural gas transmission pipelines should be designed by taking into account the transient pressure changes and compressible gas accumulation in the volume of pipelines, which are caused by the daily changes of gas consumption by consumers. A calculation of the transmission pipeline diameter on the basis of an average daily gas consumption and the minimum pressure setpoint would lead to an under design of the supply capacity. A calculation of the pipeline diameter on the basis of the maximum gas consumption, but without taking into account the transient accumulation of the gas within the transmission pipelines would lead to an over design of the pipeline and increased construction costs. Zuo et al. [40] investigated gas pipeline transients as a support to the prediction of setpoints for the action of automatic line-break control valves closure, which are used to prevent the gas release in the event of a pipeline rupture accident.

On the other hand, for the temperature profile of buried gas pipelines prediction, M. Edalat [41] developed a new analytic technique based on the corresponding states principle. This new technique can predict temperature profile quite accurately without using any additional chart or table. It can also be used for predication of gas mixture temperature profile flowing in a buried pipeline. Also, Oosterkamp et al. [42] developed a model of one-dimensional gas flow inside pipe. For comparison the developed model is coupled to three different external heat transfer models (1D steady state, 1D radial unsteady and 2D unsteady description of pipe wall layer and soil) of the ambient domain (pipe wall layers and soil). Both conduction and convection heat transfer in the soil layers were investigated. The effect of transient boundary conditions on heat transfer rates and flow parameter calculations were quantified.

A natural gas leakage and transient gas dynamic forces, which act on the pipeline structure and supports during gas pipeline blowdown accidents were numerically simulated by Stevanovic [43]. Yuan et al. performed natural gas transient calculations with the aim of detecting partial and extended blockages inside the pipelines [44].

As same as the steady-state flow models of natural gas pipelines, some transient models are based on isothermal flow, and the rest on non-isothermal flow. But a few of these models made a comparison between the two types of flow as was done by Osiadacz and Chaczykowski [11]. They used constant friction and compressibility factors, while neglecting the convective term to compare the transient models of isothermal and non-isothermal conditions for gas pipelines. They showed that there is a considerable difference within the pressure profile along the pipeline between the cases of isothermal and non-isothermal conditions, and this distinction increases with the gas density increase. Also, Thorley and Tilley [45] developed conservation laws for unsteady one-dimensional, non-isothermal compressible flow. They also surveyed several popular methods of solution for transient pipeline analysis, such as characteristics method, explicit and implicit method of finite difference, and finite-element method. The paper has an excellent review of the literature for these solution approaches.

Meanwhile, some investigators developed, presented, and solved the transient flow models numerically based on different mathematical methods. A number of numerical schemes and methods developed for the solution of differential equations were applied in numerical simulations of transient gas flows. For instance, Heath and Blunt [46] solved the mass and momentum conservation equations for slow isothermal gas transient flow by using the Crank-Nicolson semi-implicit numerical method. In case of nonlinear problems, this method is not stable according to the large time-step Neumann stability analysis; hence, this is the main disadvantage of the method. Osiadacz and Yedroudj [47] compared the application of the finite difference and the finite element methods for the simulation of gas pipeline transients. It was found that for the same level of accuracy, the finite difference method provides less computational time. Deen and Reintsema developed a technique that reduces energy equation to one single parameter in the mass equation without isothermal or isentropic flow assumption. They used the characteristics approach in combination with a finite difference method with a second-order truncation error [48]. Again, the method of characteristics was also used by Abott [49], Mekebel and Loraud [50], and Osiadacz [51] for the simulation of natural gas transient flow. It was also applied by Yow [52] and Wylie et al. [53] with an inertia multiplier modification to the equation of motion to move forward its computational capabilities for analysing natural gas pipeline flow.

Wylie et al. [53] compared the method of characteristics with an implicit finite difference method which uses central differences. The finding was that the explicit technique of the method of characteristics avoids the difficulty of simultaneous solving of a large matrix of equations, which is pertinent to the implicit methods, and therefore can generally be used on smaller computers. The drawback of the method of characteristics is the restriction of the time step of integration by the distance between adjacent nodes, as defined by the Courant criteria.

Herran-Gonzales et al. [54] prepared S-functions and used MATLAB-Simulink for unsteady flow simulation of gas networks. They derived two simplified models based on the method of characteristics and Cranke-Nicolson algorithm. While, Reddy et al. [55] used the transfer functions in Laplace domain to present an effective transient flow simulation for gas pipelines and networks. The equivalent transfer functions have been derived for the governing equations, and afterwards, the convolution theorem has been used in order to obtain the output series form in the time domain. On the other hand, Alamian et al. [56] analysed the natural gas transient flow in pipelines based on the state space equations with different boundary conditions. The state space model was applied for a large and complex network and the accuracy and computational efficiency of the proposed simulation were verified by comparing the results with those of the conventional finite difference schemes. The results showed that the proposed simulation with the state space model of the unsteady gas flow is more computationally efficient than other finite difference methods. Based on the finite volume technique and transfer function models an efficient simulation of transient flow for gas pipelines and networks has been performed by Wang et al. [57]. For different boundary conditions, the equivalent transfer functions of the nonlinear governing equations have been derived to verify the accuracy of the proposed simulation and obtained results were compared with experimental results. In this simulation, the effect of the flow inertia is considered with discretization by TVD scheme.

In addition, a significant number of analysts investigated and analysed the behaviour of natural gas flow in pipelines systems as one-dimensional flow, though, rare investigators applied two-dimensional flow. As an example, Noorbehesht and Ghaseminejad [58] utilized two-dimensional computational fluid dynamic (CFD) simulations in cylindrical coordinates to investigate the dynamic behaviour of natural gas flow in transmission pipelines. The applied modelling approach was based on the continuity, momentum and energy balance equations, a modified k-ε turbulence model and the ideal gas law. They discretized the coupled partial differential equations with the finite volume method and compared results with the experimental field data. Errors of approximately 4 to 4.5% were achieved. In addition, to simulate a 2-D natural gas transient flow phenomena a numerical procedure was developed by Ibraheem and Adewumi [59]. They used a special Runge-Kutta based method to model accurate evolution of flow characteristics. Therefore, the Total Variation Diminishing (TVD) strategy can be utilized with higher-order accuracy in order to resolve sharp discontinuous fronts.

An alternative approach for simulating the dynamics of natural gas pipelines was presented by Dorao and Fernandino [60]. They described a time-space least squares spectral method using a C^{11} type p-version hierarchical interpolations in space and time. In their formulation, both time and property space are coupled in the least squares minimization procedure. Farzaneh-Gord and Rahbari [61] developed an analytical approach to study and analyse natural gas pipeline network under transients based on the Kirchhoff's laws.

Different levels of modelling accuracy were applied in the description of transient gas flows. Issa and Spalding [62], Thorley and Tiley [45] and Price et al. [63] evolved the basic equations for one-dimensional, transient, compressible flow, comprising the effects of wall friction and heat transfer. Some previous researchers had neglected the convective term in the momentum equation, which resulted in a loss of accuracy in results of natural gas transient flow in pipelines. Hence, Zhou and Adewumi [23] solved one-dimensional natural gas transient flow in a horizontal pipeline, and they took into account all terms in the momentum conservation equation.

Price et al. [63] calculated the effective friction factor and the overall heat transfer coefficient for a high pressure natural gas pipeline under fully transient flow conditions. For pipeline boundary state, they used time-varying SCADA (Supervisory Control and Data Acquisition) measurements and implicit finite difference approximations for solving partial differential equations. This transient flow model was based on one-dimensional transient flow equations (continuity, momentum and energy) numerical solution. Tentis et al. [64] simulated the unsteady gas flow in pipelines utilizing the Adaptive Method of Lines.

Rachford et al. [65] used a Galerkin finite element method to model the isothermal transient gas flow by considering two dimensional elements in space-time. Maddox and Zhou [66] applied steady-state friction loss determination techniques to assess the unsteady state behavior of pipeline systems from pressure drop and material balance relationships in real time.

Kiuchi [67] defined a method for solving isothermal unsteady compressible flow by a fully implicit finite difference. A Von Neumann stability analysis on the finite difference equations of a pipe (after neglecting the inertia term in the momentum equation) showed that the equations are unconditionally stable. He contrasted this method with other methods such as the characteristics method, the Lax-Wendroff method, the Guys method and the Crank-Nicolson method and showed that fully implicit methods are very reliable for a small number of sections and a large time step, which is very useful for industrial gas pipelines due to the savings in calculation time. Likewise, Beam and Warming [68] developed an implicit finite difference scheme in conversation-law form for the effective numeric solution of nonlinear hyperbolic systems. The algorithm results in a second order time-accurate, two-level, non-iterative solution using a spatially factored form.

Luongo [69] presented an isothermal solution for gas pipelines using the Crank-Nicolson method for solving equations. He developed a simulation code with both linearized and non-linearized form of governing equations. By using an implicit finite difference scheme, the numerical solution is accomplished and then used to simulate transients in real pipeline networks. The results showed that 25% of the computational time is often saved by utilization of the linearized version without a serious sacrifice in accuracy.

Tao and Ti [70] extended the electric analogy method by combining resistance and capacitance, which resulted in a first order ordinary differential equation instead of partial differential equation for the solving of transient gas flow problems. It was found that the results obtained are akin to those obtained with the common techniques for solving partial differential equations.

A variety of hydraulic and thermal models and numerical methods were applied to the transient gas flow simulations. Osiadacz [71] characterized various transient flow models and assorted numerical methods which are utilized to resolve unsteady flow equations. For a given mathematical model, the challenge is to identify the numerical strategy that provides a high level of accuracy without requiring noteworthy computational resources. He used the Runge-Kutta Chebyshev (RKC) methods to solve ordinary differential equations resulting from the line approach applied to parabolic-type partial differential equations. Lewandowski [72] presented an application of an object-oriented methodology to model a network for the transmission of natural gas. For organized modeling and sensitivity analysis of dynamic systems, this approach was applied using a library of C++ classes. The model of a gas pipeline network can be formulated as a directed graph. Each arc of this graph represents a segment of the pipeline and has associated a partial differential equation which describes the gas flow through this segment. Graph nodes corresponding to gas pipeline nodes may be categorized as: source nodes, sink nodes, passive nodes, and active nodes.

A focusing on another characteristic of the natural gas flow in pipelines can be posed, such as solving of governing flow equations of state for single-phase and two-phase transient flow. It could be clearly noted that many researchers solved and developed the transient models of gas flow of state for single-phase and few investigators analyzed the flow of state for two-phase as same as Modisette [73] and Abbaspour [74].

Modisette [73] investigated the influence of the thermal model on the overall pipeline model accuracy for both gas and liquid. He coupled this model with a transient ground thermal model. The first effort to simulate the non-isothermal, one-dimensional, transient homogenous two-phase flow gas pipeline system using two-fluid conservation equations was done by Abbaspour et al. [74]. He used the modified Peng–Robinson equation of state to calculate the vapor–liquid equilibrium in multi-component natural gas to find the vapor and liquid compressibility factors. The fully implicit finite difference was the technique of solutions. This approach is robust when a large time step for gas pipeline simulations is used and thus minimizes the calculation time. The algorithm used to solve the non-linear thermo-fluid differential equations for two-phase flow through a pipe is based on the Newton – Raphson method. In the equation of momentum conservation, the inertia term is not neglected.

Most previous researchers ignored the term inertia in the momentum equation when they simulated transient flow of single-phase natural gas in pipelines. This makes the consequent set of partial differential equations linear. Formerly, numerical methods utilized to solve this system of partial differential equations such as the method of characteristics and a set of explicit and implicit finite difference schemes. Neglecting the inertia term in the momentum equation will definitely result in a loss of accuracy of the simulation results.

Dufont and Rachford described the effect of thermal changes induced by transients in gas flow and examined three different environments around the pipe and illustrated the effect of these conditions on temperature distribution [75].

Gato and Henriques [76] presented a numerical modelling of the dynamic behaviour of high-pressure natural-gas flow in pipelines. They performed numerical simulations by solving the conservation equations for one-dimensional compressible flow, using the Runge–Kutta and discontinuous Galerkin method, with third-order approximation in space and time. Chaczykowski [77] investigated the consequences gas state equation selection for the model of pipeline gas flow. He studied a non-isothermal transient gas flow model with AGA-8 and SGERG-88 equations of state. Models with SoaveRedlich-Kwong and Benedict-Webb-Rubin equations of state were solved to illustrate the overall gas flow model inaccuracies. The effect of the selection of different equations of state on the flow parameters is demonstrated and discussed.

Also, Chaczykowski [78] simulated the fast and slow fluid transients, like those normally found in high-pressure gas transmission pipelines by solving non-isothermal, one-dimensional gas flow model. Results of this simulation were applied to see the effect of different pipeline thermal models on the pressure, flow rate and temperature in the pipeline. Coelho and Pinho [79] discussed the particularities of the pressure drop equations being used in the design of natural gas pipelines. Several versions are presented according to the different flow regimes under consideration and through the presentation of these equations the basic physical support for each one was discussed as well as their feasibility.

Zhou and Adewumi [80] simulated eight field examples of engineering interest to provide some understanding of the behaviour of gas pipeline transient under operational scenarios. They solved one-dimensional natural gas transient flow in a horizontal pipeline, and they took into account all terms in the momentum conservation equation

Abbaspour and Chapman [81] solved the continuity, momentum, and energy balance equations by using the fully implicit finite-difference technique to simulate and analyse non-isothermal, one-dimensional unsteady gas flow in pipelines. Their work results show that the effect of treating the gas in a non-isothermal manner is extremely necessary for pipeline flow calculation accuracies, especially for rapid transient process.

Adeosun et al. [82] took into account all terms in the momentum equation to present unsteady-state Weymouth Equations for flow of natural gas in long pipelines. The new Weymouth Equations yield results close to steady-state flow and is able to account for the initial transient in gas volumetric flow rate.

A reduced-order modelling approach has been proposed by Behbahani-Nejad and Shekari [83]. They considered the Euler equations as the governing equations and used the method of implicit Steger-Warming flux vector splitting (FSM). Linearized form of the Euler equations has been derived and the corresponding eigensystem was obtained. Then, they used a few dominant flow eigenmodes to construct an efficient reduced-order model.

Helgaker et al. [84] utilized an implicit finite difference method to solve the governing equations for one-dimensional compressible flow, and they investigated the influence of different physical parameters which enter into the model.

Helgaker et al. [85] predicted a gas temperature change in a long transmission gas pipeline during a several days transient. The pipeline is buried in the ground and the heat transfer from the gas to the soil was predicted with and without the heat accumulation in the soil. A better agreement between calculated and measured outlet gas temperatures was obtained by taking the heat accumulation in the ground. The model with the steady-state heat transfer from the gas to the soil showed greater divergences from the measured data during periods with more intensive transient operational conditions. Nevertheless, the variation of the presented measured gas temperature at the long pipeline outlet was within 3ºC during the 4 days of the transient with the initial mass flow rate change of about 40 % and the gas pressure change variation between 150 bar and 180 bar. At the same time, there were no practical differences in the pressure predictions obtained by inclusion of thermal model with and without heat accumulation in the ground. But, regarding these presented results, no conclusions could be drawn about the uncertainty of the transient prediction that would be introduced by the assumption of the isothermal gas flow model.

Santos [86] also analysed the influence of the transient gas consumption on the optimal design and capital investments for the case of a long transmission gas pipeline. In addition, he showed the importance of the simulation and analyses of gas pipeline transients in cases of compressors' trips in the early stage of the system design. It was found that parallel arrangements of compressors would increase a reliability of gas supply. Finch and Ko [87] provided detailed information in three different areas in flow equation usage. First, a step by step development of the fundamental flow equation is included, followed by a discussion of various friction factor equations and their relation to the Moody diagram. This included the diameter dependence, the Reynolds number dependence and the recently developed explicit friction factor equation. The last area discussed the practical considerations of using the fundamental flow equation. Applicable variable ranges, sensitivity, and efficiency factor usage are included.

Gas pipeline transients caused by the time-varying consumers demand was simulated by Zhang et al. [88], with the aim of applying optimization of operational control, which should provide a minimum of energy consumption by compressor stations. Zhang [89] numerically simulated the performance of the surge avoidance system in a natural gas compression station and validated the results against experimental measurements during the emergency shutdown of compressor in an experimental piping network. Recently, Chaczykowski et al. [90] simulated natural gas pipeline transients with the tracking of gas composition propagation, which are caused by the injection of gases from unconventional sources, such as hydrogen and biomethane. Natural gas network of transient flow caused by the ambient temperature variations are numerically simulated by Farzaneh-Gord and Rahbari [61].

Table 2.1 shows the summary of the literature where it can be noted that the most of the previous investigators who studied natural gas flow in pipeline neglected the effect of heat transfer and considered that the temperature of gas remains constant. On the other hand, the most of researchers who take into account the change in temperature of natural gas flow in pipeline in their studies consider that the flow is transient; however, almost all of them neglected the heat generation due to the friction between the flowing gas and the inner surface of pipe. In addition, most of previous researches have not analysed or investigated the natural gas transmission pipeline behaviour during operational disturbances that are likely to happen during the gas pipeline exploitation.

Table 2.1: summary of the literature

Researcher	Research	Highlight	Flow mode	Solving Method
Stoner [16]	new method for obtaining a steady-state solution of gas system model of pipelines	Isoth. flow	Steady-state	New technique based on Newton-Raphson method
Ouyang and Aziz [24]	account for the pressure drop due to friction, elevation and kinetic energy change	Isoth. flow	Steady-state	new general flow equations and compared with AGA equations
Tian and Adewumi [30]	determine the flow of natural gas through a pipeline system	Isoth. flow	Steady-state	Deriving analytical equation based on mass and momentum balance
Costa et al [18]	provided a steady–state gas pipeline simulation	Isoth. flow	Steady-state	Model based on flow equation associated with the energy equation
Borujerdi and Rad [19]	analysed the gas flow in high pressure buried pipelines subjected to wall friction and heat transfer.	Non-isoth.	Steady-state	governing equations for 1D compressible pipe flow are derived and solved numerically
Zhou and Adewumi [37]	Predicting N-G flow Temp. & Press. with heat transfer with surrounding and Joule-Thompson effect	Non-isoth.	Steady-state	fourth-order Runge-Kutta method to solve ODE system
Dufont & Rachford [75]	explained the effect of thermal changes induced by transients in gas flow	Non-isoth.	Transient	
Edalat & Mansoori [41]	developed a new analytic technique for the prediction of temperature profile	Non-isoth.	Transient	new analytic technique based on the corresponding states principle
Kiuchi [67]	solving isothermal unsteady compressible flow	Isoth. flow	Transient	fully implicit finite difference method
Price et al. [63]	determined the effective friction factor and overall heat transfer a high pressure, natural gas pipeline	Non-isoth.	Transient	implicit finite difference approximations for solving PDE
Zhou & Adewumi [23]	provide a functional relationship among inlet and outlet gas density, gas mass flux, length, internal diameter and wall friction	Isoth. flow	Transient	new analytical equation based on the continuity and momentum equation for gas flow in pipelines
Osiadacz & Chaczykow-ski [11]	compared isothermal and non-isothermal transient models for gas pipelines	Isoth. & non-isoth.	Transient	Flow equations are derived from motion, continuity, energy and state equations
Issa and Spalding [62]	numerical procedure to solve 1D, unsteady, compressible, frictional gas flows with heat transfer	Non-isoth.	Transient	procedure is based on the Hartree 'hybrid' method which

2.4 Concluding remarks

The above literature review leads to the following conclusions:

- Most of the researchers focused on isothermal conditions where they neglected the effect of heat transfer from and to the gas flow in pipelines.
- Most of researchers have studied the natural gas problems in terms of steady-state and transient flow of one-phase of transported natural gas, also, in one-dimensional flow.

- Most of researchers who focused on the non-isothermal flow conditions did not take into account the heat generation due to the friction between pipe wall and the gas flows in the pipeline.
- Researchers have developed numerical schemes for a flow dynamics of natural gas pipelines using different methods such as the implicit finite difference method, the explicit finite difference method, the finite elements method, and the method of characteristics.

The presented literature survey shows that there is limited information about the natural gas transmission pipelines behaviour during operational disturbances. Some of these disturbances are likely to happen during the gas pipeline exploitation, such as: (a) the stoppage of gas delivery from gas source (wells) to consumers or storage, or (b) disruption of gas consumption while the gas input from the source is available. In such cases, it is worth to know the accumulation capacity of the long transmission pipelines or a time period during which the gas pipeline accumulation capacity can satisfy consumers' needs without disruption. Regarding a need for the insight into these transient operational characteristics under likely disturbances, the topic of research of the present PhD thesis is stated.

In addition, the literature survey shows that there is a lack of a simple method for the prediction of uncertainty that is introduced by the isothermal gas flow assumption into transient gas pipeline simulations. Hence, a derivation of an original analytical method is a topic of research in the presented thesis.

The motivation of the present research is to investigate the capacity of the long natural gas transmission pipelines to deliver gas to consumers in a case of abrupt disturbance of gas supply at the inlet point. A time period is determined from the trip of the gas supply to the instance of reaching a low pressure level at the delivery points at consumers. Also, an accumulation capacity of the transmission pipeline is evaluated in cases of cease of gas delivery to consumers under sustained gas pressure at the pipeline inlet point. The results should support the operation procedures and guidelines in cases of abnormal condition operations. In order to numerically simulate the gas transmission pipeline transients, the code GTA (Gas Transient Analysis) is developed, based on the model of one-dimensional, compressible and transient natural gas flow. The model mass and momentum balance governing equations are solved with the method of characteristics, which has the potential to produce the most accurate results (Wulff, [91]). Its high accuracy originates from the fact that it reduces partial differential equations to ordinary differential equations, as well as being the only method that accurately tracks the propagation of discontinuities in first-order derivatives. The characteristic coordinates are Lagrangian coordinates for such discontinuities. An analytical method for the evaluation of the difference between isothermal and non-isothermal transient pressure predictions and non-isothermal temperature change is derived. It supports the application of the isothermal simulations by the GTA code of transient gas accumulation and discharging of the long transmission pipeline within time periods of several hours. The motivation for the evaluation of the influence of thermal effects on the pressure changes in gas transmission pipelines was also initiated by the ambiguity of previously published results.

CHAPTER 3

FORMULATION OF NATURAL GAS FLOW IN PIPELINES - BACKGROUND

3.1 Introduction

The main goal of this research is to develop a numerical model and a code for the simulation of transient natural gas pipeline flows and to apply the developed method to analyses of natural gas transmission pipelines under different operational conditions. Hence, a numerical model and a computer code have been developed for the simulation and analyses of natural gas transients, such as those typically found in high-pressure gas transmission pipelines. The research deals with one-dimensional, compressible, frictional natural gas transient flow in pipelines. The derivation of the mathematical model is based on corresponding mass and momentum balance equations.

In this chapter, physical properties and flow dynamic parameters of natural gas, which is treated as mixture of non-ideal gases are discussed. Then the mathematical modelling of natural gas flow in pipeline systems is presented. Finally, numerical methods for computing of these natural gas flows are described.

3.2 Gas properties

In this section the properties of natural gas that influence gas flow through a pipeline are discussed. The relationship of pressure, volume, and temperature of a natural gas is presented and how the gas properties such as density, viscosity, and compressibility change with a variation of temperature and pressure.

3.2.1 Density of Gas

Density (ρ) is the ratio of the mass (m) of gas and the volume (V) that the gas occupies. Therefore, it is measured in units of mass per volume [92].

$$\rho = \frac{m}{V} \tag{3-1}$$

Density is expressed in kg/m^3 in *SI* units.

3.2.2 Specific Gravity

Specific gravity (G) is a measure of how heavy the gas is compared to air at a particular temperature. Sometimes it is called gravity or relative density.

$$G = \frac{\rho_g}{\rho_{air}} \tag{3-2}$$

where, ρ_g: density of gas.

ρ_{air}: density of air.

It is noted that ρ_{air} is the density of dry air at the temperature of 20 ^oC and the pressure of 101.325 kPa. In terms of the molecular weight (*M*), gravity of gas can be calculated as following:

$$G = \frac{M_g}{M_{air}} = \frac{M_g}{28.9625} \approx \frac{M_g}{29} \tag{3-3}$$

where, M_g: molecular weight of gas.

M_{air}: molecular weight of air.

Table 3.1 lists the molecular weights and other properties of several hydrocarbon gases [92].

Because natural gas is formed of a mixture of several gasses (methane, ethane, etc.), molecular weight M_g in equation (3-3) is referred to as the gas mixture apparent molecular weight.

$$M_g = \sum M_i y_i \tag{3-4}$$

where, M_i: molecular weight of natural gas component *i*, g/mol.

y_i: mole fraction of natural gas component *i*, %

Table 3.1: Molecular weights and critical properties
Of several hydrocarbon gases [92]

Compound	Molecular weight (g/mol)	Critical Temperature K	Critical Pressure MPa
Methane CH_4	16.043	191	4.60
Ethane C_2H_6	30.070	305	4.88
Propane C_3H_8	44.097	370	4.25
Iso-butane C_4H_{10}	58.124	408	3.65
n-butane C_4H_{10}	58.124	425	3.80
Iso-pentane C_5H_{12}	72.151	460	3.39
n-pentane C_5H_{12}	72.151	470	3.37
n-hexane C_6H_{14}	86.178	507	3.01
n-Heptane C_7H_{16}	100.205	540	2.74
n-octane C_8H_{18}	114.232	569	2.49
n-Nonane C_9H_{20}	128.259	595	2.29
n-Decane $C_{10}H_{22}$	142.286	618	2.10
Nitrogen N_2	28.016	126	3.40
Carbon dioxide CO_2	44.010	304	7.38
Hydrogen sulphide H_2S	34.076	373	8.96
Oxygen O_2	32.000	155	5.04
Hydrogen H_2	2.016	33	1.30
Water H_2O	18.015	647	22.06
Air	28.960	132	3.77
Helium He	4.000	5	0.23

3.2.3 Viscosity

The viscosity of fluid (gas or liquid) represents its resistance to flow. It depends on fluid temperature and pressure. Table 3.2 gives the viscosity of common components of natural gas [93].

Since natural gas is a mixture of pure non-ideal gases such as methane and ethane, the following formula key rule is used to calculate the viscosity from the viscosities of component gases:

$$\mu = \frac{\sum(\mu_i y_i \sqrt{M_i})}{\sum(y_i \sqrt{M_i})} \tag{3-5}$$

Where, μ_i is a dynamic viscosity of natural gas component i (kg/ms), M_i is a molecular weight of natural gas component i (g/mol), and y_i is a mole fraction of natural gas component.

A related quantity to the dynamic viscosity μ is the kinematic viscosity (v):

$$\upsilon = \frac{\mu}{\rho} \tag{3-6}$$

Table 3.2: List of common gases viscosity [93]

Gas	Viscosity (cP)	Viscosity (kg/m.s)
Methane	0.0107	1.07×10^{-5}
Ethane	0.0089	0.89×10^{-5}
Propane	0.0075	0.75×10^{-5}
i-Butane	0.0071	0.71×10^{-5}
n-Butane	0.0073	0.73×10^{-5}
i-Pentane	0.0066	0.66×10^{-5}
n-Pentane	0.0066	0.66×10^{-5}
Hexane	0.0063	0.63×10^{-5}
Heptane	0.0059	0.59×10^{-5}
Octane	0.0050	0.50×10^{-5}
Nonane	0.0048	0.48×10^{-5}
Decane	0.0045	0.45×10^{-5}
Ethylene	0.0098	0.98×10^{-5}
Carbon Monoxide	0.0184	1.84×10^{-5}
Carbon Dioxide	0.0147	1.47×10^{-5}
Hydrogen Sulphide	0.0122	1.22×10^{-5}
Air	0.0178	1.78×10^{-5}
Nitrogen	0.0173	1.73×10^{-5}
Helium	0.0193	1.93×10^{-5}

3.2.4 Ideal gas law

The ideal gas law sometimes referred to as the perfect gas equation, states that the pressure, volume, and temperature of the gas are related as following:

$$pV = nRT \tag{3-7}$$

where, p stands for pressure, T represents temperature, R is the ideal gas constant (8.314 J/mol K), and n is a number of moles which can be calculated as:

$$n = \frac{m}{M} \tag{3-8}$$

3.2.5 Real gas properties

The ideal gas equation presented in section (3.2.4) can be applied when dealing with real gases, and get adequately accurate results when the pressure levels are similar or close to the atmospheric pressure. For most real gases, the ideal gas equation will not be appropriate if the pressure values are considerably higher. To achieve reasonably accurate results, ideal gas equation should be modified.

It is necessary to define two terms which are called critical temperature and critical pressure. A real gas critical temperature is defined as the temperature above which a gas cannot be compressed to form a liquid, whatever the pressure. The critical pressure is known as the minimum pressure required for the compression of gas into a liquid at the critical temperature [92].

Real gases can be treated with a modified form of the ideal gas law described in section (3.2.4), if the modifying factor, known as the compressibility factor z is included. This factor is also called the deviation factor. It is dimensionless number less than 1 and varies with gas temperature, pressure, and gas composition.

Including the compressibility factor z, the ideal gas equation gets the following form:

$$pV = znRT \tag{3-9}$$

The ratio of the gas temperature (T) to its critical temperature (T_c) is called the reduced temperature and is defined as:

$$T_r = \frac{T}{T_c} \tag{3-10}$$

The reduced pressure is the ratio of gas pressure (p) to its critical pressure (p_c) and is given by:

$$p_r = \frac{p}{p_c} \tag{3-11}$$

3.2.6 Natural gas composition and pseudo-critical properties

In reality, natural gas is a mixture of several gaseous components. The critical temperature and critical pressure can be found for each pure component that constitutes this mixture of gases. However, the critical values of temperature and pressure of the gas mixture, which are called respectively the pseudo-reduced temperature (T_{pr}) and pseudo-reduced pressure (p_{pr}) need to be calculated as follows [92]:

$$T_{pr} = \frac{T}{T_{pc}} \quad (3\text{-}12)$$

$$p_{pr} = \frac{p}{p_{pc}} \quad (3\text{-}13)$$

where, T_{pc} and p_{pc} represent pseudo-critical temperature and pseudo-critical pressure. These quantities are determined in an analogous way to one used to calculate the molecular weight.

Therefore, the apparent molecular weight is defined in equation (3-4) as following:

$$M_g = \sum M_i y_i$$

In an analogous fashion, Kay's rule can be used as following to calculate the average pseudo-critical temperature (T_{pc}) and pseudo-critical pressure (p_{pc}) of the gas mixture:

$$T_{pc} = \sum y_i T_{ci} \quad (3\text{-}14)$$

$$p_{pc} = \sum y_i p_{ci} \quad (3\text{-}15)$$

For the given mole fractions (y_i) of gas components.

In equations (3-14) and (3-15) T_{ci} and p_{ci} represent the critical temperature and critical pressure of a pure component *i* within the gas mixture.

For the case that the composition of gas mixture is not exactly known, i e. the mole fractions of the various components in the natural gas mixture are not available, the pseudo-critical properties of the gas mixture can be computed if the specific gravity (G) of gas is known in the following approximate way [2]:

$$T_{pc} = 170.491 + 307.344G \quad (3\text{-}16)$$

$$p_{pc} = 709.604 - 58.718G \quad (3\text{-}17)$$

3.2.7 Compressibility factor

As introduced in section 3.2.5, the compressibility factor is a measure of how similar real gas is to the ideal gas. The compressibility factor *z* is defined as the ratio of the volume of gas at a given pressure and temperature to the volume of the gas would occupy at the same temperature and pressure if it were an ideal gas. The factor *z* is a dimensionless number close to 1 and its value depends on the gas gravity, gas temperature, gas pressure, and the critical gas properties.

Generalized plots showing the variation of *z* with pseudo reduced temperature (T_{pr}) and pseudo reduced pressure (p_{pr}) can be used for most gases for calculating the compressibility factor, as shown in Figure 3.1 [92].

Besides using the chart, the compressibility factor *z* can also be computed. The methods for the calculation of the compressibility factor *z* are presented in the following.

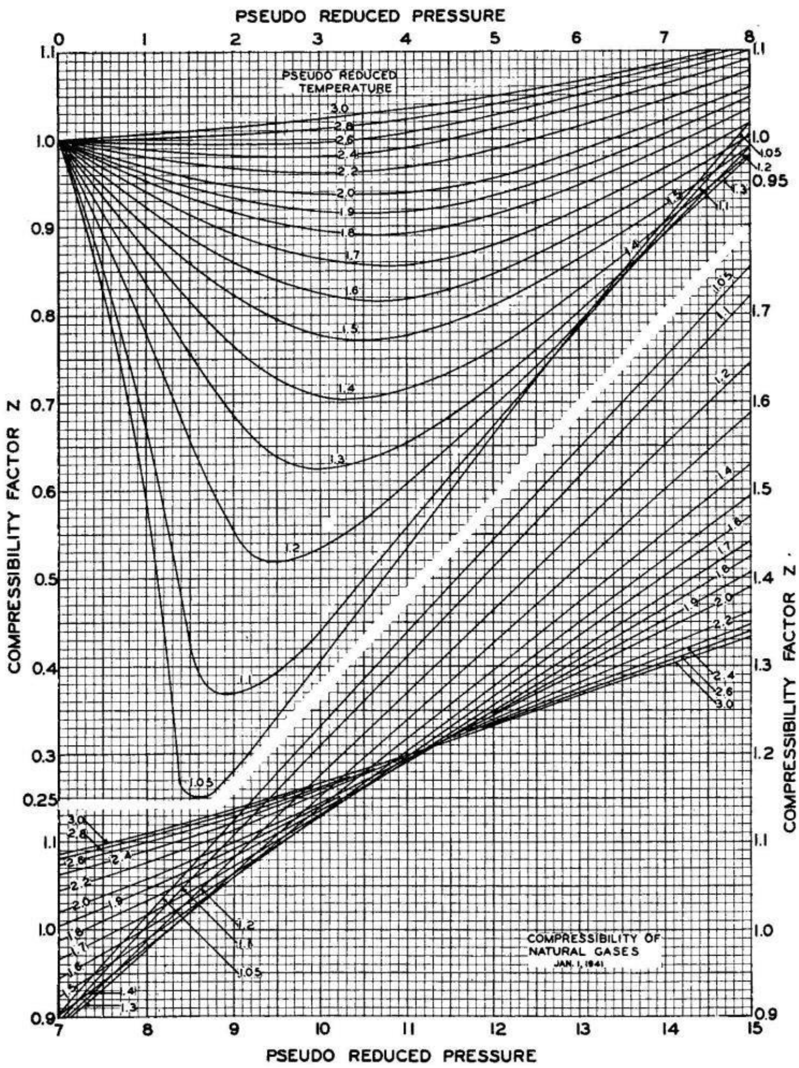

Figure 3.1: Compressibility factor chart for natural gas [93]

The available methods to calculate the compressibility factor are the Standing-Katz method, the Dranchuk, Purvis, and Robinson method, the American Gas Association (AGA) method, and the California Natural Gas Association (CNGA) method (Menon, 2005) [92].

Although the Standing-Katz method is the most common, it is not suitable for the application in a code as it is based on the use of a graph designed for binary mixtures and saturated hydrocarbon vapour. Also, the American Gas Association (AGA) method is not suitable for use in a computer code as it is based on complex mathematical algorithm, which necessities an individual computer program of significant complexity. For the above reasons, in the present thesis the approach of California Natural Gas Association (CNGA) is used to calculate the compressibility factor of natural gas flow in pipelines because of its simplicity to be applied mathematically in the algorithm (Mohitpour et. al., 2007) [93].

Therefore, according to CNGA method, the compressibility factor is computed from the following relation when the gas gravity (G), average temperature (T_{ave}), and average pressure (p_{ave}) are known [92].

$$z_{ave} = \frac{1}{\left[1+\left(\frac{p_{ave} c_1 (10)^{1.785G}}{T_{ave}^{3.825}}\right)\right]} \tag{3-18}$$

where, C_1 = 5260. For C_1 value derivation see Appendix A-3. Further, p_{ave} and T_{ave} represent the average pressure and temperature at any location on the pipeline. Therefore, for two points along the pipeline at pressure p_1 and p_2 the average pressure is $(p_1 + p_2)/2$ and average temperature $(T_1+T_2)/2$. For more accurate evaluation of average pressure the following formula can be used.

$$p_{avg} = \frac{2}{3}\left[p_1 + p_2 - \frac{p_1 p_2}{p_1 + p_2}\right] \tag{3-19}$$

In addition, at any particular point along the pipeline; the compressibility factor is determined as follows:

$$z = \frac{1}{\left[1+\left(\frac{p\ c_1 (10)^{1.785G}}{T^{3.825}}\right)\right]} \tag{3-20}$$

where, p is a gauge pressure of gas in kPa and T is in K.

3.3 Flow regimes

In high-pressure gas transmission lines with moderate to high flow rates, two types of flow regimes are normally observed, which are turbulent flow and laminar flow. A determination of whether a given flow in pipe is laminar or turbulent is necessary, since the two different flow regimes often need different methods to analyse the flow behaviour.

The laminar flow occurs in conditions with low fluid velocity and high fluid viscosity. In the case of laminar flow, all trajectories of fluid particles are parallel to the flow direction. On the other side, turbulent flow is characterized by flow mixing due to development of eddies of different size. The vectors of point velocity are in all directions but the overall flow is one-way in the direction of flow. Opposite to the laminar flow, turbulent flow appears in flow situations with high fluid velocity and low fluid viscosity.

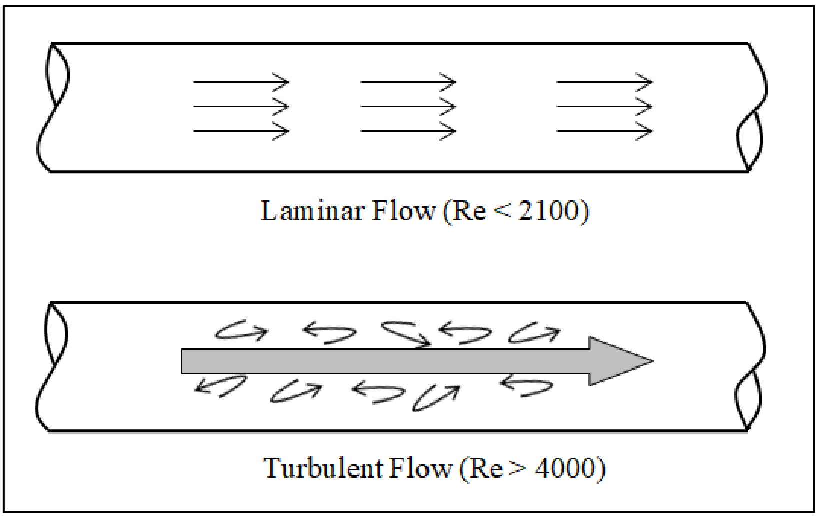

Figure 3.2 laminar and turbulent Pipe Flow

The regime of flow is defined by the Reynolds number, which is a dimensionless expression, which represents the ratio between the momentum forces of the flow to the viscous forces of the fluid:

$$\mathrm{Re} = \frac{\rho D u}{\mu} \tag{3-21}$$

where, Re: Reynolds number.

ρ: density of gas.

D: inner diameter of pipe.

u: gas flow velocity.

μ: dynamic viscosity of gas.

Reynolds number is used to characterize the type of flow in a pipe, such as laminar, transitional, or turbulent flow. It is also used to calculate the friction factor in the pipe flow. For Reynolds numbers less than 2100 the flow in pipes is normally laminar or stable. Turbulent flow in pipes occurs when the Reynolds number is greater than 4000. For the so-called the transition region (2100 < Re < 4000) the flow may be either laminar or turbulent, depending upon factors like the entrance conditions into the pipe and the roughness of the pipe surface. In general transition region conditions should be avoided in designing piping systems. In natural gas transmission the Reynolds number is much greater than 4000 [92]. Therefore, transport of natural gas in a pipeline is typically turbulent flow.

3.4 Friction factor calculation

When gas flows in a pipeline, friction occurs between the flow stream and pipeline walls and causes pressure losses. This pressure loss is computed by introducing friction factor. The friction factor is a dimensionless parameter depending on the Reynolds number of flow and roughness of pipe walls. In engineering literature, there are two formulation of friction factor; Darcy friction factor and Fanning friction factor. The relationship between the both factors is given by:

$$f_f = \frac{f_d}{4} \tag{3-22}$$

where, f_d is a Darcy friction factor, and f_f is a fanning friction factor.

Darcy friction factor is more general and will be used in this study. For the sake of simplicity, the Darcy friction factor hereafter will be denoted by the symbol f.

The friction factor for laminar flow depends only on Reynolds number:

$$f = \frac{64}{\text{Re}} \quad (3\text{-}23)$$

The friction factor for turbulent flow is a function of the Reynolds number and relative roughness of pipe walls (defined as the ratio of absolute wall roughness *e* and inside pipe diameter *D*). This dependence is graphically presented by Moody diagram in Figure 3.3. As shown in Figure 3.3, turbulent flow in pipes (Re > 4000) is divided into three zones; turbulent flow in smooth pipes, turbulent flow in rough pipes, and transition flow between smooth pipes and rough pipes.

The friction factor *f* only depends on Reynolds number for turbulent flow in smooth pipes. For fully rough pipes, *f* is more dependent on relative roughness of pipe walls (*e/D*). The value of friction factor depends on both the roughness of pipe wall, and Reynolds number in the transition zone.

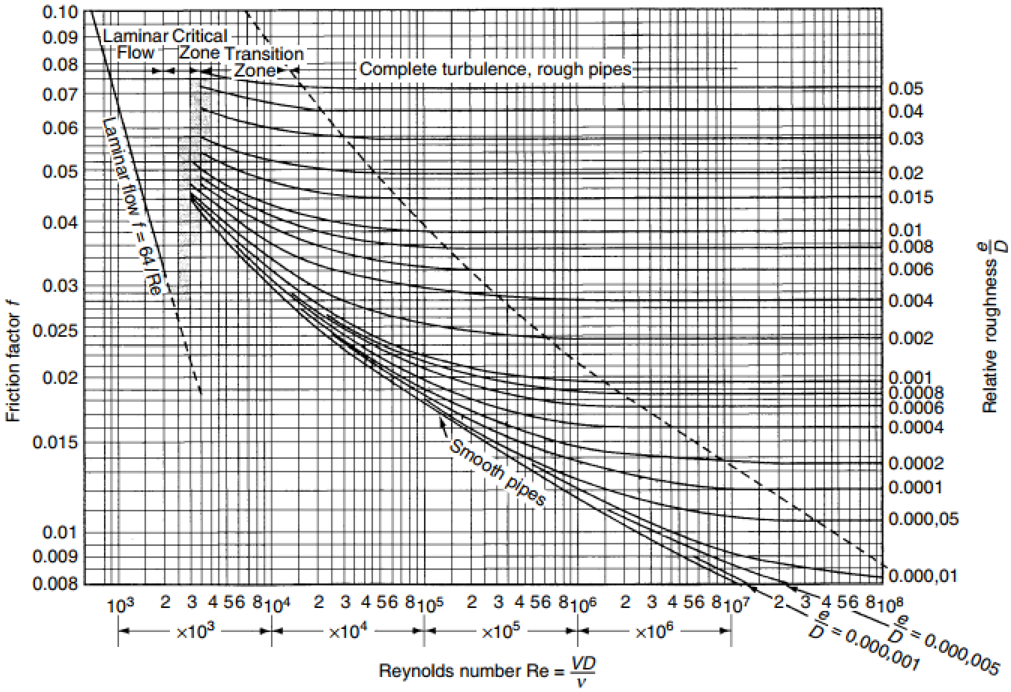

Figure 3.3: Moody diagram [93]

As shown above the roughness plays an important role in determination of friction factor. For that reason, in Table 3.3 typical values of absolute pipe roughness (*e*) are given.

Table 3.3 Typical values of absolute roughness of pipe walls [92]

Pipe Material	Roughness, (in.)	Roughness, (mm)
Riveted steel	0.0354 to 0.354	0.9 to 9.0
Commercial steel/welded steel	0.0018	0.045
Cast iron	0.0102	0.26
Galvanized iron	0.0059	0.15
Asphalted cast iron	0.0047	0.12
Wrought iron	0.0018	0.045
PVC, drawn tubing, glass	0.000059	0.0015
Concrete	0.0118 to 0.118	0.3 to 3.0

There are many correlations for calculating the friction factor. The most widely used ones for evaluation of friction factor in the gas flow in pipelines are presented below.

- **Colebrook-White correlation**

The Colebrook-White correlation relates the friction factor and the Reynolds number, pipe roughness, and inside diameter of pipe. It is the most popular equation for general gas industry transmission pipelines which combines both partially and fully turbulent flow regimes and is most suitable for cases where the pipeline is operating in transition zone (White, 1999) [94]. The following form of the Colebrook correlation is used to calculate the friction factor in gas pipelines in turbulent flow:

$$\frac{1}{\sqrt{f}} = -2 \ \log_{10}\left(\frac{e}{3.7D} + \frac{2.51}{\mathrm{Re}\sqrt{f}}\right) \qquad (3\text{-}24)$$

In order to calculate the friction factor f from equation (3-24) one must use a trial and error approach.

- **Modified Colebrook-White correlation**

The modified Colebrook-White correlation form was introduced in 1956. The main difference to Colebrook-White correlation is that it gives a higher friction factor. Because of this, conservative value of flow rate is obtained. The modified version of the Colebrook-White turbulent flow correlation reads as follows:

$$\frac{1}{\sqrt{f}} = -2\ \log_{10}\left(\frac{e}{3.7D} + \frac{2.825}{\mathrm{Re}\sqrt{f}}\right) \tag{3-25}$$

- **American Gas Association (AGA) correlation**

American Gas Association (AGA) correlation is derived as a result of a study which dealt with determination of the transmission factor for gas pipelines. The transmission factor *F* is related to the friction factor *f* in the following way:

$$F = \frac{2}{\sqrt{f}} \tag{3-26}$$

The transmission factor *F* is determined using the method of two separate equations. First, *F* is calculated for the zone of turbulent flow in rough pipe. Next, *F* is determined for the zone of turbulent flow in smooth pipe. Finally, the smaller of the two values of the transmission factor is used for pressure drop calculation.

Based on these investigations, AGA suggests using the following formula for *F* for the fully turbulent region, based on relative roughness *e/D* and independent on the Reynolds number.

$$F = \frac{2}{\sqrt{f}} = 4\log_{10}\left(\frac{3.7D}{e}\right) \tag{3-27}$$

- **Friction factor from Weymouth equation**

Weymouth equation was developed for evaluation of flow for high pressure, high flow rate, and large diameter gas gathering systems. In this method, the transmission factor *F* is determined by [92]:

$$F = 6.521\ (D)^{1/6} \tag{3-28}$$

Hence, the friction factor derived from this equation is of the following form:

$$\frac{1}{\sqrt{f}} = \frac{6.521}{2} D^{1/6} \tag{3-29}$$

- **Friction factor from Panhandle A equation**

The Panhandle A equation was developed for evaluation of flow rate in natural gas pipelines for Reynolds numbers in the range of 5 to 11 million. The roughness of the pipe is not accounted for. The friction factor extracted from this equation is given in the following form:

$$\frac{1}{\sqrt{f}} = \frac{11.85E}{2} \left(\frac{\dot{V} G}{D} \right)^{0.07305} \tag{3-30}$$

where, $\dot{V}$ is the volume flow rate of the natural gas, and E is pipeline efficiency.

- **Friction factor from Panhandle B equation**

  The Panhandle B equation, is used for evaluation of flow rate in transmission lines with large diameters, high pressure and for fully turbulent flows with Reynolds number values in the range of 4 to 40 million. The friction factor devised from this following equation has the form:

$$\frac{1}{\sqrt{f}} = \frac{19.08E}{2} \left(\frac{\dot{V} G}{D} \right)^{0.01961} \tag{3-31}$$

Summary of various correlations for friction factor used in the gas pipeline industry is presented in Table 3.4.

Table 3.4 Summary of friction factor correlations [92]

Equation	Application
Colebrook-White	Friction factor calculated for pipe roughness and Reynolds number; most popular correlation for general gas transmission pipelines
Modified Colebrook-White	Modified correlation based on U. S. Bureau of Mines experiments; gives higher pressure drop compared to the original Colebrook correlation
AGA	Transmission factor calculated for partially and fully turbulent flow considering roughness and Reynolds number
Panhandle A & B	Panhandle equations do not consider pipe roughness; instead, an efficiency factor is used; less conservative than Colebrook or AGA
Weymouth	Does not consider pipe roughness. Used for high-pressure gas gathering systems; most conservative equation that gives highest pressure drop for given flow rate

In the present thesis, for a code, it is more complicated to write all flow equations in their different forms; so, friction factor is calculated individually then substituted as an input in a code for flow calculations.

3.5 Velocity of natural gas in pipeline

Unlike a liquid pipeline, the natural gas velocity depends upon the pressure and, hence, will vary along the pipeline even if the pipeline diameter is constant, that is due to the change in compressibility of gas. In addition, if the flow is non-isothermal, the gas velocity is affected by the variation of gas flow temperature, because of its impact on the natural gas compressibility.

The highest gas velocity will be where the pressure is least and that is at the downstream end. On the opposite, the lowest value of velocity of gas will be at the upstream end, where the pressure is the highest.

Mathematically, the calculation of the velocity of the one-dimensional, compressible, frictional natural gas transient flow could be done numerically by the combination of the mass balance and momentum balance. The derivation of pressure and velocity of the natural gas transient flow in pipe will be described in detail in Chapter 4.

3.5.1 Erosional velocity

The velocity of natural gas flows in a pipeline is directly related to the pressure. The gas velocity increases as the flow pressure decreases. With the velocity increase, the vibration and noise occur. Another problematic issue is that higher velocities cause erosion of the pipeline during long period of time. If the gas velocity exceeds the erosional velocity calculated for the pipeline, the erosion of the wall is increased to rates that can significantly reduce the life of the pipeline. Therefore, it is necessary to control gas velocity in natural gas transmission lines to prevent it from rising above this limit. The upper limit of the gas velocity is usually calculated approximately from the following equation [92]:

$$u_{\max} = \frac{C_2}{\sqrt{\rho}} \tag{3-32}$$

where, C_2 is an empirical constant (C_2 = 122 for continuous service as per API 14E[2]) [95]

The recommended value for C_2 in natural gas transmission pipelines is 122 in SI units. The derivation of this constant is illustrated in Appendix A-4.

From the equation of state of gas: $\rho = \frac{p}{zRT}$

$$u_{\max} = C_2 \sqrt{\frac{zRT}{29Gp}} \tag{3-33}$$

Usually, the acceptable operational velocity (u_{acc}) in natural gas transmission pipelines is 50% from the maximum velocity [92].

$$u_{acc} = 0.5\ u_{\max} \tag{3-34}$$

3.6 Heat transfer consideration of gas flow in pipeline

Generally, in some applications, where pipelines are relatively short and at low pressure, an isothermal (i.e. constant temperature) assumption for the gas flow is fairly sufficient. There are certain characteristics of lengthy pipelines (e.g. cross-border pipelines) that make the implementation of an isothermal flow model inadequate. The majority of these pipelines transport massive amount of gas every day, which requires the line to be at high pressure values all along its route. The energy loss

[2] The American Petroleum Institute recommended practice 14E.

due to pressure drop is mostly caused by friction, this lost energy is transformed into heat that is dissipated in the ground. In some cases, when the pipeline routes from north to south or from east to west and vice versa, the climatic changes along the year create relatively large difference in soil temperature, which can pump the heat out from the gas reducing its pressure. For all these reasons, it is useful to include in some studied cases a heat transfer model that takes into consideration the heat transfers between gas and its surrounding (Osiadacz and Chaczykowski, 2001) [11].

Natural gas temperature in a pipeline is affected by the conductive and convective transfer of heat in a radial direction, by the accumulation of heat in the surrounding soil, and by the Joule-Thomson effect.

3.7 Mathematical modelling of natural gas one-dimensional unsteady compressible flow in pipelines

There are several factors that control the precise and accurate pipeline mathematical flow models, mainly serving for pipeline balance, pressure monitoring, and deliverability. There are two types of mathematical models for lengthy pipelines and networks flow; the steady-state and the transient models. The core difference between the two types of flow models lies in the equation of motion. In the transient flow models, there are terms that represent the change of transport parameters with time. When these terms are set to zero, the steady- state representation of the flow equation is obtained. Consequently, and due to this fundamental difference between the two types of models, the functionality of each of them differs. For the purposes such as pressure monitoring and leak localization, in which the change of transport parameters with time is vital, transient flow models become ideal. For other purposes such as pipeline design, sizing, line capacity estimations and line packing, where the changes of transport parameters with time are of no significance, steady-state models become ideal. The transient models are more difficult to implement compared to steady-state models.

Modelling the flow of natural gas in pipelines requires consideration of the physical processes that govern the flow. In this section, the physical laws governing the processes that take place during natural gas transportation are applied in the derivation of mathematical expressions to model natural gas flows.

3.7.1 Governing equations

The flow of natural gas in pipelines is governed by the time-dependent continuity and momentum for isothermal flow and continuity, momentum, and energy equations for non-isothermal flow and an equation of state for homogenous, geometrically one-dimensional flow. By solving these equations, the behaviour of gas parameters can be obtained along the pipe network [2]. Some of investigators developed the basic equations for one-dimensional unsteady compressible flow that include the effects of wall friction and heat transfer.

A one-dimensional unsteady flow of a homogeneous fluid in a tube with constant cross section is depicted in figure 3.4 [93], and the balance equations are as follows:

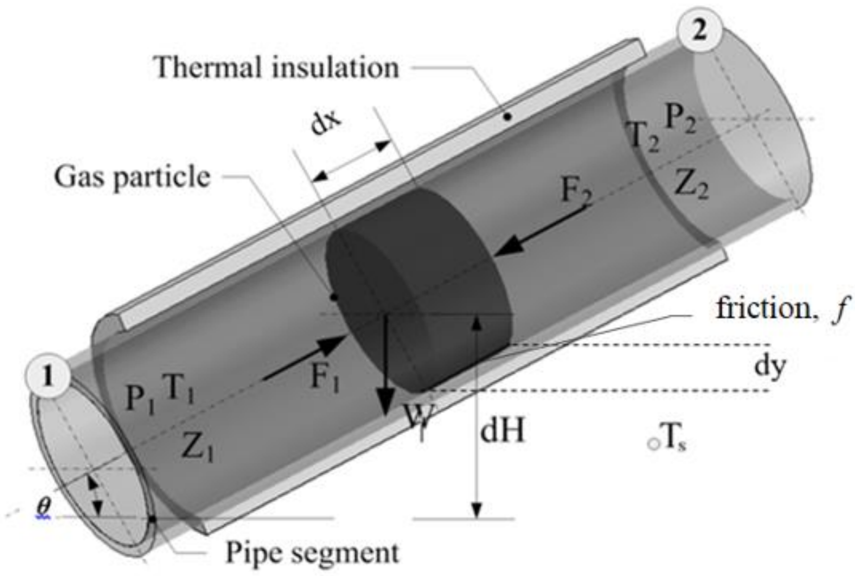

Figure 3.4 Demonstration of all forces acting on a gas particle moving in a pipeline [20]

- **Conservation of mass: continuity equation**

  The conservation of mass for the control volume shown in Figure 3.5 can be expressed in the form as follows:

$$\frac{D\rho}{Dt} + \rho\frac{\partial u}{\partial x} = 0 \quad ; \qquad (3\text{-}35)$$

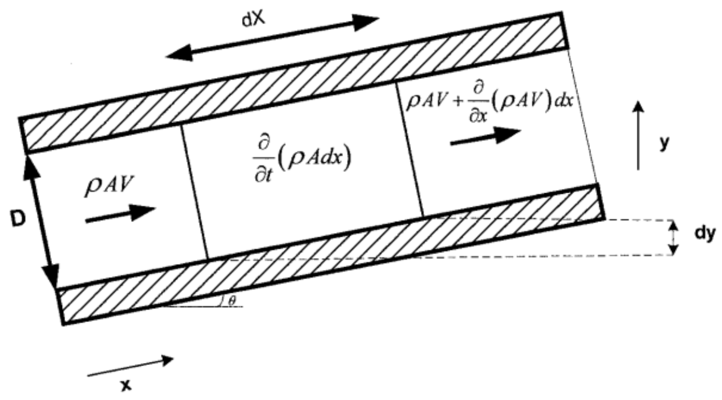

Figure 3.5: Control volume for continuity equation

where, ρ is the density of gas, u is the flow velocity. Operator $D/Dt = \partial/\partial t + u\partial/\partial x$ is the material derivative. The derivation of Eq. (3-35) is presented in Appendix A-1.

- **Momentum balance: Newton's second law of motion**

The momentum equation can be written for the control volume shown in figure 3.6 using the following force component summation:

$$\frac{Du}{Dt} + \frac{1}{\rho}\frac{\partial p}{\partial x} + \frac{fu|u|}{2D_H} + g\sin\theta = 0 \quad ; \qquad (3\text{-}36)$$

where g is the acceleration of gravity, f is the friction coefficient, and θ is the angle between the horizon and the direction x. The last two terms on the left hand side of equation (3-36) represent consequently the momentum drop due to friction on the pipeline wall and its change due to gravity. The derivation of Eq. (3-36) is presented in Appendix A-1.

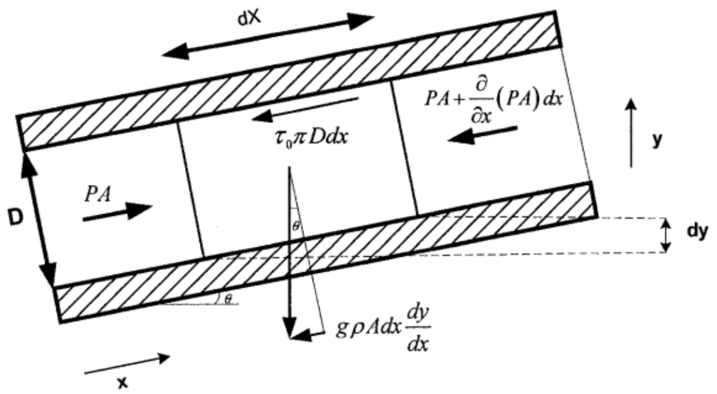

Figure 3.6: Control volume for momentum equation

- **Transformation of the balance equations**

The applied equation of state for gas under isenthalpic flow is written as

$$\rho = \rho(p) \tag{3-37}$$

The equation of state is differentiated by time t and by spatial coordinates x

$$\frac{\partial \rho}{\partial t} = \frac{d\rho}{dp}\frac{\partial p}{\partial t} \tag{3-38}$$

$$\frac{\partial \rho}{\partial x} = \frac{d\rho}{dp}\frac{\partial p}{\partial x} \tag{3-39}$$

The mass balance equation (3-35) is transformed by the introduction of derivatives (3-38) and (3-39) and the following form is obtained with the pressure material derivatives

$$\frac{Dp}{Dt} + c^2 \rho \frac{\partial u}{\partial x} = 0 \tag{3-40}$$

where the speed of sound is expressed as

$$c = \left(dp/d\rho\right)^{1/2} \tag{3-41}$$

Determination of the speed of sound is presented in Appendix A-2.

Equations (3-40) and (3-36) present a set of two partial differential equations of the hyperbolic type as follows

$$\frac{\partial p}{\partial t} + u\frac{\partial p}{\partial x} + c^2 \rho \frac{\partial u}{\partial x} = 0 \tag{3-42}$$

$$\frac{\partial u}{\partial t} + u\frac{\partial u}{\partial x} + \frac{1}{\rho}\frac{\partial p}{\partial x} = Y \quad , \tag{3-43}$$

where

$$Y = -\frac{fu|u|}{2D_H} - g\sin\theta \quad ; \tag{3-44}$$

In this system of equations dependent variables are the pressure and velocity of fluid, and the independent variables are the time and space coordinate. In order to solve the above system of equations it is necessary to specify the appropriate initial and boundary conditions. The initial conditions are defined with flow parameters of the fluid at the initial time prior to disturbance. Boundary conditions are defined on the basis of the state of the fluid at the inlet and outlet of the pipeline segment. The analytical solution of this system cannot be obtained, so a numerical method is applied to determine the particular integral.

3.7.2 Solution methods

Various numerical schemes have been developed for the solving of the mass, momentum and energy balance equations for one-dimensional transient pipeline flow, such as the method of characteristics, the finite elements method, the explicit finite deference method, and the implicit finite difference method. The choice depends partly upon the particular requirement of the system under investigation.

3.7.2.1 Method of characteristics

The method of characteristics is a technique for solving hyperbolic partial differential equations (PDE). Typically the method applies to first-order equations, although it is valid for any hyperbolic-type PDEs. The method involves the determination of special curves, called characteristics curves, along which the PDE becomes a family of ordinary differential equations (ODE). Therefore, it can be used to transform the partial differential of the continuity, momentum and energy equations into ordinary differential equations [27]. The resulting characteristics equations are solved numerically either on a grid of characteristics or on a rectangular coordinate grid. This method has the potential to produce the most accurate results (Wulff, 1987) [91]. Its high accuracy originates from the fact that it reduces partial differential equations to ordinary differential equations, as well as being the only method that accurately tracks the propagation of discontinuities in first-order derivatives. The method of characteristics was also used for the simulation of natural gas transients by Abott (1966) [49], Mekebel and Loraud (1985) [50], Osiadacz (1987) [51], and Herran-Gonzales et al. (2009) [54].

3.7.2.2 Finite element method

This method can handle some boundary conditions better than finite difference methods. On the other hand, the method has not been commonly used for gas transient flow modelling because computing time and the storage requirement are high. The element size, shape, and distribution are relatively flexible, so that nonuniform internal distribution of nodal points is possible. This method was compared with the application of the finite difference for the simulation of gas pipeline transients by Osiadacz and Yedroudj (1989) [47].

3.7.2.3 Explicit finite difference methods

There are several explicit methods of finite difference such as first-order and second-order approximations. A first-order approximation is typically not sufficiently accurate to model gas transients in a pipeline and therefore attention is focused on second-order methods [45]. The main drawback of the second-order approximation is that these techniques require a greater amount of computer time and are therefore not ideal for examining large systems or analysing unsteady flows over long periods of time.

3.7.2.4 Implicit finite difference methods

The main advantage of using an implicit method over the explicit method is that some sort of implicit method is unconditionally consistent and does not enforce any limitations on the maximum allowable time stage. Nonetheless, the approach will produce unsatisfactory results for the strong transients. In addition, some implicit methods have been known to produce erratic results during the imposition of some types of boundary conditions [45]. This method was used by Luongo (1986) [69], Abbaspour et al. (2010) [74], Helgaker et al (2014) [84], and etc.

3.7.2.5 Central difference method

In this method, the partial derivatives are approximated for sections of the pipeline rather than node points. It was used by Wiley at al. [53] to solve for the transient isothermal flow field gas pipeline network. For the non-linear equations, the Newton- Raphson method was used, and sparse matrix algebra reduced the solution time for the simultaneous equations. Although this method requires a large amount of computer storage to handle the coefficient matrix and lengthy execution times, these major disadvantages can be overcome by using a sparse matrix method.

3.7.2.6 Crank-Nicolson method

This method is a central difference solution of high-order accuracy. It was utilized by Heath and Blunt (1969) [46] to solve the conservation of mass and momentum equations for slow transients in isothermal gas flow. The main advantage of this method is that it does always give a stable solution according to the Neumann stability analysis of large time step for nonlinear problems.

3.7.2.7 Fully implicit method

Whereas the explicit finite difference methods are forward difference methods, the fully implicit method is a backward method. This method mostly is unconditionally stable. It is very robust for the gas pipeline industry because of relatively slow transient. The implicit method garantees stability for a large time step, but requires a numerical method such as the Newton-Raphson method to solve a set of nonlinear simultaneous equations at each time step.

CHAPTER 4

MODEL FORMULATION AND SOLUTION ALGORITHM

In this chapter the procedure for the computation of natural gas properties and flow field variables (pressure and velocity) is presented. The newly proposed model is based on the method of characteristics.

4.1 Application of the method of characteristics for the simulation of natural gas pipeline transients

The transient one-dimensional natural gas flow in pipelines is described with the mass and momentum balance equations. These equations are partial differential equations of the hyperbolic type. In this research, the method of characteristics is used for the numerical solution of the system of partial differential equations of hyperbolic type. This method can solve the system of two quasi-linear partial differential equations (3-42) to (3-43), with the two dependent variables (pressure and velocity) and the two independent variables (time and space coordinate).

The method of characteristics converts the quasilinear system of partial differential equations (3-42) and (3-43) into a system of differential equations with the total differential, wherein the family of curves is determined in the space-time coordinate system along which the derived transformation apply. Total differentials are then replaced by finite differences, thus obtaining two difference equations. Solving these algebraic equations by the dependent variable obtained are values of the fluid flow parameters along the pipeline during the transient.

The family of curves in the space-time coordinate system represent a physical propagation of pressure waves in the flow field. The time step of integration is determined by the Courant criterion. The Courant criterion links spatial and temporal integration step. The numerical grid for the solving of the difference equations is formed with the uniform spatial step of integration.

Multiplying equation (3-42) by λ_1 coefficient and equation (3-43) by λ_2 coefficient, and then adding the resulting equations, the following equation is obtained:

$$\lambda_1 \frac{\partial p}{\partial t} + \lambda_2 \frac{\partial u}{\partial t} + \left(\lambda_1 u + \frac{\lambda_2}{\rho} \right) \frac{\partial p}{\partial x} + \left(\lambda_1 c^2 \rho + \lambda_2 u \right) \frac{\partial u}{\partial x} = \lambda_2 Y \tag{4-1}$$

The dependant variables are marked as a general function $f \in (p,u)$ and their total derivatives are

$$df = \left(\frac{\partial f}{\partial t} \right)_x dt + \left(\frac{\partial f}{\partial x} \right)_t dx \quad . \tag{4-2}$$

By substituting corresponding equation (4-2) for each dependant flow parameter into (4-1) the following equation is obtained

$$\begin{aligned} &\left[\lambda_1 - \left(\lambda_1 u + \frac{\lambda_2}{\rho} \right) \frac{dt}{dx} \right] \frac{\partial p}{\partial t} + \left(\lambda_1 u + \frac{\lambda_2}{\rho} \right) \frac{dp}{dx} + \\ &\quad + \left[\lambda_2 - \left(\lambda_1 c^2 \rho + \lambda_2 u \right) \frac{dt}{dx} \right] \frac{\partial u}{\partial t} + \left(\lambda_1 c^2 \rho + \lambda_2 u \right) \frac{du}{dx} = \lambda_2 Y \end{aligned} \tag{4-3}$$

where coefficients λ_1 and λ_2 are determined from the condition that the expressions in equation (4-3) that multiply the partial derivatives of dependant variables *p* and *u* with respect to time *t* are zero. Hence, a system of two linear homogeneous equations is obtained

$$\begin{aligned} &\left(1 - u \frac{dt}{dx} \right) \lambda_1 - \frac{1}{\rho} \frac{dt}{dx} \lambda_2 = 0 \\ &-c^2 \rho \frac{dt}{dx} \lambda_1 + \left(1 - u \frac{dt}{dx} \right) \lambda_2 = 0 \end{aligned} \tag{4-4}$$

Solutions of this system will be nontrivial if and only if the determinant of the system is equal to zero

$$\begin{vmatrix} 1 - u \dfrac{dt}{dx} & -\dfrac{1}{\rho} \dfrac{dt}{dx} \\ -c^2 \rho \dfrac{dt}{dx} & 1 - u \dfrac{dt}{dx} \end{vmatrix} = 0 \tag{4-5}$$

Solutions by derivative $\dfrac{dt}{dx}$ represent the characteristic directions, i.e. characteristic equation

$$\frac{dt}{dx} = \left\{ \frac{1}{u+c}, \quad \frac{1}{u-c} \right\} \quad . \tag{4-6}$$

Replacement $\frac{dt}{dx}=\frac{1}{u+c}$ in equation (4-4) gives

$$\frac{\lambda_1}{\lambda_2}=\frac{1}{\rho c} \tag{4-7}$$

and $\frac{dt}{dx}=\frac{1}{u-c}$ in equation (4-4) gives

$$\frac{\lambda_1}{\lambda_2}=-\frac{1}{\rho c} \tag{4-8}$$

Substitution of equations (4-7) and (4-8) into equation (4-3) removes the partial derivatives of dependant variables and a system of ordinary differential equations is obtained as follows

for $\frac{dt}{dx}=\frac{1}{u+c}$,C^+ characteristic $\left(\frac{u}{\rho c}+\frac{1}{\rho}\right)\frac{dp}{dx}+\left(c+u\right)\frac{du}{dx}=Y$. (4-9)

for $\frac{dt}{dx}=\frac{1}{u-c}$,C^- characteristic $\left(-\frac{u}{\rho c}+\frac{1}{\rho}\right)\frac{dp}{dx}+\left(-c+u\right)\frac{du}{dx}=Y$. (4-10)

By substituting corresponding equation (4-6) in equations (4-9), and (4-10) it is obtained

for $\frac{dt}{dx}=\frac{1}{u+c}$, C^+ characteristic $dp+\rho cdu=\rho cYdt$ (4-11)

for $\frac{dt}{dx}=\frac{1}{u-c}$, C^- characteristic $dp-\rho cdu=-\rho cYdt$. (4-12)

Equations (4-11) and (4-12) are related to the propagation of the pressure waves. The laws of conservation of mass and momentum are resolved along C^+ and C^- characteristics.

The differentials in equations (4-11) and (4-12) are approximated by finite differences. The finite differences are taken along the typical straight lines. In this way a system of difference equations is obtained. The coefficients in equations (4-11) and (4-12) are considered to be constant during the integration time step, and their values are obtained by linear interpolation of the result of the previous calculation steps. The presentation of the calculation procedure follows.

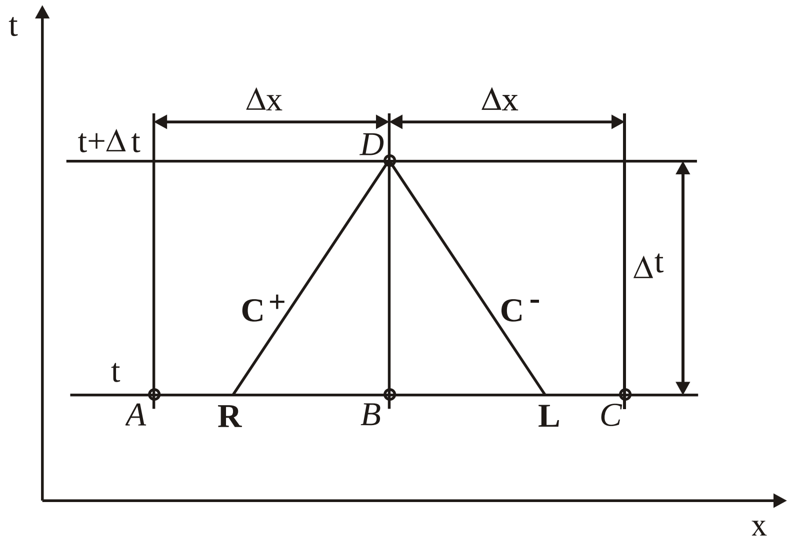

Figure 4.1 Spatial-temporal plane

Figure 4.1 shows a time instant t, which represents the initial or previous time instant, and the next time moment t+Δt. Points A, B and C are optionally selected three consecutive nodes, in the observed flow field, in which the count value depends on the variables at time t. Point D is the place in which pressure waves reaches during Δt from points **L** and **R**. Hence, at node D the two characteristic lines intersect: C^+ passing through point **R** and C^- passing through point **L**. Consequently, the point *D* represents a condition in a current area which is formed in the following point in time $t+\Delta t$ as a result of propagation of disturbances occurring at time *t*. Time step is determined from the Courant's stability criterion according to which a disturbance that starts from point R, moving with speed in $u + c$, and a disturbance that starts from point L, moving with speed $u - c$, should not exceed the point D because this would cause instability solutions. The distance along the x-axis between the nodes A and B, and B and C are identical to each other and constant over time, ie. $\overline{AB} = \overline{BC}$. Depending on variables known in all nodes in the time *t*, their values are calculated at the moment $t+\Delta t$.

By approximating the total differentials in equations (4-11) and (4-12) with finite differences along the characteristic directions, the following system of algebraic equations is obtained,

for $\frac{\Delta t}{\Delta x} = \frac{1}{u_R + c_R}$,C^+ characteristic $(p_D - p_R) + \frac{c_R}{v_R}(u_D - u_R) = \frac{c_R}{v_R} Y_R \Delta t$, (4-13)

for $\frac{\Delta t}{\Delta x} = \frac{1}{u_L - c_L}$, C^- characteristic $(p_D - p_L) - \frac{c_L}{v_L}(u_D - u_L) = -\frac{c_L}{v_L} Y_L \Delta t$, (4-14) where, $v = \frac{1}{\rho}$ is specific volume.

Solving of algebraic equations (4-13) and (4-14) provides expressions for the calculation of p_D and u_D

$$p_D = \frac{\alpha\delta + \beta\gamma}{\alpha + \beta}, \tag{4-15}$$

$$u_D = \frac{\gamma - \delta}{\alpha + \beta}, \tag{4-16}$$

where

$$\alpha = \frac{c_R}{v_R}, \tag{4-17}$$

$$\gamma = p_R + \alpha u_R + \alpha Y_R \Delta t, \tag{4-18}$$

$$\beta = \frac{c_L}{v_L}, \tag{4-19}$$

$$\delta = p_L - \beta u_L - \beta Y_L \Delta t. \tag{4-20}$$

Equations (4-15) and (4-16) provide the values of dependant variables at time t+Δt in node *D* as functions of the initial values of dependant variables at time *t* in nodes R and L. The initial values of the dependant variables are determined by linear interpolation as follows

Item **R**

$$\frac{x_B - x_R}{x_B - x_A} = \frac{u_B - u_R}{u_B - u_A}, \tag{4-21}$$

$$\frac{x_B - x_R}{x_B - x_A} = \frac{c_B - c_R}{c_B - c_A}, \tag{4-22}$$

$$\frac{x_B - x_R}{x_B - x_A} = \frac{p_B - p_R}{p_B - p_A}, \tag{4-23}$$

$$\frac{\Delta t}{x_B - x_R} = \frac{1}{u_R + c_R}. \tag{4-24}$$

Solving equations (4-21) to (4-24) by u_R, c_R and p_R it is obtained

$$u_R = \frac{(1+b)u_B - ac_B}{1+a+b}, \tag{4-25}$$

$$c_R = \frac{(1+a)c_B - bu_B}{1+a+b}, \tag{4-26}$$

$$p_R = p_B - \frac{u_B + c_B}{1+a+b}(p_B - p_A)\frac{\Delta t}{\Delta x}, \tag{4-27}$$

and

$$v_R = v_B - \frac{u_B + c_B}{1+a+b}(v_B - v_A)\frac{\Delta t}{\Delta x}, \tag{4-28}$$

where

$$a = (u_B - u_A)\frac{\Delta t}{\Delta x}, \quad b = (c_B - c_A)\frac{\Delta t}{\Delta x}. \tag{4-29}$$

Item **L**

$$\frac{x_B - x_L}{x_B - x_C} = \frac{u_B - u_L}{u_B - u_C}, \tag{4-30}$$

$$\frac{x_B - x_L}{x_B - x_C} = \frac{c_B - c_L}{c_B - c_C}, \tag{4-31}$$

$$\frac{x_B - x_L}{x_B - x_C} = \frac{p_B - p_L}{p_B - p_C}, \tag{4-32}$$

$$\frac{\Delta t}{x_B - x_L} = \frac{1}{u_L - c_L}. \tag{4-33}$$

Solving the equations (4-30) to (4-33) by u_L, c_L and p_L is obtained

$$u_L = \frac{(1+d)u_B - ec_B}{1-e+d}, \tag{4-34}$$

$$c_L = \frac{(1-e)c_B + du_B}{1-e+d}, \tag{4-35}$$

$$p_L = p_B + \frac{u_B - c_B}{1-e+d}\left(p_B - p_C\right)\frac{\Delta t}{\Delta x}, \qquad (4\text{-}36)$$

and

$$v_L = v_B + \frac{u_B - c_B}{1-e+d}\left(v_B - v_C\right)\frac{\Delta t}{\Delta x}, \qquad (4\text{-}37)$$

where

$$e = \left(u_B - u_C\right)\frac{\Delta t}{\Delta x}, \quad d = \left(c_B - c_C\right)\frac{\Delta t}{\Delta x}. \qquad (4\text{-}38)$$

Calculation of all dependent variables (p, u), as well as specific volume v, in the nodes of R and L enables the prediction of pressure and velocity in the node D according to equations (4-15) and (4-16). Specific volume of fluid in the node D is determined from the equation of state, and the local speed of sound in the fluid can be determined from the appropriate theoretical expressions or an empirical correlation for the speed of sound.

In the presented method, the spatial step, i.e. the distance between nodes, is constant. The time steps is determined by Courant criterion that provides the stability of numerical solutions

$$\Delta t \leq \min\left(\frac{\Delta x}{c_J + \left|u_J\right|}\right), \quad J = 1, 2, \ldots, n, \qquad (4\text{-}39)$$

wherein the minimum time step, for a given value of spatial step Δx, is determined by the maximum value of the sum of the speed of sound and the absolute value of the fluid velocity.

4.2 Boundary conditions

Boundary conditions are defined for the pipe inlet and outlet. In case of the pipe inlet the C^+ characteristic path in (Fig. 4.1) and corresponding characteristic equation (4-13) are not defined, while in case of the pipe outlet C^- characteristic path (Fig. 4.1) and equation (4-14) are not defined. These undefined characteristic equations are replaced by time functions $u = u(t)$ or $p = p(t)$, which should be derived from hydraulic conditions that define the transient flow problem. These hydraulic conditions might be related to gas inlet and/or outlet mass flow rates, a valve opening or closing, a leakage to the atmosphere in case of a break, a junction to the compressor, etc. A boundary condition inside a pipe network is a junction of two or more pipes (Fig. 4.2) and it is derived as follows. The pipes that transport fluid towards the junction node D in (Fig. 4.2) are denoted with J_i, while the pipes that transport fluid from the node *D* are denoted with I_j. The characteristic equations in J_i pipes can be written for C^+ paths from point R to node *D* (Fig. 4.1) as follows

$$p_D + \alpha_{R,J_i} u_{D,J_i} = \gamma_{R,J_i}, \; i = 1, 2, ...n \tag{4-40}$$

The characteristic equations in I_j pipes can be written for C^- paths from point L to node *D* (Fig. 1) in the following form

$$p_D - \beta_{L,I_j} u_{D,I_j} = \gamma_{L,I_j}, \; j = 1, 2, ...m \tag{4-41}$$

The mass balance equation is added for the node *D*

$$\sum_{i=1}^{n} \rho_D u_{D,J_i} A_{J_i} = \sum_{j=1}^{m} \rho_D u_{D,I_j} A_{I_j} \tag{4-42}$$

The velocities u_{D,J_i} and u_{D,I_j} are expressed from equations (4-40) and (4-41)

$$u_{D,J_i} = \frac{\gamma_{R,J_i} - p_D}{\alpha_{R,J_i}} \tag{4-43}$$

$$u_{D,I_j} = \frac{p_D - \delta_{L,I_j}}{\beta_{L,I_j}} \tag{4-44}$$

Finally, equations (4-43) and (4-44) are introduced into equation (4-42) and the explicit expression is obtained for the calculation of pressure in node D

$$p_D = \left(\frac{\sum_{i=1}^{n} \frac{\rho_D A_{J_i}}{\alpha_{R,J_i}} + \sum_{j=1}^{m} \frac{\rho_D A_{I_j}}{\beta_{L,I_j}}}{\sum_{i=1}^{n} \frac{\rho_D \gamma_{R,J_i} A_{J_i}}{\alpha_{R,J_i}} + \sum_{j=1}^{m} \frac{\rho_D \delta_{L,I_j} A_{I_j}}{\beta_{L,I_j}}} \right)^{-1} \tag{4-45}$$

After calculating the pressure in the junction node D with equation (4-45), the velocities in cross sections at pipe ends towards the junction node D are calculated with equations (4-43) and (4-44). The density in the node D in the new time $t + \Delta t$ is approximated with the density at the same location but from the initial time t, i.e. $\rho_D \approx \rho_B$, in order to avoid iteration in calculation process.

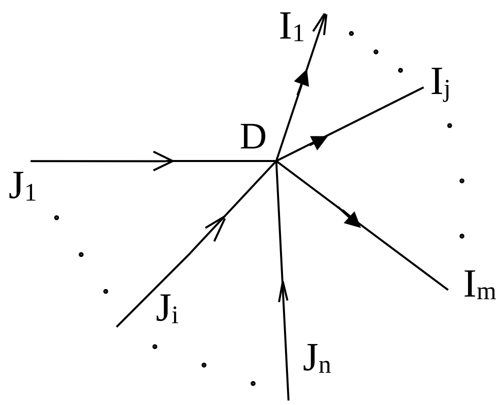

Figure 4.2 Pipes in a junction

4.3 Flowchart of the calculation process

The calculation flowchart of the GTA code is developed in a way to enable defining the pipe network and appropriate boundary conditions by input parameters. The flowchart is shown in Figure 4.3. The inlet and outlet pipe boundary conditions are defined by G(A,J) matrix, where A=1,2 denotes the pipe inlet and outlet respectively and *J*=1,2,…n denotes the pipe number. The value of matrix element G(A,J) denotes a type of the predefined boundary condition. The solution procedure is shown in figure 4.3.

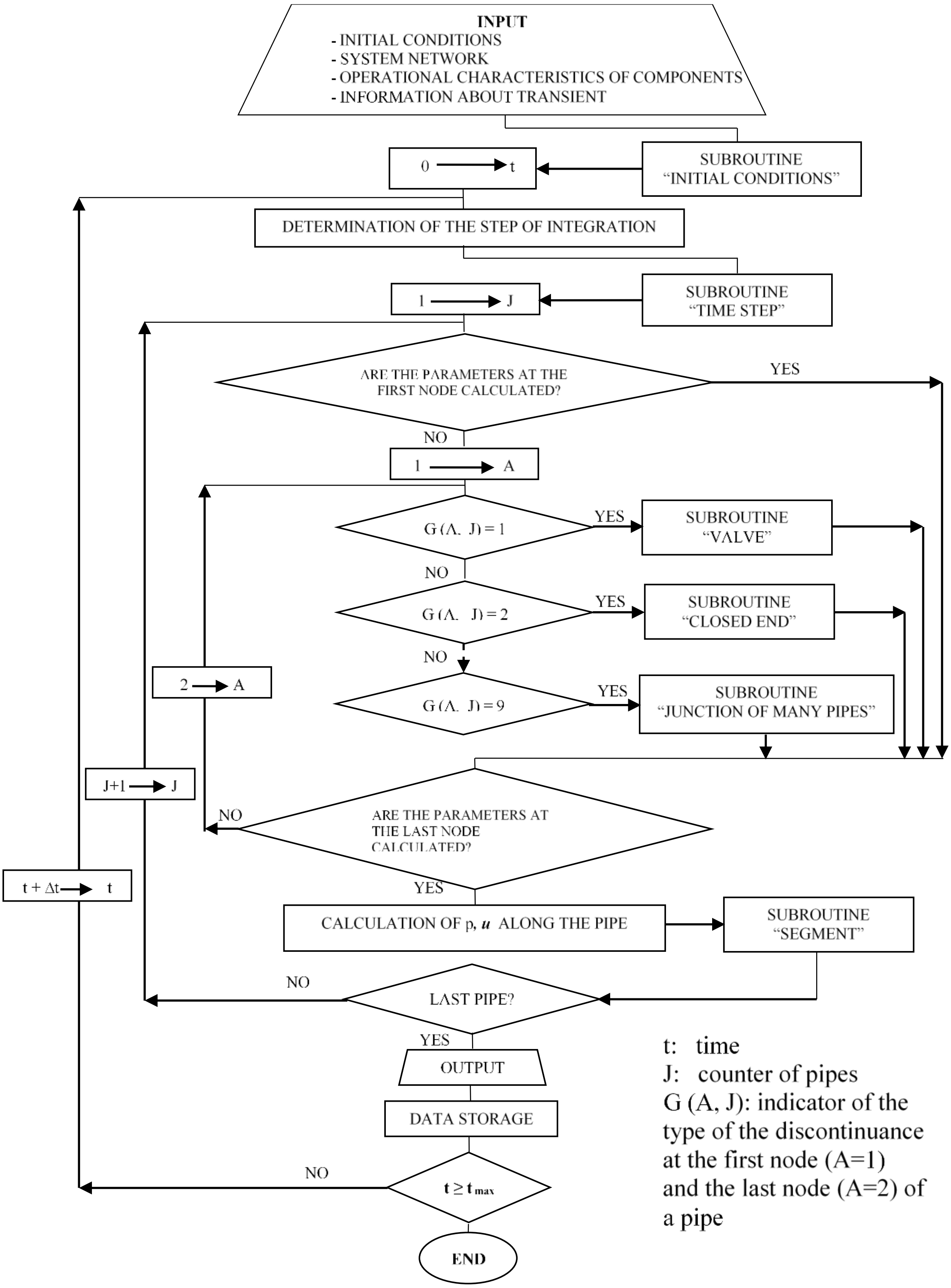

Figure 4.3 Flowchart of the calculation procedure

CHAPTER 5

CODE VALIDATION

In this chapter, the developed model and the GTA code for the simulation and analyses of gas pipeline transients are validate. Four cases are applied from the open literature as the benchmark experiments for the validation of the developed model and code GTA. Here presented results are published in [96].

5.1 Case 1

A natural gas transient in a single pipeline of 8000 m length and with 0.406 m diameter is numerically simulated. The pipeline has the upward elevation of 1 m in the flow direction. The natural gas temperature is 300 K, the specific gravity is 0.675 and the viscosity is 10^{-5} kg/(ms). The pipeline wall roughness is 0.046 mm. The gas flow rate varies at the pipeline's outlet due to the consumer's demand with a period of 6000s, as depicted in figure 5.1. The volumetric flow rate in figure 5.1 is presented in million metric standard cubic meters per day (MMSCmD). The gas pressure at the pipeline's inlet is constant during the transient and its value is 6 MPa.

The transient is simulated with the presently developed Gas Transients Analysis (GTA) code. In order to investigate the numerical calculation sensitivity on the numerical grid refinement, the pipe length is discretized with a small number of 9 nodes, as well as with a much greater number of 161 nodes, i.e. the simulations were performed with uniform distances between two adjacent numerical nodes of 1000 m and 50 m respectively.

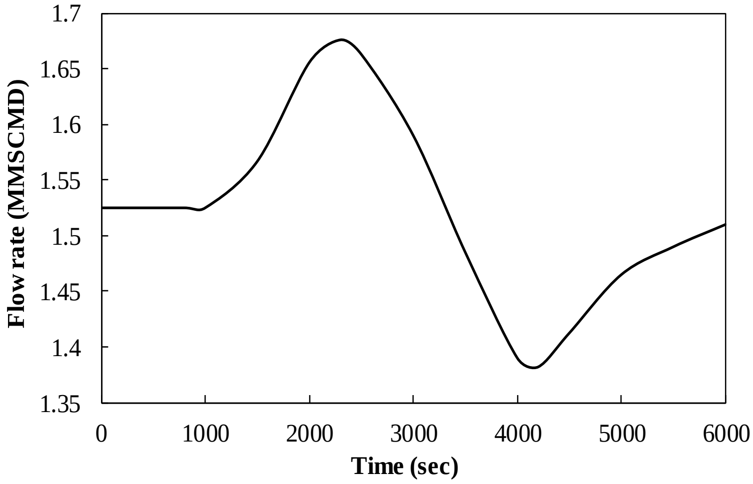

Figure 5.1: Specified volume flow rate at the pipeline outlet (Case1)

The obtained results are shown in figure. 5.2 and compared with the previously reported numerical results of Reddy et al. (2006) [55] and Alamian et al. (2012) [56]. The calculated inlet flow rate in figure 5.2 shows the same trend and values as the prescribed outlet flow rate in figure 5.1. These results indicate that during this long lasting transient the gas flow rate along the pipeline, from the inlet to the outlet, is nearly constant in every time instant, although, as shown, it changes with time. A very good agreement of GTA code results with the results of Reddy et al. (2006) [55] and Alamian et al. (2012) [56] is achieved.

A grid refinement tests were performed and the pipeline length was discretized with 9, 41, 81 and 161 nodes. Practically the same results are obtained in all these tests. The results obtained with the minimum number of 9 nodes and the maximum 161 nodes are presented in figure 5.2. It is shown that a coarse numerical grid with the distance of 1000 m between two adjacent nodes is sufficient for an accurate calculation. Such an accurate calculation with a coarse grid is possible due to the relatively short distance of the pipeline and the low gas velocity. The gas velocity along the pipeline is approximately 2.4 m/s and the pressure drop along the pipeline is lower than 0.05 MPa. Due to the low pressure change there is no influence of the gas compressibility, there is no nonlinearity caused by the gas density change, and the accurate simulation is obtained by applying the coarse grid. The time step of numerical integration is calculated according to the Courant criterion equation (4-39) and its value is approximately 2.56 s in the case with the spatial discretization with 9 nodes.

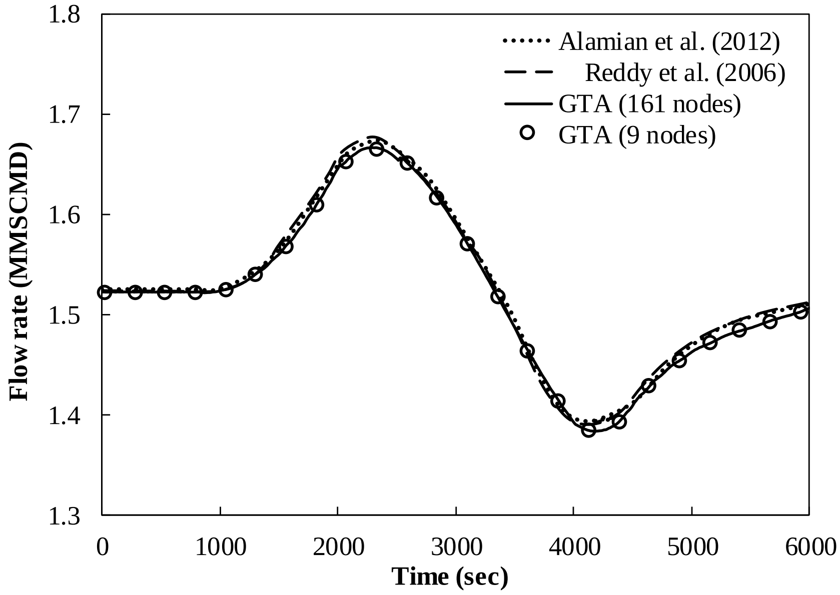

Figure 5.2: Calculated volume flow rates at the pipeline inlet (Case 1)

5.2 Case 2

This transient was previously numerically simulated by Taylor et al. (1962) [45], Zhou and Adewumi (1997) [37], Tentis et al. (2003) [64], Behbahani-Nejad and Bagheri (2008) [97] and Alamian et al. (2012) [56]. A single pipeline with the length of 72,259.5 m, the diameter of 0.2 m and the pipeline wall roughness of 0.617 mm transports natural gas. The gas pressure at the pipeline inlet is constant at 4.205 MPa. The flow is isothermal at 283 K. The specific gravity of gas is 0.675, the viscosity is 1.1831×10^{-5} kg/(ms) and the isothermal speed of sound is equal to 367.9 m/s. At the pipeline outlet the mass flow rate varies within a 24-h cycle according to consumer's daily demand changes, as shown in figure 5.3. The mass flow rate shown in figure 5.3 specifies the boundary condition at the pipeline outlet and it is the input into the simulation.

The transient was simulated with the GTA code that is developed in this presented thesis. The pipeline was discretized with 371 nodes. Further grid refinement by increasing the number of nodes provided practically the same results.

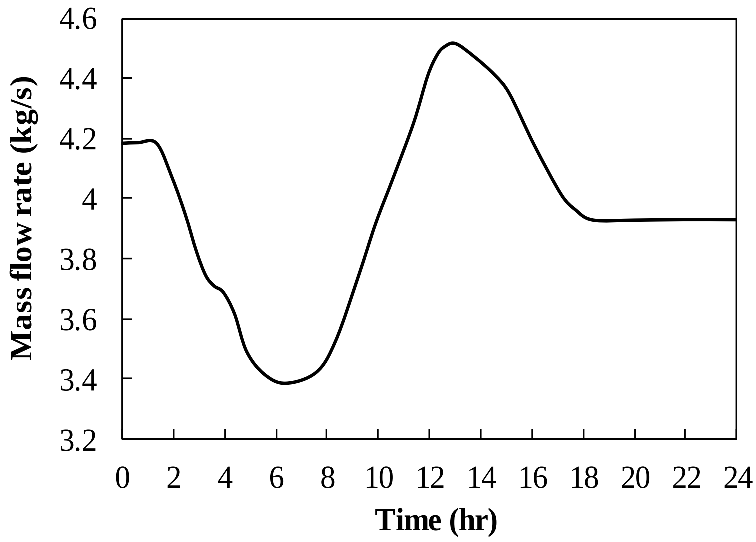

Figure 5.3: Specified daily change of the mass flow rate at the pipeline outlet (Case 2)

The calculated pressure at the pipeline outlet is shown in figure 5.4. As presented, the GTA code results are in agreement with the previously published results. The flow rate decrease in the period from 1.4 h to 6.8 h (Fig. 5.3) leads to the pressure increase at the pipeline outlet (Fig. 5.4), where the maximum pressure is reached after 8 hours. This delay of the maximum pressure occurrence compared to the time of minimum flow rate at the pipeline outlet for approximately 1.2 hours indicates an accumulation of gas and an inertia effect of the accumulated gas mass along the pipeline during the period of decreased gas flow rate from the pipeline. A similar delay is observed for the period of gas flow rate increase at the pipeline outlet.

The maximum gas flow rate at the pipeline outlet is reached after 13 hours, while the minimum pressure is reached after 15 hours. Again, the delay of minimum pressure occurrence after the maximum flow rate at the pipeline outlet is attributed to the gas accumulation in the pipeline and inertia of the gas mass along the pipeline. After 18.7 hours the gas flow rate at the pipeline outlet remains constant (Fig. 5.3). A certain discrepancy between measured and calculated data is shown.

The measured maximum pressure is higher for approximately 0.1 MPa than the calculated values after 8 hours (Fig. 5.4). The measured pressure at the outlet is nearly constant after 16 hours as shown in figure 5.4, while numerical results show transient behaviour in this period. These discrepancies are attributed to the uncertainty in the specification of the pipeline boundary flow in figure 5.3 (it might be questioned whether the gas flow rate is constant for the last five hours (in the period from 19 till 24 hours) or there is a certain decrease of the flow rate).

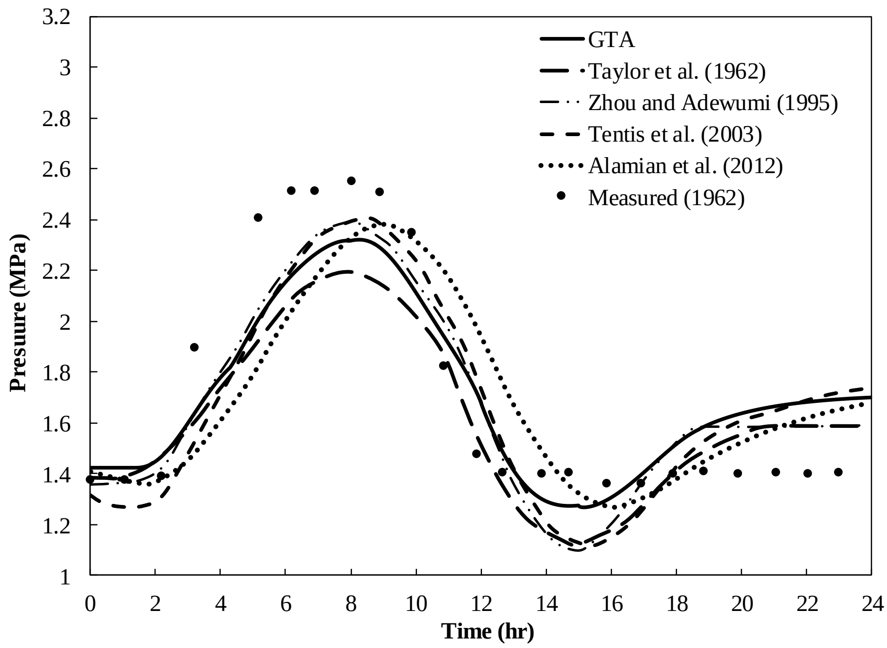

Figure 5.4: Calculated pressure at the pipeline outlet (Case 2)

5.3 Case 3

The ability of the GTA code to predict transients in gas pipeline networks is validated by a simulation of transient in the gas network shown in figure 5.5.

Dimensions of three pipelines that form the network are presented in Table 5.1. The gas specific gravity is 0.6, the operational temperature is 278 K, and the friction factor is considered to be constant and equal to 0.003.

Table 5.1: Dimensions of the pipelines in the gas network (Case 3)

Gas Pipe	**Diameter (m)**	**Length (km)**
1	0.6	80
2	0.6	90
3	0.6	100

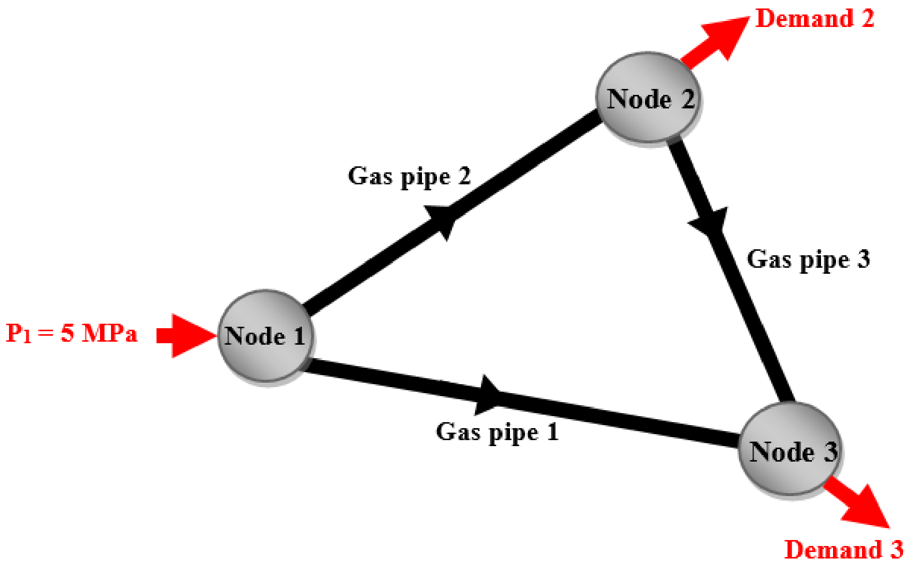

Figure 5.5: Gas pipeline network (Case 3)

Gas flows into the network at node 1 with the constant pressure of 5 MPa. Gas outflows from the network at nodes 2 and 3 with flow rates specified by figure 5.6.

The GTA code results are compared in figures 5.7 and 5.8 with numerical results obtained by Osiadacz (1987) [51], Ke and Ti (1999) [98], Behbahani-Nejad and Bagheri (2008) [97] and Alamian et al. (2012) [56].

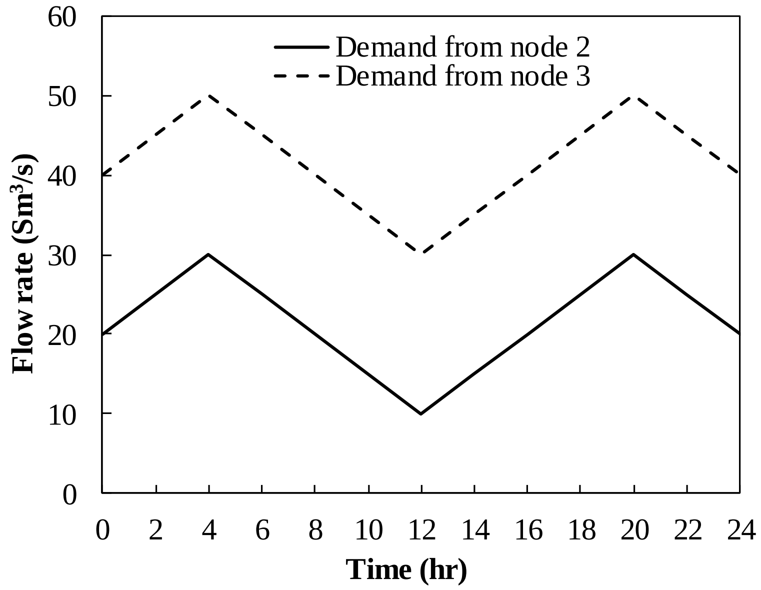

Figure 5.6: Gas demand versus time for nodes 2 and 3 of the simulated network (Case 3)

As shown in figures 5.7 and 5.8, the GTA code results are in agreement with the results of other researchers.

In the periods of increased gas demands from nodes 2 and 3 the pressure in these nodes decreases, while in the periods of decreased gas demands from nodes 2 and 3 the pressure in these nodes increases as illustrated in figures 5.7 and 5.8 respectively. The time instants when the maximum and minimum pressures are reached in nodes 2 and 3, as shown in figures 5.7 and 5.8, are delayed for about 0.3 hours to 0.5 hours compared to time instants of outlet gas flow rates changes from nodes 2 and 3 at 4 hours, 12 hours and 20 hours from the beginning of transient, as shown in figure 5.6. This effect is attributed to the accumulation and inertia of gas mass in long pipelines 1, 2 and 3. The GTA code results are obtained with the uniform distance of 2000 m between the numerical nodes along all three pipelines, i.e. the number of numerical nodes is 41, 46 and 51 in gas pipelines 1, 2 and 3 respectively.

The time step of integration is approximately 5.2 s, as predicted with equation (4-39).

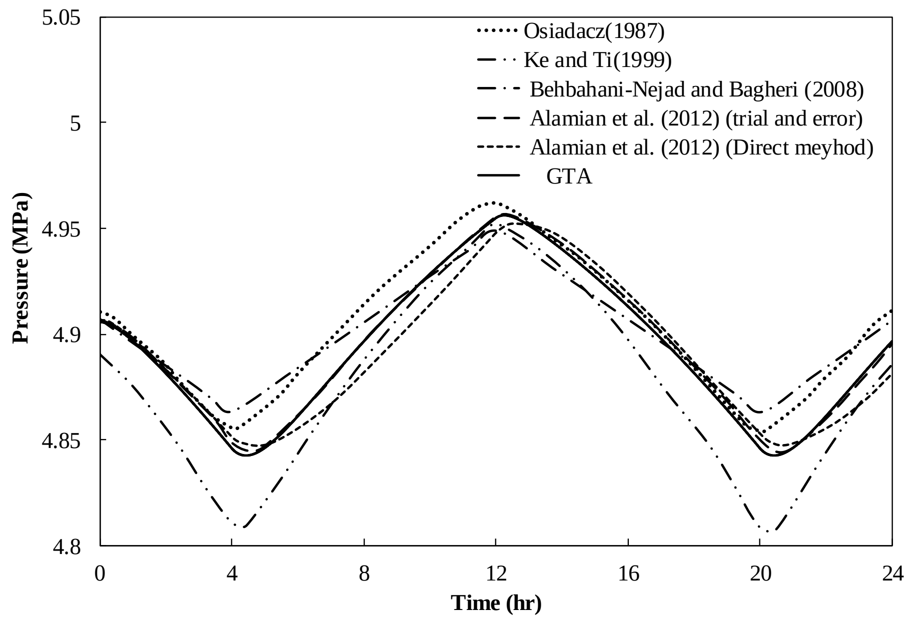

Figure 5.7: Calculated pressure in node 2 of the network (Case 3)

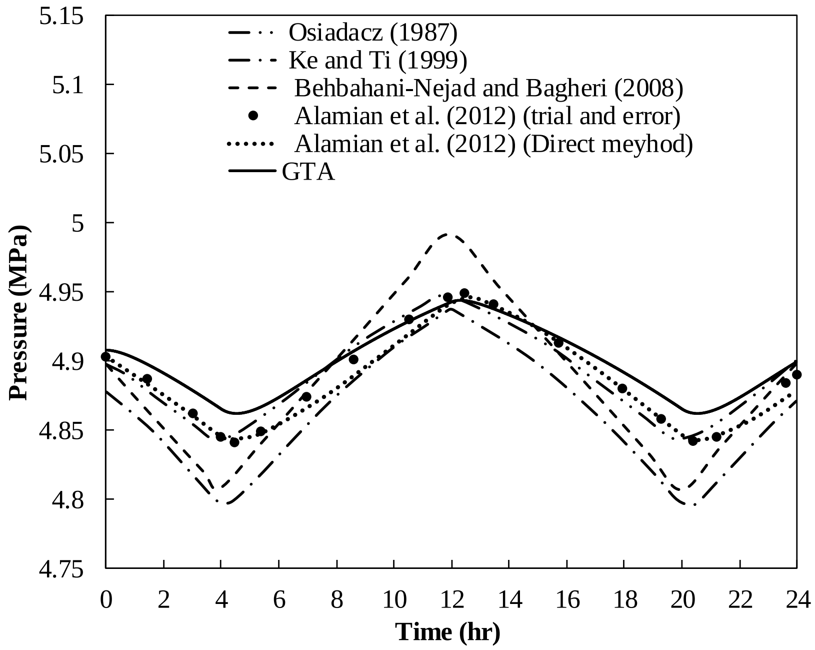

Figure 5.8: Calculated pressure in node 3 of the network (Case 3)

5.4 Case 4

A gas transient takes place in a gas pipeline with a length of 91.44 m and an inner diameter of 0.61 m. The initial gas pressure in the pipeline is 4.136 MPa, the sonic wave speed is 348.1 m/sec, and the friction factor is 0.03. The gas specific gravity is 0.67. The downstream pipeline end is closed during the whole transient, while the upstream inflow begins to increase linearly from zero and reaches 17 MMSCMD (millions of standard meter cubic per day) at 0.145 s, then decreases again linearly and reaches zero at 0.29 s. Figure 5.9 shows schematically this study case along with its boundary conditions.

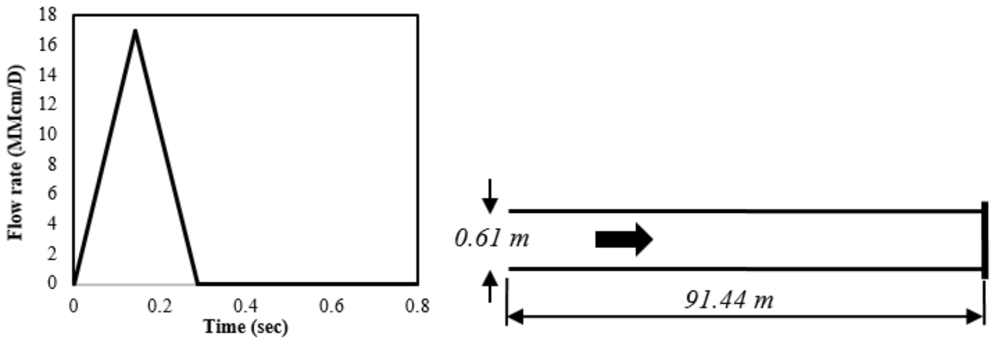

Figure 5.9: Boundary conditions and geometry of the pipeline in Case 4

Numerical results of previous simulations of this case were reported Zhou and Adewumi (1996) [80] and Behbahani-Nejad and Shekari (2010) [83], and presently by the usage of the GTA code.

Measured and calculated pressure changes at the closed end of the pipeline are shown in figure 5.10. The pressure change has the same shape as the inlet flow rate change. The pressure pulse reaches the closed end after approximately 0.26 s. This time period is determined by the sonic velocity of the gas and the pipeline length (91.44 [m]/348.1 [m/s] = 0.26 [s]).

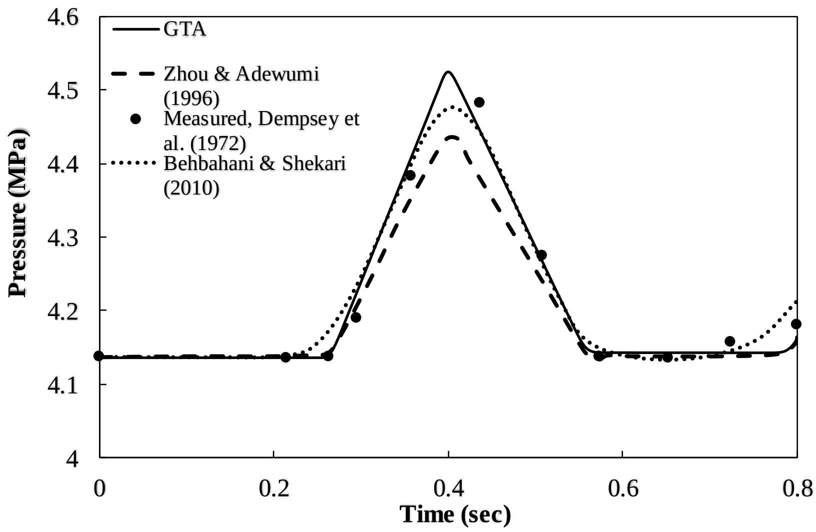

Figure 5.10: Pressure history at the outlet of the pipeline (Case 4)

The pressure change at the pipeline inlet is shown in figure 5.11. The inlet pressure increases with the gas inlet flow rate increase, and decreases with the inlet flow rate decrease. The inlet pressure increases for approximately 0.2 MPa. This amplitude is approximate to the value determined by the Joukowsky equation

$$\Delta p = \rho c \Delta u \quad (5\text{-}1)$$

where change of pressure Δp is equal to the product of density ρ, speed of sound c, and change of velocity Δu. Namely, the inlet gas velocity increases from zero to 16.2 m/s, the gas density at 4.15 MPa is 28 kg/m3, and taking into account the above reported sonic velocity of 348.1 m/s, the pressure pulse of 0.16 MPa is obtained. The amplitude of the pressure increase at the closed pipe end is approximately 0.4 MPa, which is two times greater than the amplitude at the pipeline inlet due to the pressure wave rarefaction at the rigid pipeline closed end. This greater pressure amplitude reaches later on the pipeline inlet at 0.65 s.

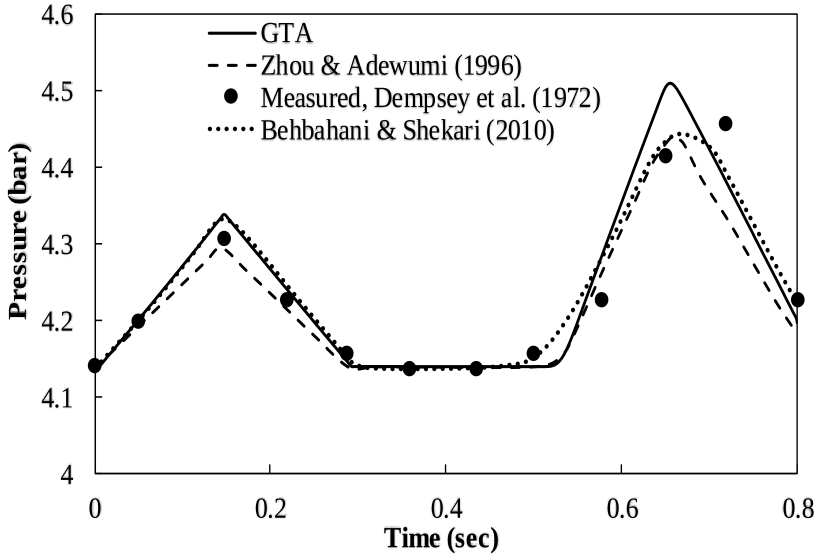

Figure 5.11: Pressure history at the inlet of the pipeline (Case 4)

The gas flow rate change at the half length of the pipeline is shown in figure 5.12, and it is determined by the compression pressure wave propagation along the pipeline. The presented GTA code results are obtained with 101 numerical nodes along the pipeline, while the influence of the number of numerical nodes is presented in figure 5.13. As shown, there is no practical difference between results obtained with 51 and 101 nodes.

The time step of integration in case with 101 nodes is approximately 0.0025 s according to equation (4-39).

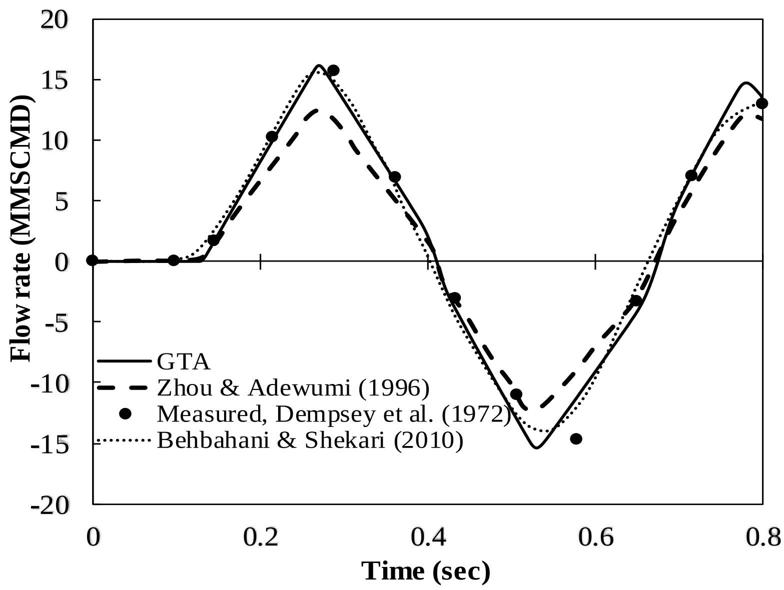

Figure 5.12: Gas volume flow rate at the pipeline midpoint (Case4)

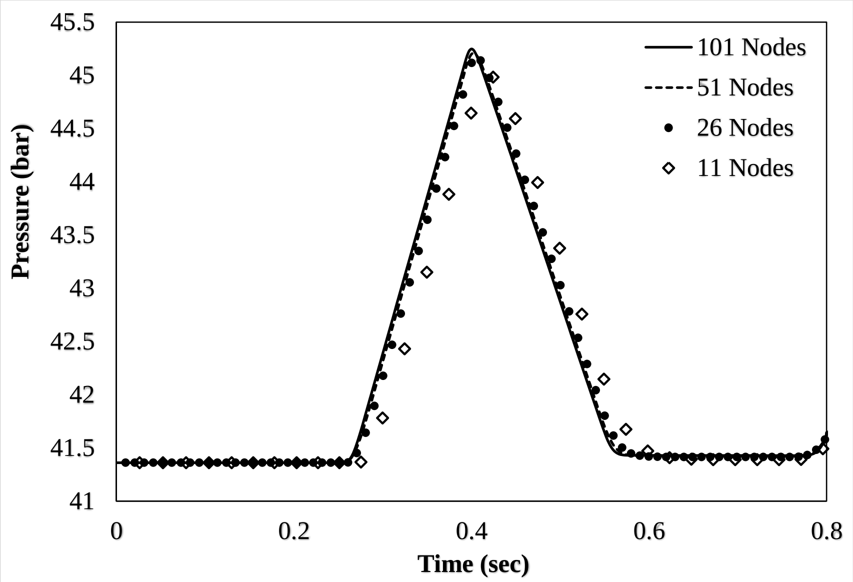

Figure 5.13: Pressure history at the pipeline closed end obtained with different number of numerical nodes (grid refinement test for Case 4)

5.5 Conclusion remarks

The GTA code is validated by computer simulations of transient cases reported in the literature. The simulated cases include transients caused by the variable gas consumption and boundary pressure pulses.

It is shown that the calculation procedure is numerically stable and the good agreement is obtained between the GTA code results and the previous published results. The presented model derivation and analysis of validation results show that the applied method is relatively easily implemented in the computer code, the calculation procedure is robust and the reliable simulations are obtained for both slow and fast gas pipeline transients.

CHAPTER 6

TRANSIENT BEHAVIOR OF A LONG TRANSMISSION GAS PIPELINE

The GTA code was used to analyse the behaviour of natural gas transient flow in long transmission pipeline. Real natural gas transmission pipeline in Libya was taken for studying, and some scenarios were assumed and simulated to predict the gas flow parameters to investigate its behaviour. Also here, the presented results are published in reference [96].

6.1 Analyses of transient behaviour of gas pipeline of the Western Libya Gas Project

The developed GTA code was applied to the analysis of transients in the onshore gas transmission pipeline of the Western Libya Gas Project shown in figure 6.1 below [99].

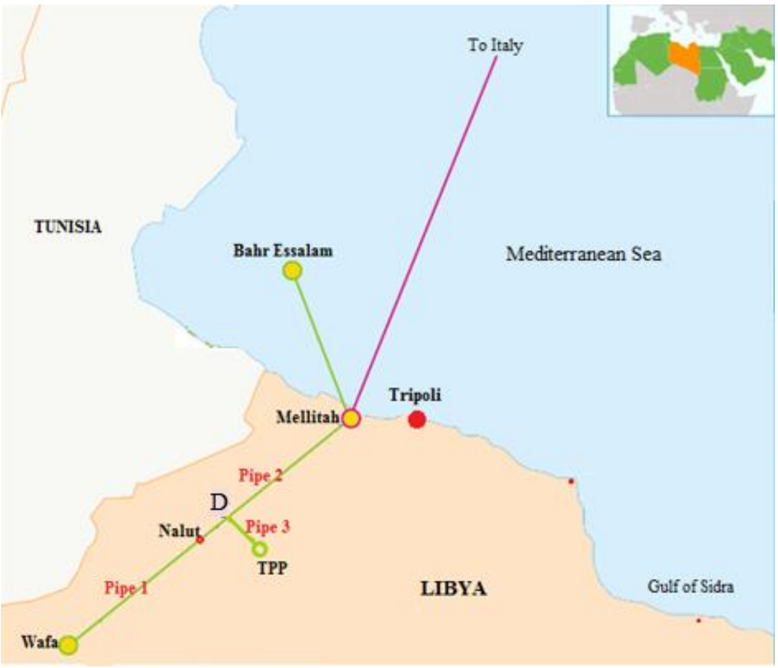

Figure 6.1 Main gas pipeline of the Western Libya Gas Project

The gas inlet to the main transmission gas pipeline is at the Wafa Desert Plant with gas wells, which is located at the 329 meters above the sea level (MASL). The pipeline extends to the Mellitah Complex at the sea coast. The pipeline length from Wafa to Mellitah is 525 km and the diameter is 0.8128 m (32 in). At the distance of 370 km from the gas inlet at Wafa, there is junction with a branch line (depicted as the junction D in Fig. 6.1) that is 5 km long and has the diameter of 0.4064 m (16 in). This branch transport gas to the Ar Ruways Gecol Thermal Power Plant (TPP) at 245 MASL. The highest elevation of the pipeline of 632 MASL is near the Nalut city. From Nalut to Mellitah at the sea level the pipeline elevation steadily decreases. The maximum total delivery of the pipeline from Wafa Desert Plant is about 530,000 Sm^3/h of gas. The design delivery to the Ar Ruways Gecol[3] TPP is 212,520 Sm^3/h, which is based on the maximum TPP capacity [99]. Based on the field data, the gas pressure and temperature at the pipeline inlet at Wafa are 6.4 MPa and 315 K. The gas viscosity is 1.71×10-5 kg/(ms) and the specific gravity is 0.67. The gas temperature at the outlet in the Mellitah Complex is about 300 K.

Gas Transient Analysis code simulations results are first compared to the real plant data for the period of 12 hours operation on the 31st of July 2017. In the presented simulation the pipeline from Wafa Desert Plant to the junction with the branch towards the TPP is denoted as pipeline 1, from the junction to the Mellitah Complex as pipeline 2 and the branch towards the TPP as pipeline 3. The inlet pressure at Wafa and outlet volume flow rates at the Mellitah Complex and the TPP are specified according to the measured data presented in figures 6.2 and 6.3.

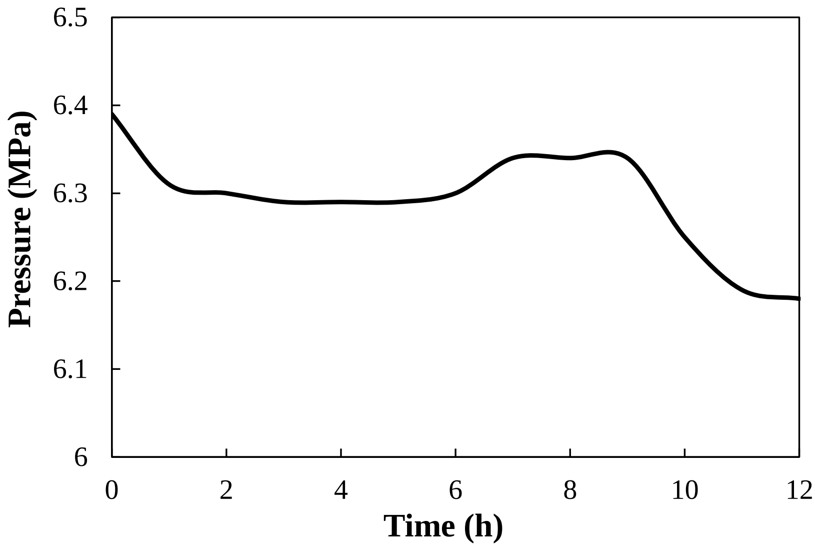

Figure 6.2 Measured pressure at the main gas pipeline inlet in the Wafa Desert Plant

[3] GECOL: General Electricity Company of Libya.

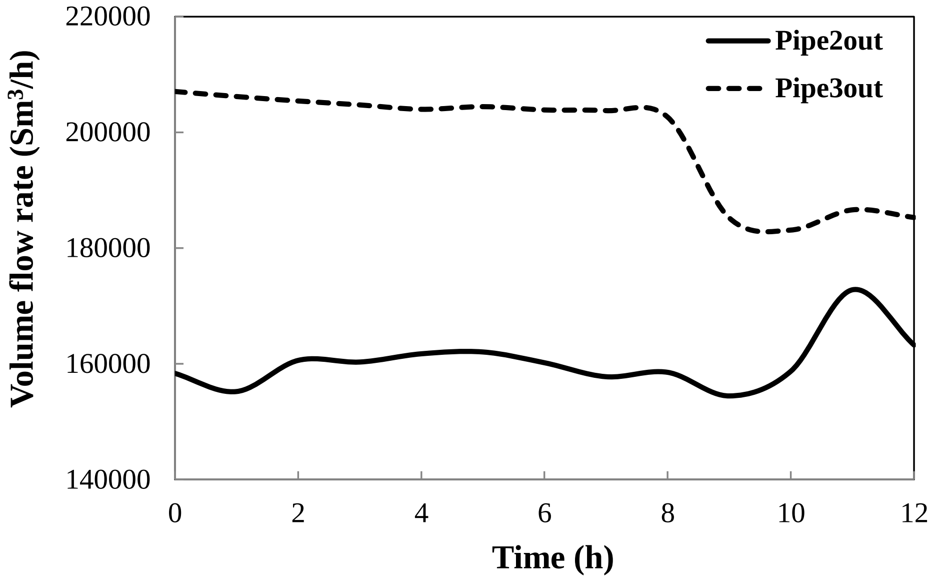

Figure 6.3 Measured volume flow rates at the delivery outlets in the Mellitah Complex and in the Ar Ruways Gecol TPP

The calculated pressure at the Mellitah Complex is compared with measured values in figure 6.4. The calculated values show the increase of pressure during the first hour, which is the result of the measured gas flow rate decrease at the pipeline outlet in the Mellitah Complex that is shown in figure 6.3 (Pipe 2 out). The measured pressure shows a decrease during the first hour in figure 6.4.

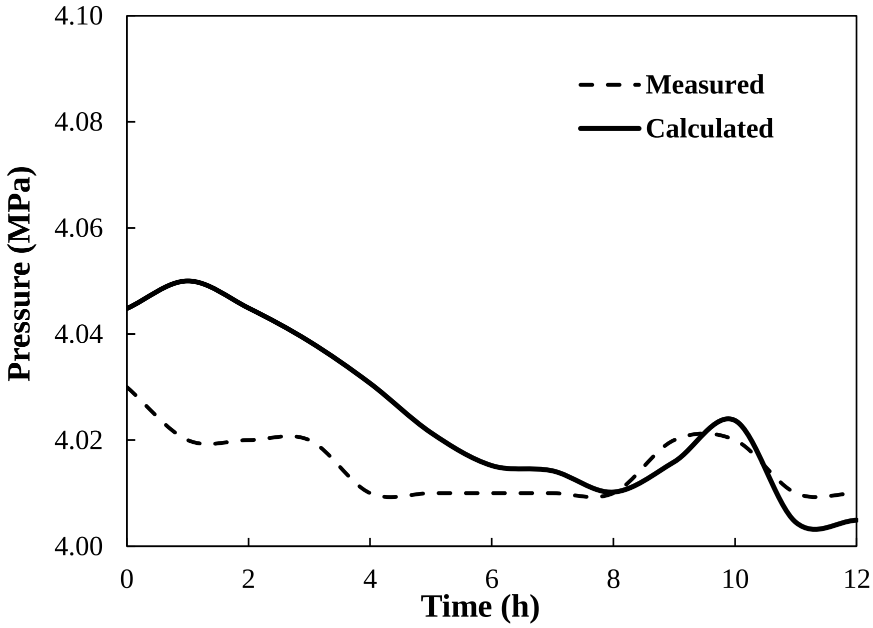

Figure 6.4 Measured and calculated pressure at the transmission pipeline outlet in the Mellitah Complex

This discrepancy between calculated and measured data is attributed to the permanent weak fluctuations of the gas pressure and flow rate during long transmission pipeline operation, which is not taken into account by the prediction of the initial condition of the pipeline (the initial condition is calculated as the steady-state condition, since the actual distribution of pressure and flow rate along the pipeline is not recorded).

In the later period between 1 and 8 hours both calculated and measured values show the pressure decrease. In the period between 8 and 9 hours the gas flow rate decreases at the outlet in the Mellitah Complex (Fig.6.3) and both measured and calculated values show the pressure increase (Fig.6.4) due to this gas flow rate change. In the period between 10 and 11 hours the gas flow rate at the outlet in the Mellitah Complex increases (Fig.6.3) and this leads to the pressure decrease as shown in Fig.6.4 by both measured and calculated values. The maximum difference between these values is lower than 0.02 MPa and the calculated pressure transient behaviour is in the complete agreement with measured behaviour in the period when the influence of the uncertainty of the initial condition is diminished.

Further work was directed towards investigation of gas pipeline transport capacity in transients caused by a trip of gas source at Wafa Desert Plant and by a trip of gas delivery at the TPP and the Mellitah Complex.

6.1.1 Scenario 1

The trip of the gas supply in Wafa Desert Plant is assumed. As presented in figure 6.5 the gas supply in Wafa Desert Plant is constant for 2 hours and then suddenly stops. The gas delivery in the Mellitah Complex and to the TPP is kept constant at the initial level that corresponds to the nominal operation. These flow rates are specified boundary conditions for this simulation.

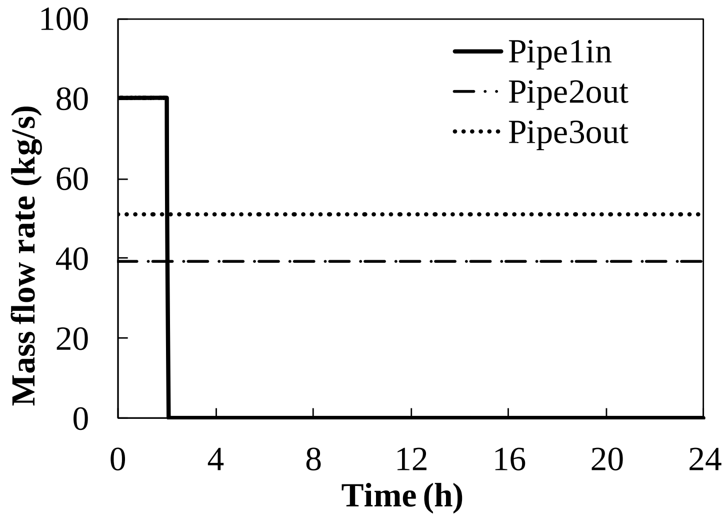

Figure 6.5 Flow rate behaviour in the gas pipeline of the Western Libya Gas Project during the gas supply trip

Calculated pressure values are shown in figure 6.6. The pressure at the main pipeline inlet at Wafa Desert Plant is denoted as (Pipe 1in) as in figure 6.6. The pressure in the junction D (Fig.6.1) equals the pressure at the outlet of Pipe 1 and inlets of Pipe 2 and Pipe 3, as presented in figure 6.6 (Pipe1out = Pipe2in = Pipe3in). The pressures at the outlet in the Mellitah Complex and at the outlet in the TPP are denoted as (Pipe 2out and Pipe 3out) in figure 6.6. All these pressure values are constant for the first 2 hours till the gas supply trip.

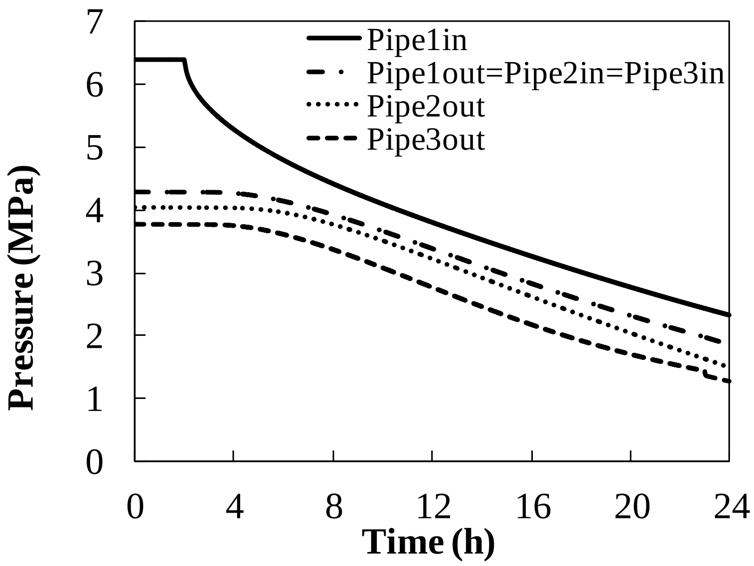

Figure 6.6 Pressure history in the gas pipeline of the Western Libya Gas Project during the gas supply trip

Later on, the pressure level in the whole pipeline system decreases, but during the whole simulated transient the pressure is the highest at the inlet in Wafa Desert Plant and gradually decreases along the pipeline to the junction D (Fig.6.1). The pressure also drops from the junction D towards the TPP and the Mellitah Complex. Although there is a pressure drop along the transmission pipeline, the required delivery flow rates at the TPP and at the Mellitah Complex are sustained for a period even longer than 24 hours, which is a result of the gas accumulation in the large volume of the main gas pipeline.

6.1.2 Scenario 2

In the second simulated scenario the gas delivery stops at the Mellitah Complex after one hour, while the gas pressure at the pipeline inlet in Wafa desert plant and the gas delivery to the TPP are kept constant at the initial value. The mass flow rates in the pipeline system are presented in figure 6.7. All flow rates are constant during the first hour. Later on, the mass flow rate at the transmission pipeline inlet in the Wafa Desert Plant gradually decreases (denoted as (Pipe1in) as in Fig.6.7). Although the delivery flow rate in the Mellitah Complex is stopped after 1 hour, the decreasing flow rate at the inlet of pipeline 2 (denoted as (Pipe2in) as in Fig.6.7) still exists in the long period of 11 hours after the outlet flow stoppage due to the pressure increase and the gas accumulation.

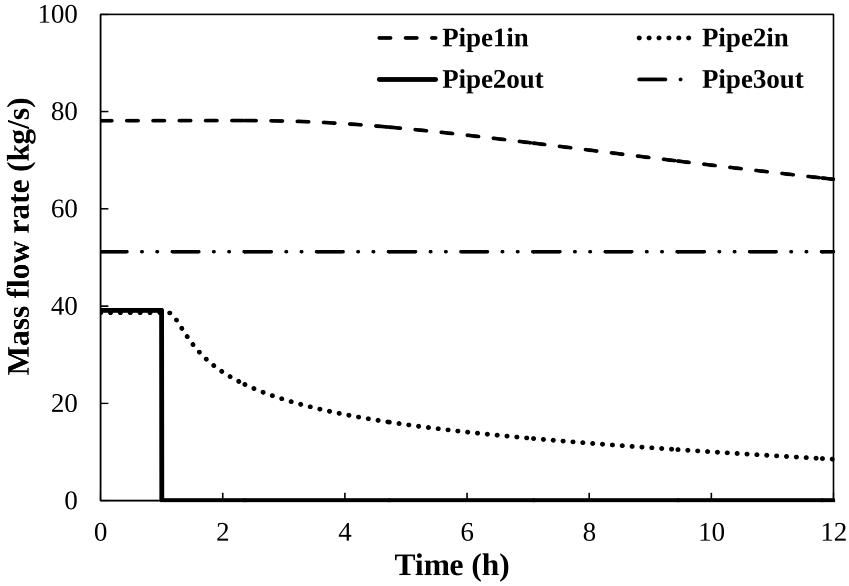

Figure 6.7 Flow rate behaviour in the gas pipeline of the Western Libya Gas Project during the trip of gas delivery to the Mellitah Complex

The pressure history during the transient is shown in figure 6.8. The gas pressure at the pipeline inlet in the Wafa Desert Plant is kept constant at 6.4 MPa. Within one hour after the trip of the gas delivery in the Mellitah Complex the gas pressure from the junction D (Fig.6.1) towards the Mellitah Complex is practically equal. The pressure drop from the junction D towards the TPP exists due to the gas delivery to the TPP and this pressure drop is practically constant because of the constant mass flow rate. The pressure increase within the whole pipeline system indicates gas accumulation.

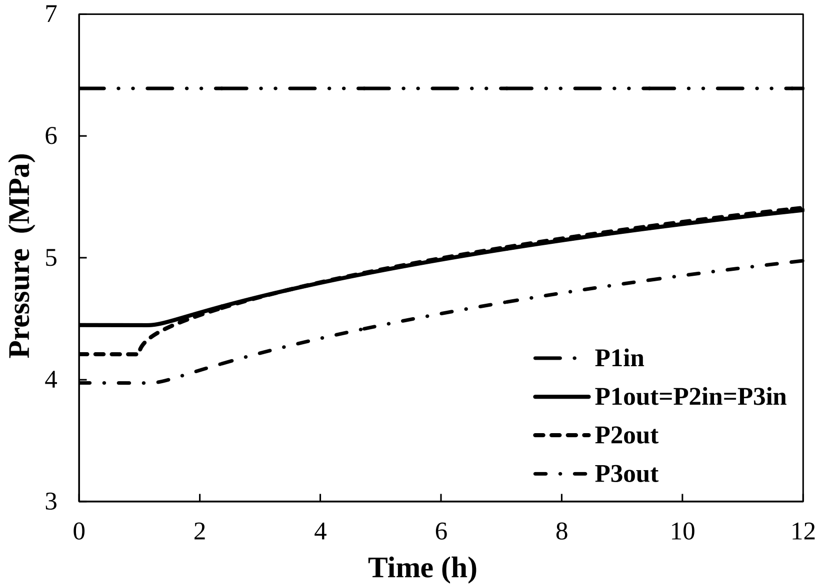

Figure 6.8 Pressure history behavior in the gas pipeline of the Western Libya Gas Project during the trip of gas delivery to the Mellitah Complex

6.1.3 Scenario 3

A trip of gas delivery both in the Mellitah Complex and in the TPP is assumed in the third simulated scenario. The flow rate change within the pipeline system is shown in figure 6.9.

It is shown that although the whole gas delivery is stopped, there is still a gas inflow at the inlet point of the transmission pipeline at the Wafa Desert Plant due to the gas packing and pressure increase, as shown in figure 6.10. Due to the short length of the pipeline branch towards the TPP of 5 km, compared to the length of the main pipeline of 525 km, the flow in the branch almost instantaneously stops with the delivery trip at the TPP.

The pressure history during the transient in figure 6.10 shows that the pressure values at the junction D (Fig.6.1) with the branch towards the TPP and at the pipeline outlet in the Mellitah Complex become practically equal about five hours after the trip of gas delivery, while in the pipeline branch towards the TPP, inlet and outlet pressure values are momentary equal and governed by the pressure in the junction D.

Although the pressure within the whole pipeline system reaches the main pipeline inlet pressure in the Wafa Desert Plant after 12 hours, the inlet flow rate at the Mellitah Complex still exists after this period due to the inertia of the gas mass within the long distance main pipeline of large volume.

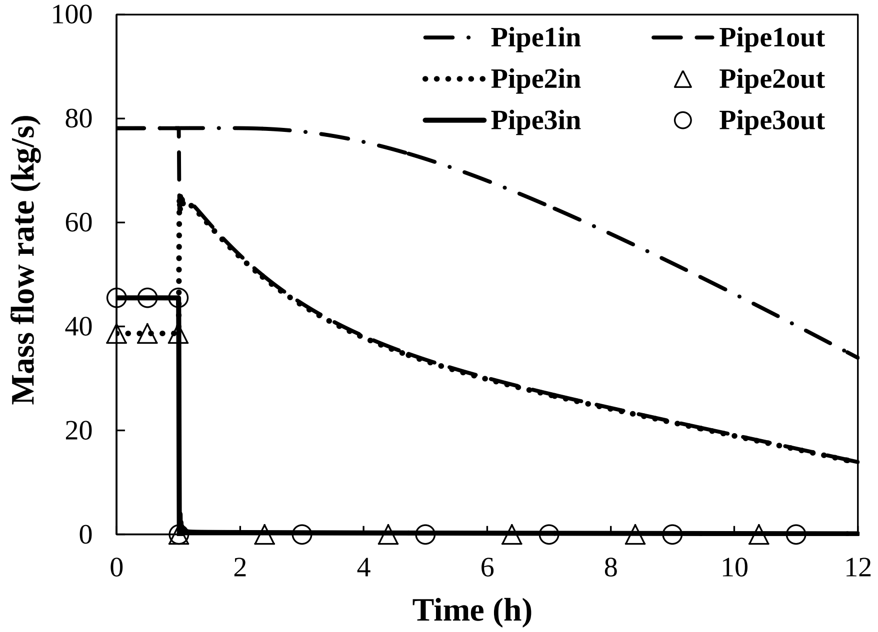

Figure 6.9 Flow rate behavior in the gas pipeline of the Western Libya Gas Project during the trip of total gas delivery

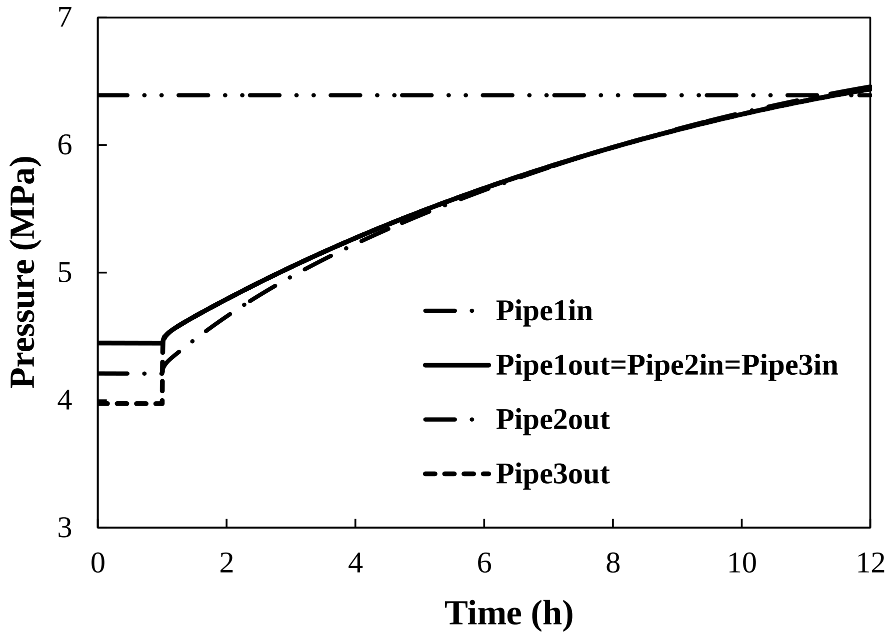

Figure 6.10 Pressure behavior in the gas pipeline of the Western Libya Gas Project during the trip of total gas delivery

The calculated velocity change along the pipeline from the inlet at the Wafa plant to the outlet at the Mellitah Complex is shown in figure 6.11 at the initial steady-state and 5 and 11 hours after the stop of gas outflows. As shown, prior to the transient, the gas velocity increases along the pipeline due to the pressure drop and corresponding density decrease. At the distance of 370 km from the inlet there is a drop of velocity since a part of the gas flow rate from the main transmission pipeline is directed towards the TPP, while the main pipeline diameter is unchanged. The velocity decreases after the stop of gas delivery at pipeline ends in the Mellitah Complex and in the TPP. At the transmission pipeline end at 525 km the velocity is zero during the transient, while along the pipeline the compressible gas still flows due to the inertia of the large gas mass and gas packing in the long pipeline. Hence, the pressure gradually increases and the velocity decreases along the pipeline.

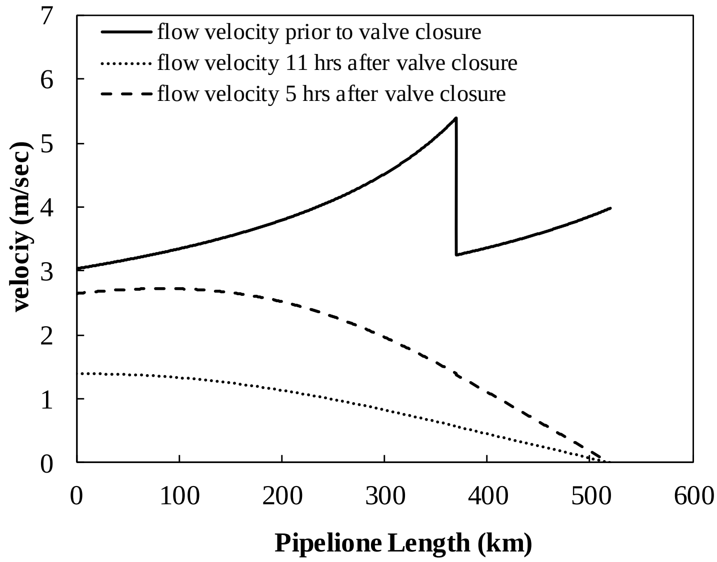

Figure 6.11 Velocity change along the pipeline at the initial steady-state and 5 and 11 hours after the trip of total gas delivery

6.2 Thermal effects in long transmission natural gas pipeline

6.2.1 The influence of temperature change along the gas pipeline on the pressure drop

The following presentation is related to the influence of the heat transfer from the gas pipeline to the surrounding medium and the heat generation due to friction between the flowing gas and the inner pipeline wall on the pressure drop in the case of the long transmission pipeline of the Western Libya Gas Project. The main transmission gas pipeline of the Western Libya Gas Project is buried in the ground with the pipeline centreline depth of approximately 1.5 m as shown in figure (6.12). The carbon steel pipeline is coated with 3.2 mm thick polyethylene. The following steady-state operating parameters are considered: the inlet gas mass flow rate is 78 kg/s and the inlet gas temperature is 315 K at Wafa plant. The mean soil temperature of 295 K is adopted at the depth of 1.5 m. The soil thermal conductivity varies between 0.64 W/(mK) for silty sand and 1.28 W/(mK) for limestone. The lower value of 0.64 W/(mK) leads to a more conservative conditions with a higher temperature and pressure increase. [96]

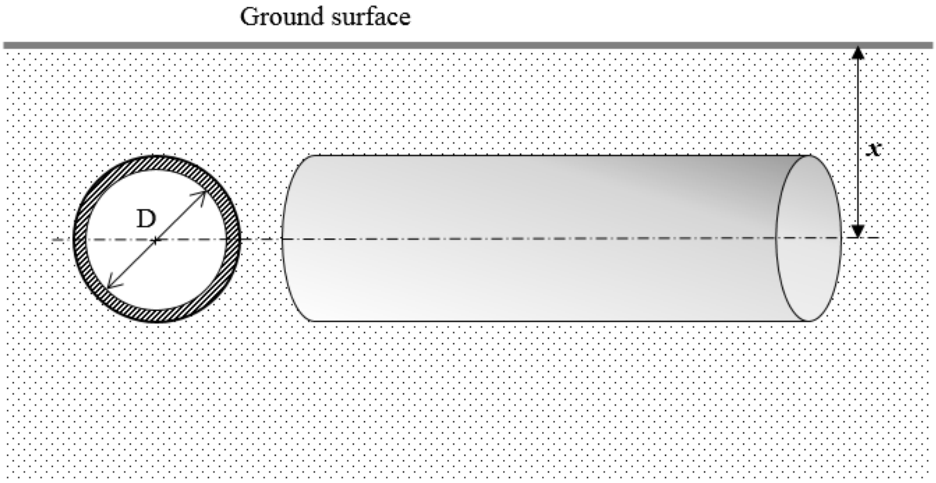

Figure 6.12 Pipeline buried in the ground at the depth x

The temperature change along the main gas pipeline is predicted by solving the energy equation in the following form

$$\frac{d(\rho u c_p T)}{dx} = f\,\frac{\rho u^3}{2D} - \frac{4k}{D}\left(T - T_s\right) \tag{6-1}$$

where the product of specific heat capacity at constant pressure c_p and temperature T represents enthalpy and k is the heat transfer coefficient from the gas to the surrounding soil at temperature T_s. The first term on the right hand side of equation (6-1) represents the heat generation due to the friction between the flowing gas and the inner pipeline wall. It is noted that the heat generation due to the wall friction is of the order of MW in long transmission gas pipelines. In case of the Western Libya Gas Project $f\rho u^3 V/(2D) \approx 4\,MW$). The second term is the heat transfer rate from the gas stream to the surrounding. Differential equation (6-1) is solved analytically by applying the following relations and assumptions:

a) The product of density and velocity ρu is constant under a steady-state condition.
b) The heat transfer coefficient is determined by the heat conduction from the pipeline outer surface through the soil.

The heat transfer rate per unit length of the buried pipeline is calculated as [100].

$$q_L = \lambda\left(T - T_s\right)\frac{2\pi}{\cosh^{-1}\left(\dfrac{2x}{D}\right)} \tag{6-2}$$

which holds for $x \approx 2D$, where x is the depth from the ground surface to the centerline of the buried pipeline. The soil temperature in the massive of the ground is T_s, T is the gas temperature in the pipeline and λ is the soil thermal conductivity. The relation between surface and linear heat flux is $q_L = \pi D q_A$. Since $q_A = k(T - T_s)$ and introducing equation (6-2), it follows

$$k = \frac{\lambda}{D}\frac{2}{\cosh^{-1}\left(\frac{2x}{D}\right)} \tag{6-3}$$

c) The gas velocity changes along the pipeline due to the pressure, temperature and consecutive density change.

d) The soil temperature depends on the ground surface temperature change, which is determined by the seasonal and day-night period changes, and on the soil conductivity. The soil conductivity changes along the pipeline, especially in cases of hundreds of kilometres long pipelines. The precise information about the soil characteristic is usually not available. Further, the soil temperature at some distance from the ground surface changes slowly with time and usually it can be assumed constant during a 24 hours day period [101]. According to the above presented analyses, the parameters (ρu), u, c_p, f, k and T_s are approximated fairly well with constant values. Therefore, Eq. (6-1) is solved analytically in the following form

$$T = \left(\frac{f\rho u^3}{8k} + T_s\right)\left(1 - \exp\left(-\frac{4k}{\rho u c_p D}x\right)\right) + T_{in}\exp\left(-\frac{4k}{\rho u c_p D}x\right) \tag{6-4}$$

Friction factor and compressibility factor were calculated respectively with Colebrook-White equation and California Natural Gas Association (CNGA) method [14].

The thermal effect is evaluated first by the introduction of the above defined parameters and the value of the heat conduction coefficient λ= 0.64 W/(mK) into equation (6-4) which leads to

$$T = 25.8\left(1 - \exp\left(-1.046 \cdot 10^{-5}x\right)\right) + 42\exp\left(-1.046 \cdot 10^{-5}x\right) \tag{6-5}$$

while for λ= 1.28 W/(mK) it leads to

$$T = 23.9\left(1 - \exp\left(-2.092 \cdot 10^{-5}x\right)\right) + 42\exp\left(-2.092 \cdot 10^{-5}x\right) \tag{6-6}$$

The calculation of natural gas temperature changes along the pipeline with equations (6-5) and (6-6) according to equation (6-4) are presented in figure 6.13 for the heat conduction coefficient values λ= 0.64 W/(mK) and 1.28 W/(mK). As shown, the gas temperature decreases within the first hundred kilometres even with the low value of the heat conduction coefficient related to the dry send. For higher values of λ, which are most common, the natural gas temperature decrease at the pipeline inlet part will be more intensive. The difference between gas temperatures calculated with λ= 0.64 W/(mK) and 1.28 W/(mK) is 2.3 K at the distance of 370 km from the pipeline inlet figure (6.13). [96]

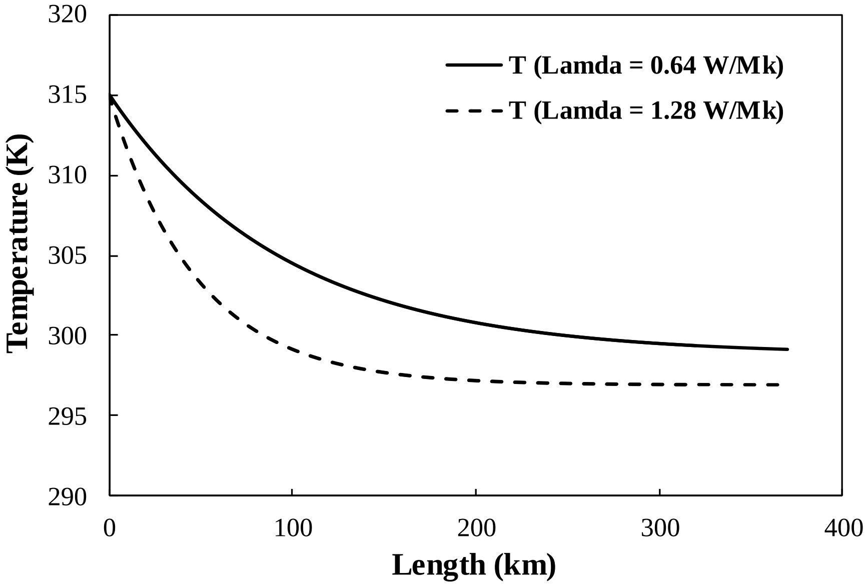

Figure 6.13 Temperature change along the entrance part of the long transmission gas pipeline for two heat conduction coefficient values

The temperature change in figure (6.13) is presented till 370 km since at that distance the gas mass flow rate is reduced in the main transmission pipeline due to the branch towards the TPP, which leads to the further decrease of difference between gas and soil temperatures. It is also noted that after 200 km the gas temperature is practically constant in case of λ= 1.28 W/(mK).

According to these results, the conclusion can be derived that the difference in the pressure change calculation with an isothermal and a non-isothermal model is small, as follows. Since the natural gas density change is about 5% with the temperature change form 315 K to 299 K (the density change with temperature is related to (315/299 = 1.05), the difference in the pressure drop calculated with the non-isothermal and isothermal models is lower than 5% (assuming that the adopted isothermal gas temperature is between the maximum value of 315 K and the minimum value of 299 K, and according to the well-known Darcy relation that $\Delta p = f\dot{m}^2/\left(2\rho A^2\right)\cdot L/D$). This uncertainty is of the same order as the change of pressure drop that is introduced by the change of the pipe wall roughness by 0.01 mm. The friction coefficient values calculated with Colebrook-White correlation which is the most popular equation for general gas industry transmission pipelines equation (3-24) are 0.01004 and 0.01054 for wall roughness 0.02 mm and 0.03 mm respectively and corresponding parameters: Re=7·10^6, D=0.8128 m (which shows the pressure drop change by 5%). According to data presented in Jia et al. (2014) [102], the change of wall roughness within a long transmission pipeline is in the span of 0.01 mm. Therefore, it is concluded that the assumption of the isothermal gas condition leads to an uncertainty of the pressure drop calculation that is of the same order as the uncertainty of the friction pressure drop calculation due to the uncertainty of the wall surface roughness prediction.

6.2.2 The influence of thermal effects on pressure transient in the long transmission gas pipeline

Scenario 3 presented in Section 6.1.3 is used for the analyses of natural gas temperature change during a long pipeline transient. It shows the greatest time rate of pressure change among presented Scenarios 1, 2 and 3 from Section 6.1 and consequently the greatest temperature change and the most intensive influence of thermal effects on the pressure change are expected during this scenario (even higher rate of pressure change can occur in case of pipeline rupture and blowdown, but this unlikely accident scenario is not considered in here presented research).

The gas temperature change during the transient of gas packing in Scenario 3 is evaluated with a model derived from the mass, energy and volume balances of the fluid control volume presented in figure (6.14).

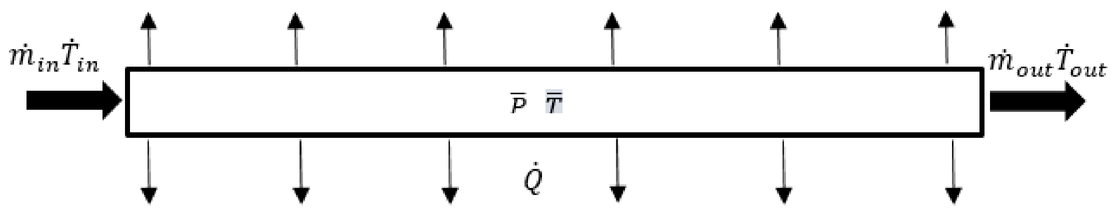

Figure 6.14 Gas control volume in the pipeline

- **Mass Balance**

$$\frac{dm}{dt} = \dot{m}_{in} - \dot{m}_{out} \tag{6-7}$$

- **Energy Balance**

$$\frac{dH}{dt} = (\dot{m}\,h)_{in} - (\dot{m}\,h)_{out} + \dot{Q} + V\,\frac{dp}{dt} \tag{6-8}$$

- **Volume of Pipeline**

$$V = \frac{M}{\rho} \tag{6-9}$$

Total enthalpy H is expressed as

$$H = m\,h \tag{6-10}$$

Where

$$h = c_p T \tag{6-11}$$

$$m = \rho\,V \tag{6-12}$$

The total enthalpy H in Eq. (6-8) is replaced with the product of fluid mass M and specific enthalpy h and the specific enthalpy is expressed as the product of the specific heat capacity c_p and temperature T. After derivation of the left hand side term in Eq. (6-8), by taking into account the mass balance Eq. (6-7) and by assuming that the change of the specific heat capacity by pressure and temperature is negligible ($c_p=const.$ in the range of pressure and temperature change during the analysed transients) the following expression is obtained for the temperature change.

$$\frac{dT}{dt} = \frac{1}{\rho V}\left[\dot{m}_{in}\left(T_{in} - T\right) - \dot{m}_{out}\left(T_{out} - T\right) + \frac{\dot{Q}}{c_p} + \frac{V}{c_p}\frac{dp}{dt}\right] \tag{6-13}$$

Differentiation of equation (6-9) gives,

$$\frac{dV}{dt} = 0 = \frac{1}{\rho}\frac{dm}{dt} - \frac{m}{\rho^2}\frac{d\rho}{dt} = \frac{1}{\rho}\frac{dm}{dt} - \frac{m}{\rho^2}\left[\left(\frac{\partial\rho}{\partial p}\right)_T \frac{dp}{dt} + \left(\frac{\partial\rho}{\partial T}\right)_p \frac{dT}{dt}\right] \tag{6-14}$$

and from equation (6-14) is derived

$$\frac{dp}{dt} = \frac{\rho}{m}\left(\frac{\partial p}{\partial\rho}\right)_T \frac{dm}{dt} - \left(\frac{\partial\rho}{\partial T}\right)_p \left(\frac{\partial p}{\partial\rho}\right)_T \frac{dT}{dt} \tag{6-15}$$

Substation of equations (6-7) and (6-13) into equation (6-15) gives

$$\frac{dp}{dt}=\frac{\left(\frac{\partial p}{\partial \rho}\right)_T\left[\rho+T\left(\frac{\partial \rho}{\partial T}\right)_p\right](\dot{m}_{in}-\dot{m}_{out})-\left(\frac{\partial \rho}{\partial T}\right)_p\left(\frac{\partial p}{\partial \rho}\right)_T\left[(\dot{m}T)_{in}-(\dot{m}T)_{out}+\frac{\dot{Q}}{c_p}\right]}{\rho V\left[1+\frac{1}{c_p\rho}\left(\frac{\partial \rho}{\partial T}\right)_p\left(\frac{\partial p}{\partial \rho}\right)_T\right]} \tag{6-16}$$

The heat rate $\dot{Q}$ is determined as

$$\dot{Q}=f\,\frac{\rho\,u^2}{2D}V-\dot{q}_L L \tag{6-17}$$

The first term on the right hand side represents the heat generation due to the gas friction on the pipeline wall, while the second term is the heat transfer rate from the gas stream to the surrounding and the linear heat transfer rate is determined with Eq. (6-2).

As an assumption, in case of the trip of gas delivery the gas flow rate at the pipeline outlet is zero $(\dot{m}_{out}=0)$; hence, equations (6-13) and (6-16) are reduced to

$$\frac{dT}{dt}=\frac{1}{\rho V}\left[\dot{m}_{in}(T_{in}-T)+\frac{\dot{Q}}{c_p}+\frac{V}{c_p}\frac{dp}{dt}\right] \tag{6-18}$$

$$\frac{dp}{dt}=\frac{\rho\left(\frac{\partial p}{\partial \rho}\right)_T\dot{m}_{in}-\left(\frac{\partial \rho}{\partial T}\right)_p\left(\frac{\partial p}{\partial \rho}\right)_T\left[\dot{m}_{in}(T_{in}-T)+\frac{\dot{Q}}{c_p}\right]}{\rho V\left[1+\frac{1}{c_p\rho}\left(\frac{\partial \rho}{\partial T}\right)_p\left(\frac{\partial p}{\partial \rho}\right)_T\right]} \tag{6-19}$$

For isothermal flow, where $\left(\frac{\partial \rho}{\partial T}\right)=0$, equation (6-19) is reduced to

$$\frac{dp}{dt}=\frac{1}{V}\frac{\partial p}{\partial \rho}\dot{m}_{in} \tag{6-20}$$

Partial derivatives $(\partial p/\partial \rho)_T$ and $(\partial \rho/\partial T)_p$ in Eq. (6-19) are obtained by the differentiation of the ideal gas law as follows. The ideal gas law is written as

$$p=z\rho R_g T \tag{6-21}$$

From this equation,

$$\left(\frac{\partial p}{\partial \rho}\right)_T = R_g T \frac{\partial}{\partial \rho}(z\rho)_T = R_g T\left[\rho\left(\frac{\partial z}{\partial \rho}\right)_T + z\right] \tag{6-22}$$

The compressibility factor z is function of p and T and its derivative is

$$dz = \left(\frac{\partial z}{\partial p}\right)_T dp + \left(\frac{\partial z}{\partial T}\right)_p dT \tag{6-23}$$

Dividing the above equation with $d\rho$ and assuming the isothermal conditions, i.e. $dT = 0$, the following expression is obtained

$$\left(\frac{\partial z}{\partial \rho}\right)_T = \left(\frac{\partial z}{\partial p}\right)_T \left(\frac{\partial p}{\partial \rho}\right)_T \tag{6-24}$$

Introduction of Eq. (6-24) into Eq. (6-22) leads to

$$\left(\frac{\partial p}{\partial \rho}\right)_T = \frac{zR_g T}{1 - R_g T\rho\left(\frac{\partial z}{\partial p}\right)_T} \tag{6-25}$$

By expressing the ideal gas law in the form

$$\rho = \frac{p}{zR_g T} \tag{6-26}$$

and differentiation by temperature for isobaric conditions leads to

$$\left(\frac{\partial \rho}{\partial T}\right)_p = \frac{p}{R_g}\left[\frac{\partial}{\partial T}\left(\frac{1}{zT}\right)\right] \tag{6-27}$$

$$\left(\frac{\partial \rho}{\partial T}\right)_p = -\frac{p}{zR_g T}\left[\frac{\left(\frac{\partial z}{\partial T}\right)_p}{z} + \frac{1}{T}\right] \tag{6-28}$$

Finally, Eq. (6-19) is written as

$$\frac{dp}{dt} = a_1 + b_1 T \tag{6-29}$$

where

$$a_1 = \frac{\left(\frac{\partial p}{\partial \rho}\right)_T \left\{\rho \dot{m}_{in} - \left(\frac{\partial \rho}{\partial T}\right)_T \left[\dot{m}_{in} T_{in} + \frac{2\pi\lambda L}{c_p \cosh^{-1}(2x/D)} T_s + f\frac{\rho u^3}{2Dc_p} V\right]\right\}}{\rho V \left[1 + \frac{1}{c_p \rho}\left(\frac{\partial p}{\partial \rho}\right)_T \left(\frac{\partial \rho}{\partial T}\right)_T\right]} \tag{6-30}$$

$$b_1 = \frac{\left(\frac{\partial p}{\partial \rho}\right)_T \left(\frac{\partial \rho}{\partial T}\right)_p \left[\dot{m}_{in} + \frac{2\pi\lambda L}{c_p \cosh^{-1}(2x/D)}\right]}{\rho V \left[1 + \frac{1}{c_p \rho}\left(\frac{\partial p}{\partial \rho}\right)_T \left(\frac{\partial \rho}{\partial T}\right)_T\right]} \tag{6-31}$$

Substitution of Eq. (6-29) into Eq. (6-18) leads to

$$\frac{dT}{dt} = a_2 - b_2 T \tag{6-32}$$

where

$$a_2 = \frac{1}{\rho V}\left[\dot{m}_{in} T_{in} + \frac{2\pi\lambda L}{c_p \cosh^{-1}(2x/D)} T_s + \frac{\left(\frac{\partial p}{\partial \rho}\right)_T \left\{\rho \dot{m}_{in} - \left(\frac{\partial \rho}{\partial T}\right)_T \left[\dot{m}_{in} T_{in} + \frac{2\pi\lambda L}{c_p \cosh^{-1}(2x/D)} T_s + f\frac{\rho u^3}{2Dc_p} V\right]\right\}}{c_p \rho + \left(\frac{\partial p}{\partial \rho}\right)_T \left(\frac{\partial \rho}{\partial T}\right)_T}\right] \tag{6-33}$$

$$b_2 = \frac{1}{\rho V}\left[\dot{m}_{in} + \frac{2\pi\lambda L}{c_p \cosh^{-1}(2x/D)} + \frac{\left(\frac{\partial p}{\partial \rho}\right)_T \left(\frac{\partial \rho}{\partial T}\right)_T \left[\dot{m}_{in} + \frac{2\pi\lambda L}{c_p \cosh^{-1}(2x/D)}\right]}{c_p \rho + \left(\frac{\partial p}{\partial \rho}\right)_T \left(\frac{\partial \rho}{\partial T}\right)_T}\right] \tag{6-34}$$

Parameters on the right hand side of Eqs. (6-30,6-31) and (6-33,6-34) are taken as constant for a certain range of gas pressure and temperature change and gas packing with the constant gas inlet mass flow rate and temperature. This assumption enables an analytical solving of the differential equations (6-29) and (6-32). Equation (6-32) is solved as

$$T - T_0 = \left(\frac{a_2}{b_2} - T_0 \right)\left(1 - \mathrm{e}^{-b_2 t}\right) \tag{6-35}$$

Substitution of Eq. (6-35) into Eq. (6-29) leads to the following solution

$$p = p_0 + \left(a_1 + \frac{a_2 b_1}{b_2} \right) t + \frac{b_1}{b_2} \left(\frac{a_2}{b_2} - T_0 \right) e^{-b_2 t} \tag{6-36}$$

In order to evaluate the temperature and pressure change during the gas packing of Scenario 3, the stated balance equations (6-7) and (6-8) and derived equations (6-35) and (6-36) are applied to the whole length of the transmission pipeline. Therefore, the pressure p and temperature T in equations (6-35) and (6-36) represent the mean values for the whole gas volume. The temperature distribution along the pipeline presented in figure (6.13) shows that approximately after one third of the pipeline length the temperature is nearly constant and the assumption of the gas mean temperature for the whole pipeline has a sense. The pressure change from the inlet to the outlet of the long transmission pipeline is about 2.5 MPa (the difference between initial inlet and outlet values in figure (6.10) and approximation of the gas pressure along the pipeline with the mean pressure seems to be rather crude. But, during the gas packing the difference between the inlet and outlet values is reduced and becomes zero at the end of transient, which diminishes the pressure change along the pipeline. Further, results of the evaluation of the mean pressure change during the gas packing, as it is presented in this section below, show that the predicted mean pressure change is in accordance with the pressure change presented in figure (6.10).

The initial mean temperature of the gas along the pipeline T_0, prior to the gas delivery trip, is expressed explicitly from equation (6-13) by taking into account that the time derivatives are equal to zero in the steady-state operation and with the introduction of relation for the heat transfer rate Eq. (6-17)

$$T_0 = T_s + \frac{\dot{m} c_p \left(T_{in} - T_{out} \right) + f \dfrac{\rho u^3}{2D} V}{\dfrac{2\pi\lambda}{\cosh^{-1}(2x/D)} L} \tag{6-37}$$

The following values of the operational parameters are taken in order to evaluate the pressure and temperature change during the gas packing: the inlet mass flow rate is assumed to be constant and $\dot{m}_{in} = 78\, kg/s$, the initial mean gas pressure is $p_0 = 53\, bar$, the solution of equation (6-37) provides the initial mean temperature $T_0 = 301.5\ K$, the soil massive temperature is constant along the pipeline with a value $T_s = 295\ K$, the gas inlet temperature is $T_{in} = 315\ K$, the natural gas constant is $R_g = 500\ J/kgK$, the mean gas density value is $\rho = 37.6\ kg/m^3$ (it is determined from the assumption that the gas mean velocity along the pipeline is $u = 4\ m/s$ and the gas mass flux is $\rho u = \dot{m}/(3.14 \cdot D^2/4) = 150.4\ kg/(m^2 s)$), the gas specific heat capacity is $c_p = 2500\ J/kgK$, the compressibility factor is $z = 0.89$, the partial derivatives are $\left(\partial p/\partial \rho\right)_T = 120000\ J/kg$ and $\left(\partial \rho/\partial T\right)_T = -0.189\ kg/m^3 K$, the soil thermal conductivity is $\lambda = 0.64\ W/mK$, pipeline inner diameter is $D = 0.8\ m$ and the length of the pipeline $L = 525 \cdot 10^3\ m$.

Introduction of these parameters into equations (6-35) and (6-36) leads to

$$T - T_0 = 4.8\left(1 - \mathrm{e}^{-6.489 \cdot 10^{-5} t}\right) \tag{6-38}$$

$$\left(p - p_0\right)_{nonisothermal} = 37.93t - 108943\left(e^{-6.489 \cdot 10^{-5} t} - 1\right) \tag{6-39}$$

According to equation (6-38) the mean temperature rise is 4.4 K during the gas packing for 11 hours (the same time period of gas packing as shown in figure (6.10)). Equation (6-39) provides the mean pressure increase during the gas packing under this non-isothermal condition, while the following integral of equation (6-20) provides the pressure change under the assumption of the isothermal gas packing

$$\left(p - p_0\right)_{isothermal} = 34.38t \tag{6-40}$$

The difference between the pressure rise during the gas packing for 11 hours and under non-isothermal and isothermal conditions is calculated with equation (6-39) and (6-40) as following

$$\left(p - p_0\right)_{nonisothermal} - \left(p - p_0\right)_{isothermal} = 1.499 - 1.361 = 0.138\ MPa \tag{6-41}$$

where the value of 0.138 MPa is the relative difference of 9.2% in comparison to the non-isothermal pressure change.

The above calculation is performed with the assumption that during the whole gas packing transient the gas velocity is constant and has the initial value of 4 m/s. According to figure (6.11) the gas velocity decreases during the transient. The heat generation due to friction is related to the third power of velocity; hence, the heat generation due to friction rapidly decreases with the velocity decrease during the gas packing transient. So, if the heat generation due to gas friction on the pipeline wall is neglected, the term $f \rho u^3 V/\left(2D\right)$ is removed from equation (6-17), as well as the term $f\rho u^3 V\big/\left(2Dc_p\right)$ from equation (6-30) and (6-33). In this case the temperature and pressure rises during the gas packing with the constant inlet flow rate are calculated as

$$T - T_0 = 4.0\left(1 - \mathrm{e}^{-6.489\cdot 10^{-5} t}\right) \tag{6-42}$$

$$\left(p - p_0\right)_{nonisothermal} = 34.36t - 91464\left(e^{-6.489\cdot 10^{-5} t} - 1\right) \tag{6-43}$$

According to equations (6-42) and (6-43) the temperature and pressure rises during the gas packing with the constant inlet flow rate is 3.7 K and 1.445 MPa. The difference between the pressure rises under non-isothermal and isothermal conditions is 0.084 MPa, obtained as next,

$$\left(p - p_0\right)_{nonisothermal} - \left(p - p_0\right)_{isothermal} = 1.445 - 1.361 = 0.084\, bar \tag{6-44}$$

which is the relative difference of 5.8% in comparison to the non-isothermal pressure change.

The presented differences between calculated temperature and pressure changes under non-isothermal and isothermal conditions in the intervals from 3.7 K and 4.4 K and 0.084 MPa and 0.138 MPa are in the range of uncertainty caused by the unknown local soil thermal conductivity and ambient temperature along the whole long pipeline. Therefore, the prediction of the pressure change during the long lasting pressure packing transient is acceptable with isothermal model and the temperature change does not have significant influence on the gas properties.

The same is concluded for the case when the gas inflow is stopped ($\dot{m}_{in} = 0$) and its delivery to the consumers is continued with unchanged flow rate, such as in Scenario 1 applied to the Western Libya Gas Project in Section 6.1. In this case the temperature and pressure change differential equations (6-13) and (6-16) have the form

$$\frac{dT}{dt} = \frac{1}{\rho V}\left[\dot{m}_{out}\left(T - T_{out}\right) + \frac{\dot{Q}}{c_p} + \frac{V}{c_p}\frac{dp}{dt}\right] \tag{6-45}$$

$$\frac{dp}{dt} = \frac{\left(\frac{\partial p}{\partial \rho}\right)_T \left\{-\rho \dot{m}_{out} - \left(\frac{\partial \rho}{\partial T}\right)_p \left[\dot{m}_{out}\left(T - T_{out}\right) + \frac{\dot{Q}}{c_p}\right]\right\}}{\rho V\left[1 + \frac{1}{c_p \rho}\left(\frac{\partial p}{\partial \rho}\right)_T \left(\frac{\partial \rho}{\partial T}\right)_p\right]} \tag{6-46}$$

During the pipeline discharge transient the gas outlet temperature T_{out} is not constant. Therefore, in the above equations the outlet temperature is approximated with the mean gas temperature. It should be noted that this approximation leads to an even more conservative approach to the estimation of the temperature and pressure change. Namely, the term $\dot{m}_{out}\left(T-T_{out}\right)$ is positive and it reduces the temperature drop calculated by equation (6-45) in case of the gas discharging transient. The same holds for the pressure drop. The partial derivative $\left(\partial\rho/\partial T\right)_p$ has a negative value and the term $\left(\partial p/\partial\rho\right)_T\left(\partial\rho/\partial T\right)_p\dot{m}_{out}\left(T-T_{out}\right)$ in the numerator of equation (6-46) reduces the pressure drop during the gas discharging from the pipeline. The solution of equations (6-45) and (6-46) is also in the form of equations (6-35) and (6-36). The related coefficients in these equations are

$$a_1=\frac{\left(\frac{\partial p}{\partial\rho}\right)_T\left\{-\rho\dot{m}_{out}-\left(\frac{\partial\rho}{\partial T}\right)_T\left[\frac{2\pi\lambda L}{c_p\cosh^{-1}(2x/D)}T_s+f\,\frac{\rho u^3}{2Dc_p}V\right]\right\}}{\rho V\left[1+\frac{1}{c_p\rho}\left(\frac{\partial p}{\partial\rho}\right)_T\left(\frac{\partial\rho}{\partial T}\right)_T\right]} \tag{6-47}$$

$$b_1=\frac{\left(\frac{\partial p}{\partial\rho}\right)_T\left(\frac{\partial\rho}{\partial T}\right)_p\frac{2\pi\lambda L}{c_p\cosh^{-1}(2x/D)}}{\rho V\left[1+\frac{1}{c_p\rho}\left(\frac{\partial p}{\partial\rho}\right)_T\left(\frac{\partial\rho}{\partial T}\right)_T\right]} \tag{6-48}$$

$$a_2=\frac{1}{\rho V}\left[\frac{2\pi\lambda L}{c_p\cosh^{-1}(2x/D)}T_s+\frac{\left(\frac{\partial p}{\partial\rho}\right)_T\left\{-\rho\dot{m}_{out}-\left(\frac{\partial\rho}{\partial T}\right)_T\left[\frac{2\pi\lambda L}{c_p\cosh^{-1}(2x/D)}T_s+f\,\frac{\rho u^3}{2Dc_p}V\right]\right\}}{c_p\rho+\left(\frac{\partial p}{\partial\rho}\right)_T\left(\frac{\partial\rho}{\partial T}\right)_T}\right] \tag{6-49}$$

$$b_2=\frac{1}{\rho V}\left[\frac{2\pi\lambda L}{c_p\cosh^{-1}(2x/D)}+\frac{\left(\frac{\partial p}{\partial\rho}\right)_T\left(\frac{\partial\rho}{\partial T}\right)_T\frac{2\pi\lambda L}{c_p\cosh^{-1}(2x/D)}}{c_p\rho+\left(\frac{\partial p}{\partial\rho}\right)_T\left(\frac{\partial\rho}{\partial T}\right)_T}\right] \tag{6-50}$$

The differences of mean temperature and pressure changes under non-isothermal and isothermal conditions, in case of the pipeline empting Scenario 1 in Section 6.1, when the gas supply at the Wafa plant is stopped and the gas delivery is continued with the value of the initial flow rate, are respectively -0.8 K and 0.17 MPa (this pressure difference is 11% of the calculated pressure change under non-isothermal conditions).

6.3 Conclusions

The GTA code is used for the simulation of transient behaviour of the 525 kilometres long distance pipeline of the Western Libya Gas Project. First, the results of simulated operational condition are compared with the available measured data and an acceptable agreement is obtained. Afterwards, simulated are transients caused by hypothetical scenarios of abrupt disturbances in gas inflow at the gas source form the wells field and trips of gas delivery to the consumers. In addition, The GTA code predictions are obtained under isothermal flow conditions, while the influence of the heat generation due to friction on the inner pipeline wall and the heat transfer to the surrounding soil is determined by the application of adequate thermal energy balance equations. The main findings are discussed in the next Chapter 7.

CHAPTER 7

CONCLUSIONS

For the prediction of transient natural gas flows in transmission pipelines and pipe networks, the numerical model and computer code GTA (Gas Transient Analysis) are developed based on one-dimensional compressible gas flow in pipeline of constant diameter. Using the method of characteristics the mass and momentum governing equations are solved numerically. The intersection of several pipes and prescribed transient mass flow rates and pressure data at inlet and outlet of pipeline are considered as boundary conditions of a model, which enable modelling of gas networks of diverse configurations.

The GTA code is validated by computer simulations of transient cases reported in the literature. Four cases are simulated to validate the code, which include transients caused by the variable gas consumption and boundary pressure pulses. Results of simulations show that the procedure of calculation is numerically stable, also the good agreement between the previous published results and the GTA results is achieved.

In addition, the gas transient analysis code is applied for the simulation of transient behavior of the several hundred kilometers long distance pipeline of the Western Libya Gas Project. The results of simulated operational condition are firstly compared with available measured data and acceptable agreement is obtained. Thereafter, transients are simulated for different suppositional scenarios of sudden disturbances in gas inflow at the gas source wells fields and trips of gas delivery to the consumers. The main findings are as following:

- In spite of the trip of the natural gas delivery to the inlet point of the pipeline from the source wells and the decreasing of corresponding pressure and flow rate along the pipeline from the Wafa Desert Plant towards the Mellitah Complex and in the branch towards the TPP, scenario 1 shows that the required delivery flow rates at the TPP and at the Mellitah Complex are maintained for a period even longer than 24 hours, due to the gas accumulation in the large volume of the gas transmission pipeline.
- Scenario 2 shows that even though the delivery flow rate in the Mellitah Complex is stopped after 1 hour, the decreasing flow rate at the inlet of the long pipeline towards Mellitah Complex still exists in the long period of 11 hours after the outlet flow stoppage due to the corresponding pressure increase and the gas accumulation. After one hour of the trip of gas delivery in the

Mellitah Complex, the pressure along the several hundred kilometers long pipeline towards the Mellitah Complex is practically constant. The pressure increase within the whole pipeline system indicates gas accumulation.

- Scenario 3 shows that although the whole gas delivery to consumers (Mellitah Complex and TPP) is stopped, there is still a gas inflow at the main pipeline inlet point for a period about 11 hours, due to the gas accumulation and corresponding pressure increase. Because of its relatively short length of 5 km, the flow rate in the branch towards the TPP practically immediately stops. The flow rate sustains for a time period longer than 11 hours in the main transmission pipeline due to its long length of 525 km.
- Furthermore, the GTA code predictions are obtained under isothermal flow conditions. In order to evaluate the error introduced by this assumption in the simulation of long transmission pipeline transients of the Western Libya Gas Project, the analytical expressions are derived based on the solving of mass, volume and energy balance equations of the pipeline gas volume. These equations provides differences between isothermal and non-isothermal mean gas pressure changes in the pipeline during the gas packing and during the gas discharge from the pipeline under the trip of gas supply, as well as the temperature changes during these transients. The results show that the mean temperature change is a few degrees Celsius and the relative difference between isothermal and non-isothermal pressure change is not greater than 9.2% in case of gas packing and up to 11% in case of pipeline discharging. These differences are in the range that can be introduced with the uncertainties of the soil thermal conductivity and ambient temperature along the long transmission pipeline. In addition, the thermal effects under steady-state conditions are analytically evaluated and their influence on the prediction of pressure change along the long transmission pipeline is within 3%. This error is in the range of the uncertainty of friction pressure drop calculation due to the uncertainty of the wall roughness prediction in the span of 0.01 mm. Therefore, these estimations of maximum errors that are introduced by the application of the isothermal gas flow model are in favor of the isothermal model application in engineering calculations, when other important conditions, such as the soil thermal conductivity, the ambient temperature or the wall surface roughness might introduce uncertainness of even higher values.
- The gas temperature in steady-state condition is determined by the heat generation due to the gas friction on the pipeline's wall and by the heat transfer from the pipeline to the surrounding ambient, as presented by equation (6-37). The heat generation by friction in the long transmission pipelines is of the order of MW and according to equation (6-37) there is a difference of the gas and soil temperatures by a few Celsius degrees. This difference should be taken into account also in case of isothermal calculations (in Subsection 6.2.1 the adopted soil

temperature is 295 K, the gas inlet temperature is 315 K and the calculated mean gas temperature in steady-state operation is 301.5 K). Hence, the assumption that in the long pipeline the gas temperature is equal to the surrounding soil temperature is not adequate. The gas temperature is a few degrees higher and, as explained, it is determined by the heat generation by friction and its transfer from the gas to the surrounding soil.

The developed GTA code and presented results are a support to planning and specification of operational and repair procedures and guidelines in cases of abnormal conditions.

REFERENCES

1. Borraz-Sanchez, C. 2010. Optimization Methods for Pipeline Transportation of Natural Gas. PhD dissertation. University of Bergen, Norway.
2. Mokhatab, M., Poe, W. A., Speight, J. G., 2006. Handbook of Natural Gas Transmission and Processing, Gulf Professional Publishing, Elsevier. USA.
3. How products are made. http://www.madehow.com/Volume-6/Natural-Gas.html. 2010
4. Pipeline and Gas Journal's 2017 Worldwide Pipeline Construction Report. January 2017, Vol. 244, No.1.
5. BP Statistical Review of World Energy. June 2018. 67th edition. UK.
6. Kelkar, M., 2008. Natural Gas: Production Engineering. Copyright by Penn Well Corporation, USA.
7. BP Statistical Review of World Energy. June 2019. 68th edition. UK.
8. International Energy Outlook 2019 with projections to 2050, the U.S. Energy Information Administration (EIA), 24 Sep. 2019. USA.
9. Rios-Mercado, R. Z., Borraz-Sa´nchez, C., 2014, "Optimization Problems in Natural Gas Transportation Systems: A State-of-the-Art Review", University Autónoma de Nuevo León (UANL), Report number: PISIS-2014-04.
10. Government of Alberta, Energy. http:www.energy.alberta.ca/NaturalGas/. 2011
11. Osiadacz, A. J., and Chaczykowski, M., 2001. Comparison of Isothermal and Non-Isothermal Pipeline Gas Flow Models. Chem. Eng. J. 81(1-3), pp. 41–51.
12. Chapman, K. S., Krishniswami, P., Wallentine, V., Abbaspour, M., Ranganathan, R., Addanki, R., Sengupta, J., Chen, L., 2005. Final Technical Report: Virtual Pipeline System Testbed to Optimize the U.S. Natural Gas Transmission Pipeline System. DE-FC26-02NT41322, USA.
13. Abbaspour, M., 2005. Simulation and Optimization of Non- Isothermal, One-Dimensional Single / Two-Phase Flow in Natural Gas Pipeline. PhD, Kansas State University, USA.
14. Wu, S., 1998. Steady State Simulation and Fuel Cost Minimization of Gas Pipeline Networks. PhD, University of Houston, USA.
15. Key World Energy Statistics, International Energy Agency (IEA), 2019.
16. Stoner, M. A., 1972. Sensitivity Analysis Applied to a Steady-State Model of Natural Gas Transportation systems. SPE 45th Annual Fall Meeting, Houston, USA.

17. Mohitpour, M., William, T., Asante, B., 1996. The Importance of Dynamic Simulation on the Design and Optimization of pipeline transmission systems. International Pipeline Conference — Vol. 2, ASME 1996

18. A.L.H. Costa, J.L. de Medeiros and F.L.P. Pessoa. 1998. Steady-State Modeling and Simulation of Pipeline Networks for Compressible Fluids. Brazilian Journal of Chemical Engineering, vol. 15 n. 4.

    http://www.scielo.br/scielo.php?script=sci_arttext&pid=S0104-66321998000400004&lng=en&tlng=en

19. Nouri-Borujerdi, A., Ziaei-Rad, M., 2009. Simulation of compressible flow in high pressure buried gas pipelines. International Journal of Heat and Mass Transfer, vol.52, pp 5751–5758.

20. Alghlam, A.S. 2012. Numerical Scheme for Modeling Natural Gas Flow in Cross-Border Pipelines. ME thesis, University of technology Malaysia.

21. Cameron, I. 1999 Using an Excel-Based Model for Steady State and Transient Simulation. TransCanada Transmission. Alberta, Canada.

22. Szoplik, J., 2010. The Steady-State Simulations for Gas Flow in a Pipeline Network. Chemical Engineering Transactions, Vol. 21, 1459-1464.

23. J. Zhou, M. A. Adewumi. The Development and Testing of a New Flow Equation. Pipeline Simulation Interest Group Annual Meeting, PSIG-9504, US.

24. Ouyang, L., Aziz, K., 1995. Steady-state gas flow in pipes. Journal of Petroleum Science and Engineering, Vol. 14, pp 137-158.

25. Rhoads, G. A., 1983. Which Flow Equation- Does It Matter?. Pipeline Simulation in Interset Group. PSIG Annual Meeting, Michigan, USA.

26. Schroeder, Jr. D. W., 2001. A Tutorial on Pipe Flow Equations. Carlisle Pennsylvania 17013-0086, pp. 1-18.

27. Stoner, M. A., 1969. Steady-state Analysis of Gas Production, Transmission and Distribution Systems. No. SPE 2554, Society of Petroleum Engineers of AIME, Texas, USA.

28. Berard, G. P., Eliason, B. G., 1978. An Improved Gas Transmission System Simulator. Society of Petroleum Engineers of AIME. No. SPE 6872, 52ND Annual Fall Technical Conference Exhibition, Denver, USA.

29. Hoeven, T. V., Gasunie, N. V.N., 1992. Some Mathematical Aspects of Gas Network Simulation. Gasunie Netherlands.

30. Tian, S., Adewumi, M. A., 1994. Development of Analytical Design Equation for Gas Pipelines. Society of Petroleum Engineers, SPE Production & Facilities, pp 100-106.

31. Sung, W., Huh, D., Lee, J., Kwon, O., 1998. Optimization of Pipeline Networks with a Hybrid MCST-CD Networking Model. SPE Production & Facilities, pp 213-219.

32. Rios-Mercado, Roger Z. A, Suming Wu, Ridgway S. L., S., Boyd, E. A., 2001. A Reduction Technique for Natural Gas Transmission. Network Optimization Problems.

33. Martinez-Romero, N., Osorio-Peralta, O., Santamaria-Vite, I., 2002. Natural Gas Network Optimization and Sensibility Analysis. Society of Petroleum Engineers, SPE 74384. International Petroleum Conference and Exhibition, Mexico.

34. Doonan, A.F., Fletcher, I. Cox, C.S., Arden W.J.B, 1998. Evaluation of a Remote Boundary Pressure Control Strategy Using SIMULINKTM. UKACC International Conference on Control. Publication No. 455, pp 129-134.

35. Fauer, D., 2002. The Making of a Useful Pipeline Simulation Model. Southern Natural Gas.

36. Greyvenstein, G. P., Laurie, D. P., 1994. A Segregated CFD Approach to Pipe Network Analysis. International Journal for Numerical Methods in Engineering, Vol. 37, pp 3685-3705.

37. Zhou, J., Adewumi, M. A., 1997. Predicting Gas Flowing Temperature and Pressure Profiles in Buried Pipelines. Society of Petroleum Engineers, SPE 38460.

38. Osiadacz, A. J., 1994. Dyanamic Optomization of High Pressure Gas Networks Using Hierarchica System Theory. State Committee for Scientific Research, No. 80565.

39. Pambour, K.A., Bolado-Lavin, R., Dijkema, G.P.J. 2016. An integrated transient model for simulating the operation of natural gas transport systems. Journal of Natural Gas Science and Engineering 28. 672-690.

40. Zuo, L., Jiang, F., Jin, B., Zhang, L., Xue, T., 2015. Value settings for the rate of pressure drop of automatic line-break control valves in natural gas pipelines. Journal of Natural Gas Science and Engineering 26. 803-809.

41. Edalat, M., Mansoori, G. A., 1988. Buried Gas Transmission Pipelines: Temperature Profile Prediction Through the Corresponding States Principle. Energy Sources, Vol. 10, 247-252

42. Oosterkamp, A., 2016. Modelling and Measuring Transient Flow in Natural Gas Pipelines, Effect of Ambient Heat Transfer Models. Norwegian University of Science and Technology.

43. Stevanovic, V. 2008. Security of gas pipelines. Proceedings of the NATO Advanced Research Workshop on Securety and Reliability of Damaged Structures and Defective Materials, Portoroz, Slovenia, Springer, pp. 253-256.

44. Yuan, Z., Deng, Z., Jiang, M., Xie, Y., Wu, Y., 2015. A modeling and analytical solution for transient flow in natural gas pipelines with extended partial blockage. Journal of Natural Gas Science and Engineering 22. 141-149.

45. Thorley, A.R.T., Tiley, C.H. 1987. Unsteady and transient flow of compressible fluids in pipelines—a review of theoretical and some experimental studies. Thermo-Fluids Engineering Research Centre, the City University of London, UK. International Journal of Heat and Fluid Flow, volume 8, issue 1, March 1987, pages 3-15.

46. Heath, M. J., Blunt J. C. 1968. Dynamic Simulation Applied to the Design and Control of a Pipeline Network. Volume 149 of Research communication, Gas Council.

47. Osiadacz, A.J., Yedrouj, M. 1989. A comparison of a finite element method and a finite difference method for transient simulation of a gas pipeline. Applied Mathematical Modelling, vol. 13.

48. Van Deen, J.K., Reintsema, S.R., 1983. Modelling of high-pressure gas transmission lines. Journal of Applied Mathematical Modelling. Vol. 7, pp 268-273 Volume 7, Issue 4, August 1983, Pages 268-273

49. Abott, M.B. 1966. An Introduction to the Method of Characteristics. (Book) New York, American Elsevier.

50. Mekebel, S., Loraud, J.C. 1985. Study of a variable flow in natural gas pipelines. International Chemical Engineering, vol.:25:2.

51. Osiadacz, A. J., 1987. Ke Simulation and Analysis of Gas Networks. Gulf Publishing Company, Houston.

52. Yow, W., 1971, Analysis and Control of Transient Flow in Natural Gas Piping Systems. Ph.D. dissertation, U. of Michigan.

53. Wylie, E. B., Streeter, V. L., Stoner, M. A., 1974. Unsteady-State Natural-Gas Calculations in Complex Pipe Systems. Society of Petroleum Engineers Journal, SPE 4004

54. Herran-Gonzalez, A., De La Cruz, J.M., De Andres-Toro, B., Risco-Martın, J.L. 2009. Modeling and simulation of a gas distribution pipeline network. Applied Mathematical Modelling 33, (1584–1600).

55. Reddy, H.P., Narasimhan, S., Bhallamudi, S.M. 2006. Simulation and State Estimation of Transient Flow in Gas Pipeline Networks Using a Transfer Function Model. Industrial & Engineering Chemistry Research 45(11).

56. Alamian, R., Behbahani-Nejad, M., Ghanbarzadeh, A., 2012. A state space model for transient flow simulation in natural gas pipelines. Journal of Natural Gas Science and Engineering 9, 51-59.

57. Wang, H., Liu, X., L., Zhou, W. 2011. Transient flow simulation of municipal gas pipelines and networks using semi implicit finite volume method. SREE

Conference on Engineering Modelling and Simulation (CEMS 2011), Procedia Engineering 12, 217–223.

58. Noorbehesht N., Ghaseminejad P., 2013. Numerical Simulation of the Transient Flow in Natural Gas Transmission Lines Using a Computational Fluid Dynamic Method. American Journal of Applied Sciences, 10 (1): 24-34, 2013. ISSN: 1546-9239.

59. Ibraheem, S. O., Adewumi, M. A., 1996. Higher-Resolution Numerical Solution for 2-D Transient Natural Gas Pipeline Flows. Society of Petroleum Engineers, SPE 35626.

60. Dorao, C.A., Fernandino, M. 2011. Simulation of transients in natural gas pipelines. Journal of Natural Gas Science and Engineering 3, pp 349-355.

61. Farzaneh-Gord, M., Rahbari, H.R. 2016. Unsteady natural gas flow within pipeline network, an analytical approach. Journal of Natural Gas Science and Engineering 28, 397-409.

62. Issa, R. I., and Spalding, D. B., 1972, “Unsteady One-Dimensional Compressible Frictional Flow with Heat Transfer”, Journal of Mechanical Engineering Science, 14 (6), pp. 365-369.

63. Price, G. R., McBrien, R. K., Rizopoulos S. N., Golshan, H., 1999. Evaluating the Effective Friction Factor and Overall Heat Transfer Coefficient During Unsteady Pipeline Operation. Journal of offshore Mechanics and Arctic Engineering. Vol. 121, ASME.

64. Tentis, E., Margaris, D., Papanikas, D. 2003. Transient gas flow simulation using an Adaptive Method of Lines. C. R. Mecanique, 331, pp 481–487.

65. Rachford, Jr. H. H., Rice U, Dupont T., 1974. A Fast Highly Accurate Means of Modeling Transient Flow in Gas Pipeline Systems by Variational Methods. SPE-AIME 47th Annual Fall Meeting, SPE 4005A, pp 165-178

66. Maddox, R. N., Zhou, P., 1983. Use of Steady State Equations for Transient Flow Calculations. Pipeline Simulation in Interest Group.

67. T. Kiuchi. An Implicit Method for Transient Gas Flow in Pipe Networks. 1994

68. Beam, R. M., Warming, R. F., 1976. An Implicit Finite-Difference Algorithm for Hyperbolic Systems in Conservation-Low Form. Journal of Computational Physics 22, pp 87-l 10.

69. Luongo, C. A., 1986. An Efficient Program for Transient Flow Simulation In Natural Gas Pipelines. Pipeline Simulation in Interest Group, PSIG Annual Meeting.

70. Tao, W. Q., Ti, H. C., 1998. Transient Analysis of Natural Gas Network. Chemical Engineering Journal 69, pp 47-52

71. Osiadacz, A. J., 1996, "Different Transient Models- Limitations, Advantages and Disadvantages", Proceedings of the Pipeline Simulation Interest Group, PSIG Annual Meeting, 23-25 October, San Francisco, California.

72. Lewandowski, A., 1995. New Numerical Methods for Transient Modeling of Gas Pipeline Networks. Pipeline Simulation Interest Group. PSIG-9510.

73. Modisette, J., 2002. Pipeline Thermal Models, PhD. Energy Solutions International.

74. Abbaspour, M., Chapman, K.S., Glasgow, L.A. 2010. Transient modeling of non-isothermal dispersed two-phase flow in natural gas pipelines. Applied Mathematical Modelling 34, 495–507.

75. Dufont, T., Rachford. Jr. H. H., The Effect of Thermal Changes Induced by Transients in Gas Flow. University of Chicago and Dupont-Rachford Engineering Mathimatics Company. 1980

76. Gato, L.M.C., Henriques, J.C.C. 2005. Dynamic behavior of high-pressure natural-gas flow in pipelines. International Journal of Heat and Fluid Flow 26, 817–825.

77. Chaczykowski, M., 2009. Sensitivity of pipeline gas flow model to the selection of the equation of sate. Journal of chemical engineering research and design 87, 1596–1603.

78. Chaczykowski, M., 2010. Transient flow in natural gas pipeline – The effect of pipeline thermal model. Applied Mathematical Modelling 34, pp 1051–1067

79. Coelho, P. M., Pinho, C., 2007. Considerations about Equations for Steady State Flow in Natural Gas Pipelines. J. of the Braz. Soc. of Mech. Sci. & Eng., Vol. XXIX, No. 3, pp 262-273.

80. Zhou, J., Adewumi, M.A., 1996. Simulation of transient flow in natural gas pipelines, the Pennsylvania State University. Petroleum and Natural Gas Engineering. GRIPA 16802.

81. Abbaspour, M., Chapman, K. S., 2008. Non-isothermal Transient Flow in Natural Gas Pipeline. Journal of Applied Mechanics, ASME, Vol. 75.

82. Adeosun, T. A., Olatunde, O. A., Aderohunmu, J. O., Ogunjare, T. O., 2009. Development of unsteady-state Weymouth equations for gas volumetric flow rate in horizontal and inclined pipes. Journal of Natural Gas Science and Engineering 1, pp 113–117.

83. Behbahani-Nejad, M., Shekari, Y., 2010. The accuracy and efficiency of a reduced-order model for transient flow analysis in gas pipelines. Journal of Petroleum Science and Engineering 73 (1-2), 13-19.

84. Helgaker, J. F., Muller, B., Ytrehus, T., 2014. Transient Flow in Natural Gas Pipelines Using Implicit Finite Difference Schemes. Journal of Offshore Mechanics and Arctic Engineering. ASME, vol. 136

85. Helgaker, J. F., Oosterkamp, A., Langelandsvik, L.I.,Ytrehus, T. 2014. Validation of 1D flow model for high pressure offshore natural gas pipelines. Journal of Natural Gas Science and Engineering 16. 44-56

86. Santos, S.P., 1997. Transient Analysis, a Must in Gas Pipeline Design. Pipeline Simulation Interest Group, Engineering Service of Petrobras - SEGEN

87. Finch, J. F., Ko, D. W., 1988. Tutorial: Fluid Flow Formula. Pipeline Simulation Interest Group

88. Zhang, X., Wu, C., Zuo, L., 2016. Minimizing fuel consumption of a gas pipeline in transient states by dynamic programming. Journal of Natural Gas Science and Engineering 28. 193-203.

89. Zhang, L., 2016. Simulation of the transient flow in a natural gas compression system using a high-order upwind scheme considering the real-gas behaviors. Journal of Natural Gas Science and Engineering 28. 479-490.

90. Chaczykowski, M., Sund, F., Zarodkiewicz, P., Hope, S.M., 2018. Gas composition tracking in transient pipeline flow. Journal of Natural Gas Science and Engineering 55, 321-330.

91. Wulff, W., 1987. Computational Methods for Multiphase Flow. Proceedings of the Second International Workshop on Two-phase Flow Fundamentals, New York, USA, Rensselaer Polytechnic Institute.

92. Menon, E. S., 2005. Gas pipeline hydraulics. Taylor & Francis Group, LLC.

93. Mohitpour, M., Golshan, H., Murray, A., 2007. Pipeline Design and Construction: A Practical Approach. 2nd Edition.

94. White, F. M., 1999, Viscous Fluid Flow, McGraw-Hill, NY.

94 Sani, F. M., Huiainga, S., Esaklul, K. A., Nestic, S., 2019. Review of the API RP 14E erosional velocity equation: Origin, applications, misuses, limitations and alternatives. An International Journal on the Science and Technology of Friction, Lubrication and Wear, 426–427 (2019) 620–636.

96. Alghlam, A. S., Stevanovic, V. D., Elgazdori, E. A., Banjac, M., 2019. Numerical Simulation of Natural Gas Pipeline Transients. Journal of Energy Resources Technology, ASME, Vol. 141, article No. 102002, pp. 1-14.

97. Behbahani-Nejad, M., Bagheri, A. 2008. A MATLAB Simulink Library for Transient Flow Simulation of Gas Networks. World Academy of Science, International Journal of Mechanical, Aerospace, Industrial, Mechatronic and Manufacturing Engineering Vol. 2, No:7.

98. Ke, S.L., Ti, H.C., 2000. Transient analysis of isothermal gas flow in pipeline network. Chemical Engineering Journal 76, 169-177.

99. Eni Gas B.V., 2007, Western Libya Gas Project, Onshore Pipelines, Ar Ruways Branch Line, Final Document. Book No: 1/1.Vol. 15.

100. Rohsenow, W. M., and Hartnett, J. P., 1998, Handbook of Heat Transfer, Y.I. Cho. 3rd ed., McGraw-Hill.

101. Badache, M., Eslami-Nejad, P., Ouzzane, M., Aidoun, Z., and Lamarche, L., 2016. A new modeling approach for improved ground temperature profile determination. Renewable Energy, 85, pp. 436-444.

102. Jia, W, Li, C., and Wu, X., 2014. Internal Surface Absolute Roughness for Large-Diameter Natural Gas Transmission Pipelines. Oil Gas European Magazine, 4, pp. 1-3.

APPENDIX A-1

FLOW GOVERNING EQUATIONS

- **Continuity Equation**

In figure A1 below, the control volume of the continuity is shown, where the conservation of mass can be written as follows:

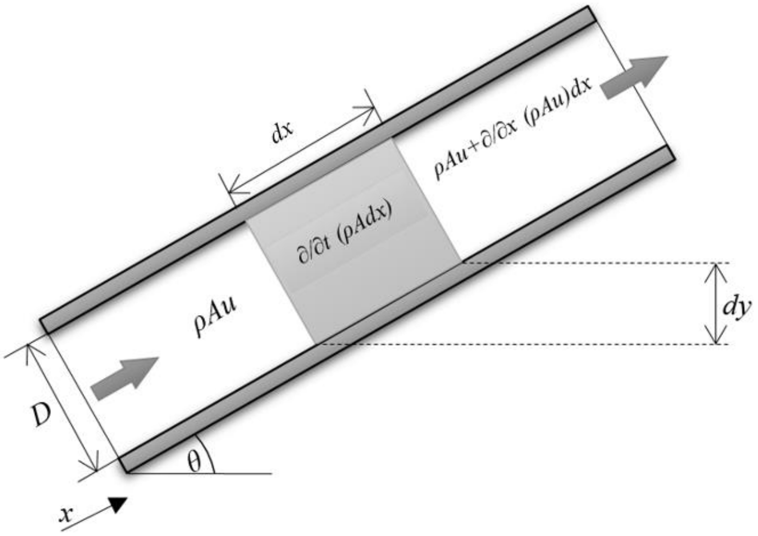

Figure A1 Control volume of continuity equation

$$\rho Au - \rho Au - \frac{\partial}{\partial x}(\rho Au)dx = \frac{\partial}{\partial t}(\rho Adx) \qquad \text{(A-1)}$$

$$\frac{\partial}{\partial x}(\rho Au)dx + \frac{\partial}{\partial t}(\rho Adx) = 0$$

$$\frac{\partial}{\partial x}(\rho u)dx + \frac{\partial}{\partial t}(\rho dx) = 0$$

$$\left[u\frac{\partial \rho}{\partial x} + \rho\frac{\partial u}{\partial x}\right]dx + \frac{\partial \rho}{\partial t}dx = 0$$

$$u\frac{\partial \rho}{\partial x} + \rho\frac{\partial u}{\partial x} + \frac{\partial \rho}{\partial t} = 0$$

$$\frac{D\rho}{Dt} + \rho\frac{\partial u}{\partial x} = 0 \qquad \text{(A-2)}$$

- **Momentum Equation**

For the control volume illustrated in figure A2, and using the following force component summation, the momentum equation can be written as below:

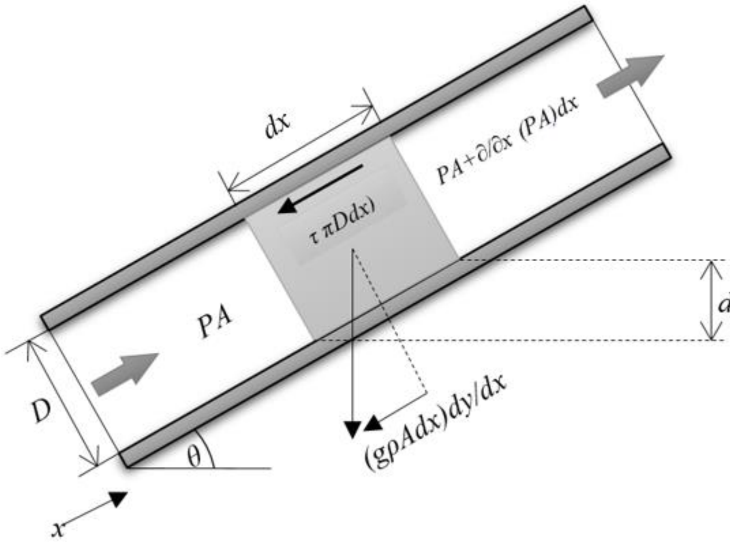

Figure A2 Control volume of momentum equation

$$pA - pA - \frac{\partial}{\partial x}(pA)dx - \tau\pi Ddx - \rho gAdx\left(\frac{dy}{dx}\right) = (\rho Adx)\left(u\frac{\partial u}{\partial x} + \frac{\partial u}{\partial t}\right)$$

Dividing by dx and the cross section area A leads to

$$-\frac{\partial p}{\partial x} - \frac{\tau\pi D}{A} - \rho g\left(\frac{dy}{dx}\right) = \rho\left(u\frac{\partial u}{\partial x} + \frac{\partial u}{\partial t}\right)$$

where: the hydraulic diameter D_H equals the pipeline inner diameter D in case of pipe flow;

u is the absolute value of flow velocity;

τ is the shear stress between the fluid and pipe wall which can be obtained by the next equation:

$$\tau = \frac{f\rho u|u|}{8} \quad \text{(A-3)}$$

f is the Darcy friction factor

Introducing $\left(\frac{dy}{dx}\right) = \sin\theta$ and the cross section area of pipe $A = \frac{\pi}{4}D_H^2$ the following equation is obtained

$$-\frac{\partial p}{\partial x} - \frac{f\rho u|u|\pi D_H}{8\frac{\pi}{4}D_H^2} - \rho g\sin\theta = \rho\frac{Du}{Dt}$$

Dividing by ρ

$$-\frac{1}{\rho}\frac{\partial p}{\partial x}-\frac{f\,u|u|}{2D_H}-g\sin\theta=\frac{Du}{Dt}$$

and the final form of the momentum equation reads

$$\frac{Du}{Dt}+\frac{1}{\rho}\frac{\partial p}{\partial x}+\frac{f\,u|u|}{2D_H}+g\sin\theta=0 \qquad \text{(A-4)}$$

- **Conservation of Energy**

The basic form of energy equation is written for the control volume illustrated in figure A3 by applying the first law of thermodynamics

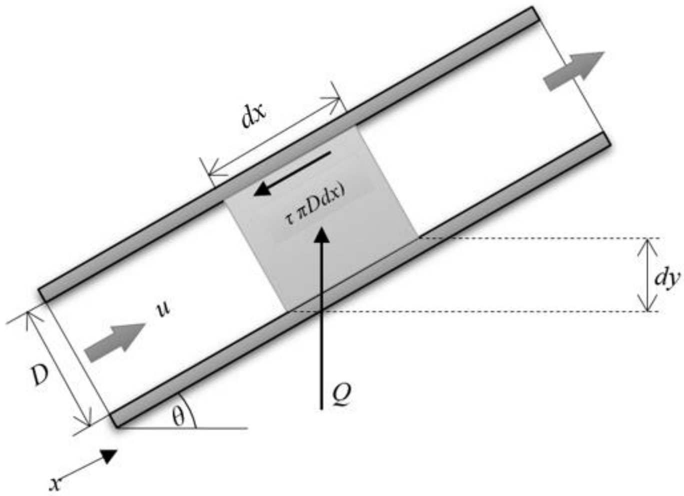

Figure A3 Control volume of energy equation

$$\dot{Q}=\dot{q}Adx=\frac{\partial}{\partial t}\left[\rho Adx\left(e+\frac{u^2}{2}+gy\right)\right]+\frac{\partial}{\partial x}\left[\rho uA\left(e+\frac{u^2}{2}+gy+\frac{p}{\rho}\right)\right]dx \qquad \text{(A-5)}$$

where: $\dot{q}$ is the heat transfer per unit volume, W/m^3, e is the internal energy per unit mass in J/kg and Q is the heat transfer in W. The separation of the second term leads to

$$\dot{Q}=\dot{q}Adx=\rho Adx\left[\frac{\partial}{\partial t}\left(e+\frac{u^2}{2}+gy\right)+u\frac{\partial}{\partial x}\left(e+\frac{u^2}{2}+gy\right)\right]+$$

$$\left[\left(e+\frac{u^2}{2}+gy\right)\left(\frac{\partial(\rho A)}{\partial t}+\frac{\partial(\rho uA)}{\partial x}\right)\right]dx+\left[\frac{p}{\rho}\frac{\partial(\rho uA)}{\partial x}+(\rho uA)\frac{\partial}{\partial x}\left(\frac{p}{\rho}\right)\right]dx$$

From continuity equation (A-2), the term $\left(\frac{\partial(\rho A)}{\partial t}+\frac{\partial(\rho uA)}{\partial x}\right)=0$ and

dividing by ρAdx the energy equation reduces to

$$\frac{\dot{q}}{\rho} = \frac{D}{Dt}\left(e + \frac{u^2}{2} + gy\right) + \frac{p}{\rho A}\frac{\partial(uA)}{\partial x} + \frac{u}{\rho}\frac{\partial p}{\partial x}$$

From momentum equation (A-4) and multiplying by *u* it is obtained

$$u\frac{\partial u}{\partial t} + u^2\frac{\partial u}{\partial x} + \frac{u}{\rho}\frac{\partial p}{\partial x} = -\frac{uw}{\rho A} - ug\sin\theta \qquad \text{(A-6)}$$

where w is a work of frictional force per unit length of pipe $w = \frac{f\rho u|u|}{8}\pi\ D_H$

The above equation is written as

$$\frac{u}{\rho}\frac{\partial p}{\partial x} = -u\frac{Du}{Dt} - \frac{wu}{\rho A} - ug\sin\theta$$

The continuity equation (A-2) is written as

$$\frac{\partial}{\partial x}(uA) = -\frac{A}{\rho}\frac{D\rho}{Dt}$$

Introduction of the above momentum and continuity equations in the energy equation (A-6) leads to

$$\frac{\dot{q}}{\rho} = \frac{D}{Dt}\left(e + \frac{u^2}{2} + gy\right) - \frac{p}{\rho^2}\frac{D\rho}{Dt} - u\frac{Du}{Dt} - \frac{wu}{\rho A} - ug\sin\theta$$

On the other hand, it is known that $\left(\frac{dy}{dx}\right) = sin\theta$, so, we can consider the following equation:

$\frac{D}{Dt}(gy) = g\left(\frac{\partial y}{\partial t} + u\frac{dy}{dx}\right) = gusin\theta$ and $\frac{D}{Dt}\left(\frac{u^2}{2}\right) = u\frac{Du}{Dt}$

Introduction of these two relations into energy equation gives

$$\frac{\dot{q}}{\rho} = \frac{De}{Dt} - \frac{p}{\rho^2}\frac{D\rho}{Dt} - \frac{uw}{\rho A}$$

Introducing enthalpy as $h = e + \frac{p}{\rho}$ and its material derivative as

$\frac{Dh}{Dt} = \frac{De}{Dt} + \frac{D}{Dt}\left(\frac{p}{\rho}\right)$ the final form of energy equation is obtained as

$$\frac{Dh}{Dt} - \frac{1}{\rho}\frac{Dp}{Dt} - \frac{fu^2|u|}{2D_H} - \frac{\dot{q}}{\rho} = 0 \qquad \text{(A-7)}$$

APPENDIX A-2

DETERMINING THE SPEED OF SOUND

The speed of sound is defined under the assumption of an isentropic propagation of infinitesimal mechanical disturbance in an elastic medium, with the following equation

$$c^2 = \left(\frac{\partial p}{\partial \rho}\right)_s . \tag{A-8}$$

By using the coupling between the density and specific volume, ($\rho = \frac{1}{v}$) the velocity of sound can be expressed as a function of the pressure and specific volume as

$$c^2 = -v^2 \left(\frac{\partial p}{\partial v}\right)_s . \tag{A-9}$$

For the purposes of the calculation with the GTA code developed in this thesis, the following derivation is introduced.

The equation of state v=v(p,h) is derived

$$dv = \left(\frac{\partial v}{\partial p}\right)_h dp + \left(\frac{\partial v}{\partial h}\right)_p dh . \tag{A-10}$$

Since the definition of the speed of sound indicates that the square of the speed of sound equals partial derivative of pressure with respect to density at constant entropy, the second law of thermodynamics is taken into account ($ds = \frac{\delta q}{T}$) followed by $\delta q = 0$. Further, inclusion of this equality in the first law of thermodynamics ($\delta q = du + pdv$), and by using the definition of enthalpy ($dh = du + d(pv)$), the following equation is derived

$$dh = vdp . \tag{A-11}$$

Substituting equation (A-11) into equation (A-10) gives

$$\left(\frac{\partial v}{\partial p}\right)_s = \left(\frac{\partial v}{\partial p}\right)_h + v\left(\frac{\partial v}{\partial h}\right)_p , \tag{A-12}$$

which is further introduced into equation (A-9) and we get the equation for the determination of the speed of sound as a function of pressure and enthalpy

$$c = \sqrt{\frac{-1}{\frac{1}{v^2}\left(\frac{\partial v}{\partial p}\right)_h + \frac{1}{v}\left(\frac{\partial v}{\partial h}\right)_p}}\,. \tag{A-13}$$

In case of gas flow Eq. (A-21) can be further simplified by introducing the assumption of applicability of the ideal gas low. The ideal gas law is introduced in the form

$$v = R_g T / p = R_g h / (c_p p) \tag{A-14}$$

where the gas constant is the ratio of the universal gas constant R and the molar mass M, i.e. R_g=R/M. Derivative of the specific volume v by p under constant h reads

$$\left(\frac{\partial v}{\partial p}\right)_h = -\frac{R_g h}{c_p p^2} \tag{A-15}$$

and derivative by h under constant p reads

$$\left(\frac{\partial v}{\partial h}\right)_p = \frac{R_g}{c_p p} \tag{A-16}$$

Introduction of Eqs. (A-15) and (A-16) into (A-13) and application of the relation $R_g = c_p - c_v$ leads to

$$c = \sqrt{\kappa R_g T} \tag{A-17}$$

where $\kappa = c_p / c_v$.

APPENDIX A-3

DETERMINING THE CONSTANT C_1

In many references, C_1 is given only in USCS (United States Customary System) units and it has not been found in SI units. Because the code works in SI units, hence, it is necessary to determine constant C_1 in SI units.

From (Menon, 2005) [92], it is found that in USCS units the compressibility factor of natural gas flow in pipeline is given by the CNGA method, equation (3-20):

$$z = \frac{1}{\left[1 + \left(\frac{p\ C_1 (10)^{1.785G}}{T^{3.825}}\right)\right]}$$

where in the USCS $C_1 = 344400$

From the same reference (Menon, 2005) [92] and from example 12 chapter 1:

T = 530 R, G = 0.6 and P = 1200 Psig

So, the calculation of compressibility factor results to, *Z = 0.844*

To determine C_1 in SI units, all variable must be converted to SI units as following:

T = 294.26 K, G = 0.6 and P = 8273.71 kPa.

Substitute these variables in equation (3-20):

$$0.844 = \frac{1}{\left[1 + \left(\frac{8273.71 \times C_1 (10)^{1.785 \times 0.6}}{294.26^{3.825}}\right)\right]}$$

So, in SI units $C_1 = 5260$

APPENDIX A-4

DETERMINING THE CONSTANT C_2

As same in the previous section, the constant C_2 is given only in USCS units in many references and it has been found in SI units. Again, the GTA code works in SI units, hence, constant C_2 must be determined in SI units.

From section 2.7 in reference [92], it is found that in USCS units the maximum velocity of natural gas flow in pipeline is given in equation (3-32):

$$u_{max} = \frac{C_2}{\sqrt{\rho}} = C_2 \sqrt{\frac{zRT}{29Gp}}$$

Where in USCS $C_2 = 100$

From the same reference [92] and from example 1 in section 2.7:

Z=0.9, R = 10.73 psia. ft^3/ lb mol.°R, T = 520 R, G = 0.6, and P = 1014.7 Psia

So, the calculated maximum velocity is, $u_{max} = 53.33$ *ft/sec*

To determine C_2 in SI units, all variables must be converted to SI units as following:

Z = 0.9, R = 8.314 kPa.m^3/kmol.K, T = 288.7 K, G = 0.6, P = 6996.1 kPa and

u_{max}= 16.255 m/sec.

Substitute these variables in equation (3-34):

$$16.255 = C_2 \sqrt{\frac{0.9 \times 8.314 \times 288.7}{29 \times 0.6 \times 6996.1}}$$

So, in SI units C_2 = 122

APPENDIX B

CASES OF STUDY CALCULATION RESULTS

Chapter 5: Code Validation

- **Case 1:** (grid independency of Code)

  8 segments (9 nodes)

Time (s)	M (kg/s)	V (MMSCMD)
26.2	14.497	1.521435
282.7	14.497	1.521435
539.2	14.497	1.521435
795.7	14.497	1.521435
1052.2	14.522	1.524045
1308.7	14.668	1.539287
1565.1	14.938	1.567474
1821.5	15.329	1.608293
2077.9	15.748	1.652035
2334.2	15.867	1.664458
2590.6	15.728	1.649947
2847	15.4	1.615705
3103.4	14.958	1.569562
3359.8	14.451	1.516633
3616.4	13.935	1.462764
3872.9	13.462	1.413385
4129.6	13.171	1.383006
4386.2	13.262	1.392506
4642.8	13.598	1.427583
4899.4	13.847	1.453578
5156	14.015	1.471116
5412.5	14.13	1.483122
5669	14.22	1.492517
5925.6	14.314	1.502331

- 160 segments (161 nodes)

Time (s)	M (kg/s)	V (MMSCMD)
0	14.504	1.522166
13.1	14.505	1.52227
26	14.504	1.522166
38.8	14.504	1.522166
51.6	14.504	1.522166
64.4	14.504	1.522166
77.3	14.504	1.522166
90.1	14.506	1.522375
102.9	14.505	1.52227
115.7	14.504	1.522166
128.6	14.506	1.522375
141.4	14.505	1.52227
154.2	14.505	1.52227
167	14.505	1.52227
179.9	14.505	1.52227
192.7	14.506	1.522375
205.5	14.505	1.52227
218.3	14.506	1.522375
231.2	14.505	1.52227
244	14.505	1.52227
256.8	14.506	1.522375
269.6	14.504	1.522166
282.5	14.505	1.52227
295.3	14.505	1.52227
308.1	14.506	1.522375
320.9	14.505	1.52227
333.7	14.505	1.52227
346.6	14.505	1.52227
359.4	14.505	1.52227
372.2	14.506	1.522375
385	14.504	1.522166
397.9	14.505	1.52227
410.7	14.505	1.52227
423.5	14.504	1.522166
436.3	14.505	1.52227
449.2	14.504	1.522166
462	14.505	1.52227
474.8	14.505	1.52227
487.6	14.505	1.52227
500.4	14.505	1.52227
513.3	14.505	1.52227
526.1	14.505	1.52227
538.9	14.506	1.522375
551.7	14.505	1.52227
564.6	14.505	1.52227
577.4	14.505	1.52227

590.2	14.504	1.522166
603	14.504	1.522166
615.9	14.505	1.52227
628.7	14.506	1.522375
641.5	14.505	1.52227
654.3	14.505	1.52227
667.2	14.504	1.522166
680	14.506	1.522375
692.8	14.504	1.522166
705.6	14.506	1.522375
718.4	14.505	1.52227
731.3	14.505	1.52227
744.1	14.505	1.52227
756.9	14.504	1.522166
769.7	14.504	1.522166
782.6	14.504	1.522166
795.4	14.504	1.522166
808.2	14.505	1.52227
821	14.504	1.522166
833.9	14.501	1.521853
846.7	14.5	1.521748
859.5	14.498	1.52154
872.3	14.498	1.52154
885.2	14.499	1.521644
898	14.5	1.521748
910.8	14.5	1.521748
923.6	14.502	1.521957
936.4	14.505	1.52227
949.3	14.506	1.522375
962.1	14.507	1.522479
974.9	14.51	1.522792
987.7	14.513	1.523106
1000.6	14.517	1.523523
1013.4	14.521	1.523941
1026.2	14.524	1.524254
1039	14.528	1.524672
1051.9	14.532	1.525089
1064.7	14.536	1.525507
1077.5	14.544	1.526342
1090.4	14.546	1.526551
1103.2	14.551	1.527073
1116	14.557	1.527699
1128.9	14.561	1.528117
1141.7	14.568	1.528847
1154.5	14.573	1.529369
1167.3	14.579	1.529996
1180.2	14.585	1.530622
1193	14.592	1.531353

1205.8	14.6	1.532188
1218.7	14.608	1.533023
1231.5	14.619	1.534172
1244.3	14.627	1.535007
1257.1	14.639	1.53626
1270	14.65	1.537408
1282.8	14.66	1.538452
1295.6	14.672	1.539705
1308.5	14.682	1.540749
1321.3	14.693	1.541897
1334.1	14.7	1.542628
1346.9	14.71	1.543672
1359.8	14.721	1.54482
1372.6	14.731	1.545864
1385.4	14.744	1.547221
1398.2	14.757	1.548578
1411	14.773	1.550249
1423.8	14.789	1.551919
1436.7	14.805	1.553589
1449.5	14.817	1.554842
1462.3	14.83	1.556199
1475.1	14.843	1.557556
1487.9	14.854	1.558705
1500.7	14.868	1.560166
1513.6	14.883	1.561732
1526.4	14.901	1.563611
1539.2	14.92	1.565595
1552	14.94	1.567683
1564.8	14.957	1.569458
1577.7	14.971	1.570919
1590.5	14.984	1.572276
1603.3	14.999	1.573842
1616.1	15.016	1.575617
1628.9	15.036	1.577705
1641.7	15.059	1.580106
1654.6	15.08	1.582298
1667.4	15.1	1.584386
1680.2	15.117	1.586161
1693	15.132	1.587727
1705.8	15.149	1.589502
1718.6	15.171	1.591798
1731.5	15.197	1.594513
1744.3	15.219	1.59681
1757.1	15.24	1.599002
1769.9	15.257	1.600777
1782.7	15.276	1.60276
1795.5	15.297	1.604952
1808.4	15.325	1.607876

1821.2	15.35	1.610485
1834	15.373	1.612887
1846.8	15.394	1.615079
1859.6	15.414	1.617167
1872.5	15.436	1.619464
1885.3	15.464	1.622387
1898.1	15.492	1.62531
1910.9	15.513	1.627502
1923.7	15.536	1.629903
1936.5	15.558	1.6322
1949.4	15.588	1.635332
1962.2	15.618	1.638464
1975	15.643	1.641074
1987.8	15.668	1.643684
2000.6	15.69	1.64598
2013.4	15.721	1.649217
2026.3	15.709	1.647964
2039.1	15.725	1.649634
2051.9	15.737	1.650887
2064.7	15.749	1.65214
2077.5	15.767	1.654019
2090.3	15.78	1.655376
2103.2	15.792	1.656629
2116	15.801	1.657568
2128.8	15.813	1.658821
2141.6	15.822	1.659761
2154.4	15.832	1.660805
2167.3	15.844	1.662057
2180.1	15.853	1.662997
2192.9	15.862	1.663936
2205.7	15.868	1.664563
2218.5	15.873	1.665085
2231.3	15.877	1.665502
2244.2	15.881	1.66592
2257	15.883	1.666129
2269.8	15.884	1.666233
2282.6	15.885	1.666338
2295.4	15.885	1.666338
2308.2	15.884	1.666233
2321.1	15.885	1.666338
2333.9	15.883	1.666129
2346.7	15.879	1.665711
2359.5	15.875	1.665294
2372.3	15.87	1.664772
2385.1	15.865	1.66425
2398	15.858	1.663519
2410.8	15.852	1.662892
2423.6	15.844	1.662057

2436.4	15.834	1.661013
2449.2	15.825	1.660074
2462.1	15.814	1.658925
2474.9	15.802	1.657673
2487.7	15.789	1.656315
2500.5	15.777	1.655063
2513.3	15.764	1.653706
2526.1	15.787	1.656107
2539	15.783	1.655689
2551.8	15.777	1.655063
2564.6	15.766	1.653914
2577.4	15.75	1.652244
2590.2	15.736	1.650782
2603	15.722	1.649321
2615.9	15.709	1.647964
2628.7	15.695	1.646502
2641.5	15.681	1.645041
2654.3	15.665	1.64337
2667.1	15.65	1.641804
2679.9	15.636	1.640343
2692.8	15.62	1.638672
2705.6	15.603	1.636898
2718.4	15.588	1.635332
2731.2	15.573	1.633766
2744	15.554	1.631782
2756.9	15.535	1.629799
2769.7	15.518	1.628024
2782.5	15.501	1.626249
2795.3	15.482	1.624266
2808.1	15.461	1.622073
2820.9	15.444	1.620299
2833.8	15.424	1.618211
2846.6	15.404	1.616123
2859.4	15.384	1.614035
2872.2	15.362	1.611738
2885	15.341	1.609546
2897.8	15.321	1.607458
2910.7	15.301	1.60537
2923.5	15.28	1.603178
2936.3	15.258	1.600881
2949.1	15.233	1.598271
2961.9	15.212	1.596079
2974.7	15.19	1.593782
2987.6	15.168	1.591485
3000.4	15.148	1.589397
3013.2	15.123	1.586787
3026	15.099	1.584282
3038.8	15.076	1.581881

3051.7	15.052	1.579375
3064.5	15.029	1.576974
3077.3	15.006	1.574573
3090.1	14.981	1.571963
3102.9	14.955	1.569249
3115.7	14.93	1.566639
3128.6	14.907	1.564238
3141.4	14.884	1.561837
3154.2	14.86	1.559331
3167	14.834	1.556617
3179.8	14.807	1.553798
3192.6	14.782	1.551188
3205.5	14.757	1.548578
3218.3	14.733	1.546073
3231.1	14.707	1.543359
3243.9	14.682	1.540749
3256.7	14.655	1.53793
3269.5	14.63	1.53532
3282.4	14.606	1.532814
3295.2	14.579	1.529996
3308	14.553	1.527281
3320.8	14.526	1.524463
3333.6	14.499	1.521644
3346.5	14.475	1.519139
3359.3	14.45	1.516529
3372.1	14.424	1.513814
3384.9	14.398	1.5111
3397.7	14.371	1.508281
3410.5	14.344	1.505463
3423.4	14.319	1.502853
3436.2	14.293	1.500138
3449	14.268	1.497528
3461.8	14.242	1.494814
3474.6	14.215	1.491995
3487.4	14.188	1.489177
3500.3	14.163	1.486567
3513.1	14.138	1.483957
3525.9	14.112	1.481243
3538.7	14.086	1.478528
3551.5	14.062	1.476023
3564.3	14.035	1.473204
3577.2	14.009	1.47049
3590	13.984	1.46788
3602.8	13.96	1.465374
3615.6	13.935	1.462764
3628.4	13.909	1.46005
3641.3	13.883	1.457336
3654.1	13.859	1.45483

3666.9	13.836	1.452429
3679.7	13.811	1.449819
3692.5	13.786	1.447209
3705.3	13.761	1.444599
3718.2	13.736	1.44199
3731	13.711	1.43938
3743.8	13.689	1.437083
3756.6	13.667	1.434786
3769.4	13.643	1.432281
3782.3	13.619	1.429775
3795.1	13.594	1.427165
3807.9	13.571	1.424764
3820.8	13.551	1.422676
3833.6	13.53	1.420484
3846.5	13.51	1.418396
3859.3	13.487	1.415995
3872.1	13.465	1.413698
3885	13.44	1.411088
3897.8	13.416	1.408583
3910.7	13.397	1.406599
3923.5	13.378	1.404616
3936.4	13.359	1.402632
3949.2	13.339	1.400544
3962	13.318	1.398352
3974.9	13.297	1.39616
3987.7	13.276	1.393967
4000.6	13.257	1.391984
4013.4	13.24	1.390209
4026.2	13.232	1.389374
4039.1	13.224	1.388539
4051.9	13.217	1.387808
4064.8	13.21	1.387077
4077.6	13.203	1.386346
4090.5	13.195	1.385511
4103.3	13.19	1.384989
4116.1	13.184	1.384363
4129	13.181	1.38405
4141.8	13.177	1.383632
4154.7	13.176	1.383528
4167.5	13.174	1.383319
4180.3	13.173	1.383214
4193.2	13.175	1.383423
4206	13.176	1.383528
4218.9	13.178	1.383736
4231.7	13.179	1.383841
4244.6	13.182	1.384154
4257.4	13.187	1.384676
4270.2	13.188	1.38478

4283.1	13.194	1.385407
4295.9	13.202	1.386242
4308.8	13.207	1.386764
4321.6	13.217	1.387808
4334.4	13.222	1.38833
4347.3	13.232	1.389374
4360.1	13.241	1.390313
4373	13.253	1.391566
4385.8	13.267	1.393028
4398.7	13.283	1.394698
4411.5	13.299	1.396368
4424.3	13.319	1.398456
4437.2	13.337	1.400335
4450	13.355	1.402215
4462.9	13.368	1.403572
4475.7	13.383	1.405138
4488.5	13.401	1.407017
4501.4	13.423	1.409313
4514.2	13.448	1.411923
4527.1	13.465	1.413698
4539.9	13.485	1.415786
4552.8	13.5	1.417352
4565.6	13.518	1.419231
4578.4	13.529	1.42038
4591.3	13.54	1.421528
4604.1	13.555	1.423094
4617	13.571	1.424764
4629.8	13.587	1.426435
4642.7	13.605	1.428314
4655.5	13.622	1.430088
4668.3	13.64	1.431968
4681.2	13.657	1.433742
4694	13.667	1.434786
4706.9	13.678	1.435935
4719.7	13.689	1.437083
4732.5	13.7	1.438231
4745.4	13.712	1.439484
4758.2	13.726	1.440946
4771.1	13.739	1.442303
4783.9	13.755	1.443973
4796.8	13.769	1.445435
4809.6	13.781	1.446687
4822.4	13.795	1.448149
4835.3	13.805	1.449193
4848.1	13.816	1.450341
4861	13.825	1.451281
4873.8	13.834	1.45222
4886.6	13.841	1.452951

4899.5	13.85	1.453891
4912.3	13.859	1.45483
4925.2	13.867	1.455666
4938	13.88	1.457023
4950.9	13.889	1.457962
4963.7	13.901	1.459215
4976.5	13.912	1.460363
4989.4	13.922	1.461407
5002.2	13.933	1.462556
5015.1	13.942	1.463495
5027.9	13.952	1.464539
5040.7	13.958	1.465166
5053.6	13.966	1.466001
5066.4	13.974	1.466836
5079.3	13.979	1.467358
5092.1	13.985	1.467984
5105	13.991	1.468611
5117.8	13.996	1.469133
5130.6	14.003	1.469863
5143.5	14.009	1.47049
5156.3	14.015	1.471116
5169.2	14.022	1.471847
5182	14.029	1.472578
5194.8	14.037	1.473413
5207.7	14.045	1.474248
5220.5	14.052	1.474979
5233.4	14.059	1.47571
5246.2	14.067	1.476545
5259.1	14.074	1.477276
5271.9	14.08	1.477902
5284.7	14.087	1.478633
5297.6	14.092	1.479155
5310.4	14.098	1.479781
5323.3	14.103	1.480303
5336.1	14.108	1.480825
5349	14.113	1.481347
5361.8	14.117	1.481765
5374.6	14.122	1.482287
5387.5	14.126	1.482704
5400.3	14.131	1.483226
5413.2	14.134	1.483539
5426	14.138	1.483957
5438.8	14.143	1.484479
5451.7	14.148	1.485001
5464.5	14.151	1.485314
5477.4	14.155	1.485732
5490.2	14.159	1.486149
5503.1	14.163	1.486567

5515.9	14.167	1.486984
5528.7	14.173	1.487611
5541.6	14.178	1.488133
5554.4	14.183	1.488655
5567.3	14.188	1.489177
5580.1	14.194	1.489803
5592.9	14.199	1.490325
5605.8	14.205	1.490952
5618.6	14.21	1.491474
5631.5	14.215	1.491995
5644.3	14.22	1.492517
5657.2	14.225	1.493039
5670	14.23	1.493561
5682.8	14.236	1.494188
5695.7	14.24	1.494605
5708.5	14.243	1.494919
5721.4	14.248	1.495441
5734.2	14.252	1.495858
5747	14.256	1.496276
5759.9	14.261	1.496798
5772.7	14.265	1.497215
5785.6	14.269	1.497633
5798.4	14.273	1.49805
5811.3	14.277	1.498468
5824.1	14.28	1.498781
5836.9	14.284	1.499199
5849.8	14.289	1.499721
5862.6	14.294	1.500243
5875.5	14.297	1.500556
5888.3	14.303	1.501182
5901.1	14.307	1.5016
5914	14.311	1.502018
5926.8	14.317	1.502644
5939.7	14.323	1.50327
5952.5	14.33	1.504001
5965.4	14.336	1.504627
5978.2	14.343	1.505358
6000	14.35	1.506089

Note: because of the huge number of data, the other results of this calculation of code stability (code validation-case1) for 320 segments (321 nodes) are in the CD.

- **Case 2:** Single pipeline
    - Pressure at the pipeline outlet

Time (s)	Time (hr)	Pressure (MPa)
0	0	2.6226
398.8	0.110778	2.6227
656.2	0.182278	2.6227
913.6	0.253778	2.6228
1171.1	0.325306	2.6228
1428.5	0.396806	2.6229
1685.9	0.468306	2.6229
1943.4	0.539833	2.623
2200.8	0.611333	2.623
2458.3	0.682861	2.6231
2715.7	0.754361	2.6231
2973.2	0.825889	2.6232
3230.6	0.897389	2.6232
3488	0.968889	2.6232
3745.5	1.040417	2.6233
4002.9	1.111917	2.6233
4260.4	1.183444	2.6234
4517.8	1.254944	2.6234
4775.2	1.326444	2.6234
5032.6	1.397944	2.6234
5290.1	1.469472	2.6236
5547.5	1.540972	2.6238
5804.9	1.612472	2.6241
6062.3	1.683972	2.6247
6319.7	1.755472	2.6254
6577.2	1.827	2.6263
6834.6	1.8985	2.6274
7092	1.97	2.6287
7349.4	2.0415	2.6301
7606.9	2.113028	2.6318
7864.3	2.184528	2.6336
8121.7	2.256028	2.6355
8379.1	2.327528	2.6377
8636.5	2.399028	2.64
8894	2.470556	2.6424
9151.4	2.542056	2.645
9408.8	2.613556	2.6477
9666.2	2.685056	2.6505
9923.7	2.756583	2.6534
10181.1	2.828083	2.6565
10438.5	2.899583	2.6595
10695.9	2.971083	2.6627
10953.3	3.042583	2.6659
11210.8	3.114111	2.6691

11468.2	3.185611	2.6724
11725.6	3.257111	2.6756
11983	3.328611	2.6788
12240.4	3.400111	2.682
12497.9	3.471639	2.6851
12755.3	3.543139	2.6882
13012.7	3.614639	2.6912
13270.1	3.686139	2.6941
13527.6	3.757667	2.6968
13785	3.829167	2.6995
14042.4	3.900667	2.702
14299.8	3.972167	2.7044
14557.2	4.043667	2.7066
14814.7	4.115194	2.7086
15072.1	4.186694	2.7105
15329.5	4.258194	2.7122
15586.9	4.329694	2.7149
15844.4	4.401222	2.7188
16101.8	4.472722	2.7232
16359.2	4.544222	2.7278
16616.6	4.615722	2.7325
16874	4.687222	2.7372
17131.5	4.75875	2.742
17388.9	4.83025	2.7467
17646.3	4.90175	2.7513
17903.7	4.97325	2.7558
18161.2	5.044778	2.7602
18418.6	5.116278	2.7645
18676	5.187778	2.7687
18933.4	5.259278	2.7728
19190.8	5.330778	2.7767
19448.3	5.402306	2.7804
19705.7	5.473806	2.7841
19963.1	5.545306	2.7876
20220.5	5.616806	2.7909
20477.9	5.688306	2.7942
20735.4	5.759833	2.7973
20992.8	5.831333	2.8003
21250.2	5.902833	2.8032
21507.6	5.974333	2.8059
21765.1	6.045861	2.8086
22022.5	6.117361	2.8111
22279.9	6.188861	2.8136
22537.3	6.260361	2.8159
22794.7	6.331861	2.8182
23052.2	6.403389	2.8204
23309.6	6.474889	2.8225
23567	6.546389	2.8244

23824.4	6.617889	2.8263
24081.9	6.689417	2.8281
24339.3	6.760917	2.8299
24596.7	6.832417	2.8315
24854.1	6.903917	2.833
25111.5	6.975417	2.8344
25369	7.046944	2.8357
25626.4	7.118444	2.8369
25883.8	7.189944	2.8379
26141.2	7.261444	2.8388
26398.7	7.332972	2.8395
26656.1	7.404472	2.8401
26913.5	7.475972	2.8405
27170.9	7.547472	2.8407
27428.3	7.618972	2.8407
27685.8	7.6905	2.8405
27943.2	7.762	2.84
28200.6	7.8335	2.8392
28458	7.905	2.8382
28715.4	7.9765	2.8368
28972.9	8.048028	2.8366
29230.3	8.119528	2.8363
29487.7	8.191028	2.8359
29745.1	8.262528	2.8351
30002.6	8.334056	2.8341
30260	8.405556	2.8328
30517.4	8.477056	2.8311
30774.8	8.548556	2.8291
31032.2	8.620056	2.8268
31289.7	8.691583	2.8241
31547.1	8.763083	2.8212
31804.5	8.834583	2.818
32061.9	8.906083	2.8145
32319.4	8.977611	2.8108
32576.8	9.049111	2.8069
32834.2	9.120611	2.8028
33091.6	9.192111	2.7985
33349	9.263611	2.7941
33606.5	9.335139	2.7897
33863.9	9.406639	2.7851
34121.3	9.478139	2.7804
34378.7	9.549639	2.7758
34636.2	9.621167	2.7711
34893.6	9.692667	2.7664
35151	9.764167	2.7618
35408.4	9.835667	2.7571
35665.8	9.907167	2.7526
35923.3	9.978694	2.7481

36180.7	10.05019	2.7437
36438.1	10.12169	2.7393
36695.5	10.19319	2.7351
36952.9	10.26469	2.7309
37210.4	10.33622	2.7269
37467.8	10.40772	2.7229
37725.2	10.47922	2.7191
37982.6	10.55072	2.7154
38240.1	10.62225	2.7117
38497.5	10.69375	2.7082
38754.9	10.76525	2.7047
39012.3	10.83675	2.7014
39269.7	10.90825	2.6981
39527.2	10.97978	2.6949
39784.6	11.05128	2.6917
40042	11.12278	2.6886
40299.4	11.19428	2.6855
40556.9	11.26581	2.6824
40814.3	11.33731	2.6794
41071.7	11.40881	2.6763
41329.1	11.48031	2.6732
41586.5	11.55181	2.6701
41844	11.62333	2.6669
42101.4	11.69483	2.6637
42358.8	11.76633	2.6604
42616.2	11.83783	2.657
42873.7	11.90936	2.6535
43131.1	11.98086	2.65
43388.5	12.05236	2.6449
43645.9	12.12386	2.6413
43903.3	12.19536	2.6381
44160.8	12.26689	2.6351
44418.2	12.33839	2.6324
44675.6	12.40989	2.6299
44933	12.48139	2.6276
45190.4	12.55289	2.6254
45447.9	12.62442	2.6234
45705.3	12.69592	2.6215
45962.7	12.76742	2.6197
46220.1	12.83892	2.6181
46477.6	12.91044	2.6166
46735	12.98194	2.6152
46992.4	13.05344	2.6139
47249.8	13.12494	2.6128
47507.2	13.19644	2.6117
47764.7	13.26797	2.6107
48022.1	13.33947	2.6097
48279.5	13.41097	2.6089

48536.9	13.48247	2.6081
48794.4	13.554	2.6074
49051.8	13.6255	2.6068
49309.2	13.697	2.6063
49566.6	13.7685	2.6058
49824	13.84	2.6054
50081.5	13.91153	2.605
50338.9	13.98303	2.6047
50596.3	14.05453	2.6044
50853.7	14.12603	2.6042
51111.2	14.19756	2.604
51368.6	14.26906	2.6039
51626	14.34056	2.6039
51883.4	14.41206	2.6038
52140.8	14.48356	2.6039
52398.3	14.55508	2.6039
52655.7	14.62658	2.604
52913.1	14.69808	2.6041
53170.5	14.76958	2.6043
53427.9	14.84108	2.6044
53685.4	14.91261	2.6046
53942.8	14.98411	2.6048
54200.2	15.05561	2.6037
54457.6	15.12711	2.6036
54715.1	15.19864	2.6038
54972.5	15.27014	2.6041
55229.9	15.34164	2.6045
55487.3	15.41314	2.6049
55744.7	15.48464	2.6054
56002.2	15.55617	2.606
56259.6	15.62767	2.6066
56517	15.69917	2.6073
56774.4	15.77067	2.608
57031.9	15.84219	2.6088
57289.3	15.91369	2.6097
57546.7	15.98519	2.6106
57804.1	16.05669	2.6115
58061.5	16.12819	2.6125
58319	16.19972	2.6136
58576.4	16.27122	2.6147
58833.8	16.34272	2.6158
59091.2	16.41422	2.617
59348.7	16.48575	2.6182
59606.1	16.55725	2.6194
59863.5	16.62875	2.6207
60120.9	16.70025	2.622
60378.3	16.77175	2.6234
60635.8	16.84328	2.6248

60893.2	16.91478	2.6261
61150.6	16.98628	2.6276
61408	17.05778	2.629
61665.4	17.12928	2.6304
61922.9	17.20081	2.6319
62180.3	17.27231	2.6333
62437.7	17.34381	2.6348
62695.1	17.41531	2.6363
62952.6	17.48683	2.6377
63210	17.55833	2.6391
63467.4	17.62983	2.6406
63724.8	17.70133	2.642
63982.2	17.77283	2.6433
64239.7	17.84436	2.6447
64497.1	17.91586	2.646
64754.5	17.98736	2.6473
65011.9	18.05886	2.6485
65269.4	18.13039	2.6496
65526.8	18.20189	2.6507
65784.6	18.2735	2.6518
66042.4	18.34511	2.6528
66300.2	18.41672	2.6537
66558	18.48833	2.6545
66815.8	18.55994	2.6552
67073.6	18.63156	2.6559
67331.5	18.70319	2.6565
67589.3	18.77481	2.6573
67847.1	18.84642	2.6579
68104.9	18.91803	2.6585
68362.7	18.98964	2.659
68620.5	19.06125	2.6595
68878.3	19.13286	2.6599
69136.1	19.20447	2.6603
69394	19.27611	2.6607
69651.8	19.34772	2.6611
69909.6	19.41933	2.6615
70167.4	19.49094	2.6618
70425.2	19.56256	2.6622
70683	19.63417	2.6625
70940.8	19.70578	2.6628
71198.6	19.77739	2.6631
71456.5	19.84903	2.6634
71714.3	19.92064	2.6636
71972.1	19.99225	2.6639
72229.9	20.06386	2.6641
72487.7	20.13547	2.6644
72745.5	20.20708	2.6646
73003.3	20.27869	2.6648

73261.1	20.35031	2.665
73519	20.42194	2.6652
73776.8	20.49356	2.6654
74034.6	20.56517	2.6656
74292.4	20.63678	2.6658
74550.2	20.70839	2.6659
74808	20.78	2.6661
75065.8	20.85161	2.6663
75323.6	20.92322	2.6664
75581.5	20.99486	2.6666
75839.3	21.06647	2.6667
76097.1	21.13808	2.6668
76354.9	21.20969	2.667
76612.7	21.28131	2.6671
76870.5	21.35292	2.6672
77128.3	21.42453	2.6673
77386.1	21.49614	2.6674
77644	21.56778	2.6675
77901.8	21.63939	2.6676
78159.6	21.711	2.6677
78417.4	21.78261	2.6678
78675.2	21.85422	2.6679
78933	21.92583	2.668
79190.8	21.99744	2.6681
79448.6	22.06906	2.6682
79706.5	22.14069	2.6682
79964.3	22.21231	2.6683
80222.1	22.28392	2.6684
80479.9	22.35553	2.6685
80737.7	22.42714	2.6685
80995.5	22.49875	2.6686
81253.3	22.57036	2.6687
81511.1	22.64197	2.6687
81769	22.71361	2.6688
82026.8	22.78522	2.6688
82284.6	22.85683	2.6689
82542.4	22.92844	2.6689
82800.2	23.00006	2.669
83058	23.07167	2.669
83315.8	23.14328	2.6691
83573.6	23.21489	2.6691
83831.5	23.28653	2.6691
84089.3	23.35814	2.6692
84347.1	23.42975	2.6692
84604.9	23.50136	2.6693
84862.7	23.57297	2.6693
85120.5	23.64458	2.6693
85378.3	23.71619	2.6694

85636.1	23.78781	2.6694
85894	23.85944	2.6694
86400	24	2.6694

- **Case 3:** The ability of the GTA code to predict transients in gas pipeline networks
  - Pressure and mass flow rate in the three nodes of the pipeline network.

Time (hr)	Node 1		Node 2		Node 3	
	P (Mpa)	m (kg/s)	P (Mpa)	m (kg/s)	P (Mpa)	m (kg/s)
0	4.969	48.97	4.9058	42.989	2.9385	14.735
0.049917	4.969	48.97	4.9057	42.989	2.9456	14.808
0.099583	4.969	48.969	4.9056	42.993	2.9538	14.893
0.151	4.969	48.967	4.9054	43.008	2.9625	14.98
0.200639	4.9689	48.964	4.9051	43.035	2.9709	15.065
0.250306	4.9689	48.961	4.9049	43.073	2.9793	15.151
0.3035	4.9688	48.958	4.9045	43.128	2.9884	15.243
0.502083	4.9683	48.94	4.9028	43.424	3.0229	15.592
0.562361	4.9682	48.934	4.9022	43.537	3.0335	15.699
0.571222	4.9681	48.933	4.9021	43.554	3.0351	15.715
0.580083	4.9681	48.932	4.902	43.573	3.0365	15.73
0.590722	4.9681	48.931	4.9019	43.594	3.0384	15.749
0.601361	4.9681	48.93	4.9018	43.615	3.0403	15.768
0.603139	4.9681	48.93	4.9017	43.618	3.0406	15.771
0.604917	4.968	48.93	4.9017	43.623	3.0409	15.773
0.606694	4.968	48.929	4.9017	43.626	3.0412	15.777
0.608444	4.968	48.929	4.9017	43.63	3.0416	15.78
0.610222	4.968	48.929	4.9017	43.633	3.0419	15.783
0.651	4.9679	48.924	4.9012	43.72	3.049	15.856
0.700639	4.9677	48.919	4.9006	43.829	3.0578	15.945
0.750278	4.9676	48.913	4.9	43.943	3.0667	16.034
0.801694	4.9674	48.906	4.8994	44.066	3.0757	16.126
0.851333	4.9672	48.9	4.8988	44.187	3.0845	16.216
0.900972	4.967	48.893	4.8981	44.313	3.0934	16.305
0.950583	4.9668	48.887	4.8975	44.441	3.1022	16.394
1.000222	4.9666	48.88	4.8968	44.572	3.1111	16.484
1.051639	4.9664	48.873	4.8961	44.711	3.1203	16.577
1.053389	4.9664	48.872	4.8961	44.715	3.1206	16.58
1.055167	4.9664	48.872	4.896	44.721	3.1209	16.584
1.056944	4.9664	48.872	4.896	44.725	3.1212	16.586
1.058722	4.9664	48.872	4.896	44.73	3.1215	16.59
1.0605	4.9664	48.871	4.896	44.735	3.1218	16.593
1.06225	4.9664	48.871	4.8959	44.74	3.1222	16.597
1.064028	4.9664	48.871	4.8959	44.744	3.1225	16.599
1.065806	4.9664	48.871	4.8959	44.749	3.1229	16.603
1.067583	4.9663	48.87	4.8959	44.754	3.1231	16.606
1.069361	4.9663	48.87	4.8958	44.759	3.1234	16.609
1.071111	4.9663	48.87	4.8958	44.764	3.1237	16.612
1.072889	4.9663	48.87	4.8958	44.77	3.1241	16.615
1.074667	4.9663	48.869	4.8958	44.774	3.1245	16.618
1.076444	4.9663	48.869	4.8957	44.778	3.1247	16.622
1.078222	4.9663	48.869	4.8957	44.783	3.125	16.625
1.079972	4.9663	48.869	4.8957	44.788	3.1253	16.628

1.08175	4.9663	48.868	4.8957	44.793	3.1257	16.631
1.083528	4.9663	48.868	4.8956	44.798	3.126	16.634
1.085306	4.9663	48.868	4.8956	44.803	3.1263	16.638
1.087083	4.9663	48.868	4.8956	44.808	3.1266	16.642
1.088861	4.9663	48.867	4.8956	44.813	3.127	16.644
1.090611	4.9662	48.867	4.8955	44.818	3.1273	16.648
1.092389	4.9662	48.867	4.8955	44.822	3.1276	16.651
1.094167	4.9662	48.867	4.8955	44.827	3.1279	16.653
1.095944	4.9662	48.866	4.8955	44.832	3.1282	16.657
1.097722	4.9662	48.866	4.8954	44.837	3.1285	16.66
1.099472	4.9662	48.866	4.8954	44.842	3.1288	16.663
1.10125	4.9662	48.866	4.8954	44.847	3.1291	16.666
1.103028	4.9662	48.865	4.8954	44.852	3.1295	16.67
1.104806	4.9662	48.865	4.8953	44.857	3.1298	16.673
1.106583	4.9662	48.865	4.8953	44.862	3.1301	16.676
1.108333	4.9662	48.865	4.8953	44.867	3.1304	16.68
1.110111	4.9662	48.864	4.8953	44.871	3.1308	16.682
1.111889	4.9662	48.864	4.8952	44.876	3.131	16.686
1.113667	4.9662	48.864	4.8952	44.882	3.1314	16.689
1.115444	4.9661	48.864	4.8952	44.886	3.1317	16.692
1.117194	4.9661	48.863	4.8952	44.891	3.1321	16.695
1.118972	4.9661	48.863	4.8951	44.896	3.1324	16.699
1.12075	4.9661	48.863	4.8951	44.901	3.1326	16.702
1.122528	4.9661	48.863	4.8951	44.905	3.133	16.705
1.124306	4.9661	48.862	4.8951	44.91	3.1333	16.708
1.126056	4.9661	48.862	4.895	44.916	3.1336	16.711
1.127833	4.9661	48.862	4.895	44.921	3.134	16.714
1.129611	4.9661	48.862	4.895	44.926	3.1342	16.718
1.131389	4.9661	48.861	4.895	44.931	3.1345	16.722
1.133167	4.9661	48.861	4.8949	44.935	3.1349	16.724
1.134917	4.9661	48.861	4.8949	44.941	3.1352	16.727
1.136694	4.9661	48.861	4.8949	44.945	3.1355	16.731
1.138472	4.966	48.86	4.8949	44.95	3.1358	16.734
1.14025	4.966	48.86	4.8948	44.954	3.1361	16.737
1.142028	4.966	48.86	4.8948	44.96	3.1364	16.741
1.143778	4.966	48.86	4.8948	44.965	3.1367	16.743
1.145556	4.966	48.859	4.8948	44.97	3.1371	16.747
1.147333	4.966	48.859	4.8947	44.974	3.1374	16.75
1.149111	4.966	48.859	4.8947	44.98	3.1377	16.753
1.150889	4.966	48.858	4.8947	44.984	3.1381	16.756
1.152639	4.966	48.858	4.8947	44.99	3.1384	16.759
1.154417	4.966	48.858	4.8946	44.994	3.1386	16.762
1.156194	4.966	48.858	4.8946	44.999	3.139	16.766
1.157972	4.966	48.857	4.8946	45.004	3.1394	16.769
1.15975	4.966	48.857	4.8946	45.009	3.1396	16.772
1.1615	4.9659	48.857	4.8945	45.014	3.1399	16.776
1.163278	4.9659	48.857	4.8945	45.02	3.1403	16.779
1.165056	4.9659	48.856	4.8945	45.024	3.1406	16.782

1.166833	4.9659	48.856	4.8945	45.029	3.1409	16.785
1.168611	4.9659	48.856	4.8944	45.035	3.1413	16.789
1.170389	4.9659	48.856	4.8944	45.04	3.1416	16.792
1.172139	4.9659	48.855	4.8944	45.045	3.1419	16.795
1.173917	4.9659	48.855	4.8944	45.049	3.1422	16.798
1.175694	4.9659	48.855	4.8943	45.054	3.1425	16.802
1.177472	4.9659	48.855	4.8943	45.059	3.1428	16.804
1.17925	4.9659	48.854	4.8943	45.065	3.1431	16.807
1.181	4.9659	48.854	4.8943	45.069	3.1434	16.811
1.182778	4.9659	48.854	4.8942	45.075	3.1438	16.814
1.184556	4.9658	48.854	4.8942	45.08	3.1441	16.818
1.186333	4.9658	48.853	4.8942	45.084	3.1444	16.82
1.188111	4.9658	48.853	4.8942	45.089	3.1447	16.824
1.189861	4.9658	48.853	4.8941	45.094	3.145	16.827
1.191639	4.9658	48.853	4.8941	45.099	3.1454	16.83
1.193417	4.9658	48.852	4.8941	45.105	3.1457	16.834
1.195194	4.9658	48.852	4.8941	45.109	3.146	16.837
1.196972	4.9658	48.852	4.894	45.114	3.1463	16.84
1.198722	4.9658	48.852	4.894	45.119	3.1466	16.843
1.2005	4.9658	48.851	4.894	45.124	3.147	16.847
1.202278	4.9658	48.851	4.894	45.13	3.1472	16.85
1.204056	4.9658	48.851	4.8939	45.135	3.1476	16.853
1.205833	4.9658	48.85	4.8939	45.14	3.1479	16.856
1.207583	4.9657	48.85	4.8939	45.144	3.1482	16.859
1.209361	4.9657	48.85	4.8938	45.149	3.1486	16.863
1.211139	4.9657	48.85	4.8938	45.154	3.1489	16.866
1.212917	4.9657	48.849	4.8938	45.16	3.1492	16.869
1.214694	4.9657	48.849	4.8938	45.164	3.1495	16.872
1.216444	4.9657	48.849	4.8937	45.17	3.1498	16.875
1.218222	4.9657	48.849	4.8937	45.175	3.1501	16.879
1.22	4.9657	48.848	4.8937	45.18	3.1505	16.882
1.221778	4.9657	48.848	4.8937	45.185	3.1508	16.885
1.223556	4.9657	48.848	4.8936	45.19	3.1511	16.888
1.225306	4.9657	48.848	4.8936	45.195	3.1514	16.891
1.227083	4.9657	48.847	4.8936	45.201	3.1517	16.894
1.50175	4.9644	48.806	4.8895	46.002	3.2011	17.393
2.001333	4.962	48.725	4.8815	47.522	3.2912	18.304
2.277583	4.9606	48.678	4.8769	48.376	3.3411	18.808
2.500694	4.9595	48.64	4.8731	49.069	3.3814	19.216
3.001639	4.9568	48.551	4.8643	50.627	3.4719	20.131
3.500611	4.9541	48.461	4.8553	52.172	3.5618	21.042
4.001167	4.9513	48.367	4.846	53.713	3.6521	21.955
4.501528	4.9496	48.333	4.8427	54.629	3.5765	21.177
4.996611	4.9503	48.368	4.8462	54.278	3.4926	20.325
5.500583	4.9522	48.437	4.8531	53.253	3.404	19.426
5.995861	4.9546	48.519	4.8612	51.907	3.3153	18.528
6.500167	4.9574	48.609	4.8701	50.354	3.2239	17.606
7.001167	4.9601	48.7	4.8791	48.709	3.1328	16.685

7.500583	4.9629	48.79	4.888	47.011	3.0417	15.765
8.000222	4.9656	48.877	4.8966	45.277	2.9503	14.843
8.500083	4.9683	48.962	4.9051	43.517	2.8588	13.921
9.009056	4.9709	49.046	4.9133	41.705	2.7655	12.98
9.498694	4.9733	49.124	4.9209	39.946	2.6758	12.076
10.00106	4.9757	49.2	4.9285	38.126	2.5834	11.146
10.51958	4.9781	49.275	4.9359	36.233	2.4882	10.187
10.99217	4.9801	49.341	4.9423	34.497	2.4013	9.313
11.5005	4.9823	49.408	4.9489	32.615	2.3079	8.372
12.00022	4.9842	49.471	4.955	30.756	2.2159	7.446
12.52686	4.9847	49.475	4.9553	30.218	2.2998	8.304
12.98214	4.9837	49.437	4.9516	31.25	2.3805	9.118
13.50142	4.9819	49.38	4.9461	32.842	2.4744	10.064
14.05061	4.9799	49.313	4.9395	34.638	2.5742	11.069
15.0595	4.9758	49.18	4.9265	37.966	2.7576	12.917
15.49975	4.9739	49.119	4.9204	39.411	2.8376	13.725
16.06222	4.9714	49.036	4.9123	41.246	2.9397	14.754
17.00031	4.9671	48.892	4.898	44.279	3.1098	16.471
17.50008	4.9646	48.811	4.89	45.879	3.2003	17.385
18.00144	4.9621	48.727	4.8817	47.472	3.291	18.302
18.50081	4.9595	48.641	4.8732	49.049	3.3813	19.215
19.00019	4.9568	48.552	4.8644	50.613	3.4714	20.128
20.00128	4.9513	48.367	4.846	53.712	3.6521	21.955
21.00233	4.9503	48.369	4.8463	54.269	3.4916	20.314
21.50111	4.9522	48.437	4.8531	53.252	3.4039	19.425
22.00164	4.9547	48.52	4.8613	51.89	3.3142	18.518
23.00344	4.9601	48.7	4.8792	48.701	3.1324	16.681
23.50281	4.9629	48.79	4.888	47.004	3.0412	15.761
23.59136	4.9634	48.806	4.8896	46.698	3.0251	15.598
24	4.9656	48.877	4.8967	45.275	2.9502	14.843

Note: in this case, data has been shortened because it is too large. All data of results could be provided if it is needed.

- **Case 4:** short single pipeline.
  - Pressure history at the inlet and outlet of the pipeline.

Time (s)	P_{in} (MPa)	P_{out} (MPa)
0	4.1368	4.136
0.0053	4.1396	4.136
0.0105	4.1467	4.136
0.0157	4.1539	4.136
0.021	4.161	4.136
0.0262	4.1682	4.136
0.0314	4.1753	4.136
0.0366	4.1825	4.136
0.0418	4.1896	4.136
0.0522	4.2039	4.136
0.0573	4.2111	4.136
0.0599	4.2147	4.136
0.0651	4.2219	4.136
0.0702	4.2291	4.136
0.0754	4.2363	4.136
0.0805	4.2435	4.136
0.0856	4.2507	4.136
0.0907	4.2579	4.136
0.0959	4.2651	4.136
0.101	4.2724	4.136
0.106	4.2796	4.136
0.1111	4.2869	4.136
0.1162	4.2941	4.136
0.1238	4.3051	4.136
0.1263	4.3087	4.136
0.1289	4.3124	4.136
0.1314	4.316	4.136
0.1339	4.3197	4.136
0.1364	4.3234	4.136
0.1389	4.327	4.136
0.1415	4.3307	4.136
0.144	4.3344	4.136
0.1465	4.3381	4.136
0.149	4.3376	4.136
0.1514	4.3341	4.136
0.1538	4.3308	4.136
0.1562	4.3275	4.136
0.1585	4.3242	4.136
0.1609	4.3209	4.136
0.1657	4.3142	4.136
0.1705	4.3076	4.136
0.1753	4.301	4.136
0.1801	4.2943	4.136
0.1849	4.2876	4.136

0.1922	4.2776	4.136
0.1946	4.2743	4.136
0.2019	4.2642	4.136
0.2043	4.2609	4.136
0.2116	4.2508	4.136
0.2164	4.2441	4.136
0.2213	4.2373	4.136
0.2262	4.2306	4.136
0.2311	4.2239	4.136
0.2335	4.2205	4.136
0.236	4.2171	4.136
0.2384	4.2137	4.136
0.2409	4.2104	4.136
0.2458	4.2036	4.136
0.2507	4.1968	4.136
0.2556	4.1901	4.1361
0.2605	4.1833	4.1375
0.2655	4.1765	4.1427
0.2704	4.1697	4.1528
0.2754	4.163	4.166
0.2803	4.1562	4.1803
0.2853	4.1494	4.195
0.2903	4.1426	4.2097
0.2953	4.1396	4.2244
0.3003	4.1396	4.2391
0.3152	4.1396	4.2831
0.3202	4.1396	4.2978
0.3252	4.1396	4.3125
0.3302	4.1396	4.3271
0.3352	4.1396	4.3418
0.3402	4.1396	4.3565
0.3452	4.1396	4.3712
0.3502	4.1395	4.3859
0.3552	4.1395	4.4006
0.3602	4.1395	4.4153
0.3652	4.1395	4.43
0.3702	4.1395	4.4448
0.3777	4.1395	4.4669
0.3801	4.1395	4.4743
0.3901	4.1395	4.5039
0.4001	4.1395	4.5247
0.4101	4.1395	4.5092
0.4151	4.1395	4.4973
0.4201	4.1395	4.4851
0.4251	4.1395	4.4729
0.4301	4.1395	4.4607
0.4351	4.1395	4.4484
0.4401	4.1395	4.4361

0.4451	4.1395	4.4238
0.45	4.1395	4.4114
0.455	4.1395	4.3991
0.46	4.1395	4.3867
0.465	4.1395	4.3743
0.47	4.1395	4.3619
0.475	4.1395	4.3495
0.48	4.1395	4.3371
0.485	4.1395	4.3247
0.49	4.1395	4.3122
0.495	4.1395	4.2998
0.5	4.1395	4.2874
0.505	4.1395	4.275
0.51	4.1395	4.2626
0.5149	4.1396	4.2503
0.5199	4.1402	4.2379
0.5249	4.1424	4.2255
0.5299	4.1475	4.2132
0.5349	4.1562	4.2009
0.5399	4.1682	4.1887
0.5449	4.1824	4.1764
0.5499	4.1976	4.1647
0.5548	4.2131	4.1547
0.5598	4.2288	4.148
0.5648	4.2444	4.1447
0.5698	4.26	4.1434
0.5748	4.2756	4.143
0.5798	4.2911	4.1429
0.5847	4.3066	4.1429
0.5872	4.3144	4.1429
0.5897	4.3221	4.1429
0.5922	4.3298	4.1429
0.5947	4.3375	4.1429
0.5997	4.3529	4.1429
0.6047	4.3683	4.1429
0.6097	4.3837	4.1429
0.6146	4.399	4.1428
0.6196	4.4142	4.1428
0.6246	4.4295	4.1428
0.6296	4.4447	4.1428
0.6346	4.4599	4.1428
0.6396	4.4751	4.1428
0.6445	4.4901	4.1428
0.6495	4.5034	4.1428
0.6545	4.5097	4.1428
0.6595	4.5074	4.1428
0.6645	4.4997	4.1428
0.667	4.4949	4.1428

0.6695	4.4898	4.1428
0.672	4.4846	4.1428
0.6745	4.4793	4.1428
0.677	4.4739	4.1428
0.6795	4.4685	4.1428
0.6819	4.4631	4.1428
0.6844	4.4577	4.1428
0.6869	4.4523	4.1428
0.6894	4.4469	4.1428
0.6919	4.4414	4.1428
0.6944	4.436	4.1428
0.6994	4.425	4.1428
0.7044	4.414	4.1428
0.7094	4.403	4.1428
0.7144	4.392	4.1428
0.7218	4.3754	4.1427
0.7243	4.3698	4.1427
0.7318	4.3531	4.1427
0.7343	4.3476	4.1427
0.7368	4.342	4.1427
0.7393	4.3364	4.1427
0.7418	4.3308	4.1427
0.7443	4.3253	4.1427
0.7468	4.3197	4.1427
0.7493	4.3141	4.1427
0.7517	4.3085	4.1427
0.7542	4.3029	4.1427
0.7567	4.2973	4.1427
0.7592	4.2917	4.1427
0.7617	4.2861	4.1427
0.7642	4.2805	4.1427
0.7667	4.2749	4.1427
0.7692	4.2693	4.1427
0.7717	4.2638	4.1427
0.7742	4.2582	4.1428
0.7767	4.2526	4.1429
0.7792	4.247	4.1431
0.7842	4.2358	4.1441
0.7866	4.2302	4.145
0.7891	4.2247	4.1465
0.7966	4.208	4.1549
0.7991	4.2024	4.1593
0.8	4.1969	4.1644

Note: in this case, data has been shortened because it is too large. All data of results could be provided if it is needed.

- **Case 5:** Influence of the natural gas wall friction.
  - Temperature change along transmission gas pipeline.

L(km)	T (K)
0	315.65
1.22	314.7094
2.44	313.7984
3.66	312.9159
4.88	312.0613
6.1	311.2335
7.32	310.4317
8.54	309.6552
9.76	308.9032
10.98	308.1749
12.2	307.4696
13.42	306.7866
14.64	306.1251
15.86	305.4845
17.08	304.8642
18.3	304.2635
19.52	303.6818
20.74	303.1185
21.96	302.5731
23.18	302.0449
24.4	301.5335
25.62	301.0383
26.84	300.5588
28.06	300.0946
29.28	299.645
30.5	299.2098
31.72	298.7883
32.94	298.3803
34.16	297.9852
35.38	297.6027
36.6	297.2324
37.82	296.8739
39.04	296.5267
40.26	296.1906
41.48	295.8653
42.7	295.5502
43.92	295.2453
45.14	294.95
46.36	294.6642
47.58	294.3875
48.8	294.1196
50.02	293.8602
51.24	293.6092
52.46	293.3661

53.68	293.1309
54.9	292.9031
56.12	292.6826
57.34	292.4692
58.56	292.2626
59.78	292.0626
61	291.869
62.22	291.6817
63.44	291.5003
64.66	291.3247
65.88	291.1547
67.1	290.9902
68.32	290.831
69.54	290.6769
70.76	290.5277
71.98	290.3833
73.2	290.2435
74.42	290.1083
75.64	289.9774
76.86	289.8506
78.08	289.728
79.3	289.6093
80.52	289.4944
81.74	289.3833
82.96	289.2757
84.18	289.1715
85.4	289.0708
86.62	288.9733
87.84	288.8789
89.06	288.7875
90.28	288.6992
91.5	288.6136
92.72	288.5309
93.94	288.4508
95.16	288.3733
96.38	288.2983
97.6	288.2258
98.82	288.1556
100.04	288.0876
101.26	288.0219
102.48	287.9583
103.7	287.8968
104.92	287.8373
106.14	287.7797
107.36	287.724
108.58	287.6701
109.8	287.618
111.02	287.5675

112.24	287.5188
113.46	287.4716
114.68	287.4259
115.9	287.3818
117.12	287.3391
118.34	287.2978
119.56	287.2578
120.78	287.2192
122	287.1818

➢ **Case 5-Scenario 1:** thermal effect of the heat generation by wall friction.

- Temperature flow with and without gas wall friction (Fig. 5.16)

L (km)	k=0.8 W/m² K Temp. (K)		k=1.6 W/m² K Temp. (K)		k=5.8 W/m² K Temp. (K)	
	with	without	with	without	with	without
0	315.65	315.65	315.65	315.65	315.65	315.65
1.5	315.522508	315.4805	315.354641	315.3119446	314.498313	314.452087
3	315.3949596	315.31194	315.061783	314.9776178	313.390907	313.300993
4.5	315.2674093	315.14432	314.771454	314.6469785	312.326115	312.194888
6	315.139908	314.97762	314.483678	314.3199859	311.302329	311.132014
7.5	315.0125034	314.81184	314.198476	313.9966	310.318001	310.11068
9	314.88524	314.64698	313.915866	313.6767808	309.371637	309.129264
10.5	314.7581593	314.48303	313.635862	313.3604891	308.461799	308.186206
12	314.6313002	314.31999	313.358476	313.047686	307.5871	307.280005
13.5	314.5046987	314.15784	313.083716	312.7383329	306.746206	306.409222
15	314.3783886	313.9966	312.811589	312.4323919	305.93783	305.572472
16.5	314.2524014	313.83625	312.542098	312.1298252	305.160733	304.768426
18	314.1267663	313.67678	312.275247	311.8305957	304.413722	303.995804
19.5	314.0015106	313.5182	312.011034	311.5346666	303.695649	303.25338
21	313.8766597	313.36049	311.749457	311.2420015	303.005408	302.539972
22.5	313.752237	313.20365	311.490514	310.9525643	302.341933	301.854446
24	313.6282645	313.04769	311.234199	310.6663194	301.7042	301.195714
25.5	313.5047623	312.89258	310.980505	310.3832317	301.091223	300.562727
27	313.3817494	312.73833	310.729423	310.1032664	300.50205	299.954479
28.5	313.2592431	312.58494	310.480946	309.8263889	299.93577	299.370004
30	313.1372594	312.43239	310.235062	309.5525652	299.391501	298.808372
31.5	313.0158132	312.28069	309.99176	309.2817617	298.868398	298.268691
33	312.8949182	312.12983	309.751027	309.0139451	298.365645	297.750103
34.5	312.7745869	311.9798	309.512851	308.7490823	297.88246	297.251783
36	312.6548309	311.8306	309.277216	308.4871409	297.418089	296.772939
37.5	312.5356608	311.68222	309.044107	308.2280885	296.971806	296.31281
39	312.4170862	311.53467	308.81351	307.9718934	296.542913	295.870665
40.5	312.299116	311.38793	308.585408	307.718524	296.130739	295.4458
42	312.1817581	311.242	308.359783	307.4679491	295.734639	295.03754
43.5	312.06502	311.09688	308.13662	307.220138	295.35399	294.645237
45	311.948908	310.95256	307.915899	306.9750601	294.988197	294.268266
46.5	311.8334282	310.80904	307.697602	306.7326853	294.636685	293.906029
48	311.7185858	310.66632	307.481711	306.4929838	294.2989	293.557949
49.5	311.6043855	310.52438	307.268207	306.255926	293.974312	293.223474
51	311.4908314	310.38323	307.057071	306.021483	293.66241	292.902071
52.5	311.3779272	310.24286	306.848282	305.7896257	293.362701	292.593229
54	311.2656761	310.10327	306.641822	305.5603257	293.074714	292.296458
55.5	311.1540807	309.96444	306.43767	305.3335547	292.797994	292.011287

57	311.0431433	309.82639	306.235805	305.109285	292.532105	291.73726
58.5	310.9328658	309.6891	306.036209	304.8874888	292.276625	291.473944
60	310.8232497	309.55257	305.838859	304.668139	292.031151	291.220919
61.5	310.7142961	309.41679	305.643736	304.4512085	291.795296	290.977783
63	310.6060059	309.28176	305.45082	304.2366706	291.568684	290.744149
64.5	310.4983795	309.14748	305.260088	304.024499	291.350958	290.519647
66	310.3914174	309.01395	305.071521	303.8146675	291.141771	290.30392
67.5	310.2851193	308.88115	304.885098	303.6071504	290.940793	290.096623
69	310.179485	308.74908	304.700799	303.4019221	290.747705	289.897429
70.5	310.0745141	308.61775	304.518601	303.1989573	290.562199	289.70602
72	309.9702057	308.48714	304.338485	302.9982312	290.38398	289.522091
73.5	309.866559	308.35726	304.160431	302.799719	290.212766	289.345352
75	309.7635728	308.22809	303.984416	302.6033963	290.048284	289.17552
76.5	309.6612458	308.09964	303.810422	302.4092389	289.890272	289.012325
78	309.5595767	307.97189	303.638426	302.217223	289.738479	288.855509
79.5	309.4585636	307.84486	303.46841	302.027325	289.592661	288.704822
81	309.358205	307.71852	303.300352	301.8395214	289.452588	288.560024
82.5	309.2584989	307.59289	303.134233	301.6537893	289.318034	288.420886
84	309.1594434	307.46795	302.970032	301.4701056	289.188786	288.287185
85.5	309.0610362	307.3437	302.807729	301.2884479	289.064636	288.15871
87	308.9632752	307.22014	302.647305	301.1087938	288.945387	288.035256
88.5	308.8661581	307.09726	302.488739	300.9311213	288.830847	287.916628
90	308.7696825	306.97506	302.332012	300.7554083	288.720832	287.802635
91.5	308.6738458	306.85354	302.177104	300.5816334	288.615168	287.693098
93	308.5786456	306.73269	302.023997	300.4097752	288.513683	287.587842
94.5	308.4840792	306.6125	301.87267	300.2398125	288.416216	287.4867
96	308.3901438	306.49298	301.723105	300.0717243	288.322609	287.389511
97.5	308.2968369	306.37413	301.575283	299.9054901	288.232713	287.29612
99	308.2041555	306.25593	301.429185	299.7410895	288.146382	287.20638
100.5	308.1120968	306.13838	301.284793	299.578502	288.063479	287.120146
102	308.020658	306.02148	301.142088	299.4177079	287.983868	287.037283
103.5	307.9298361	305.90523	301.001051	299.2586872	287.907423	286.957659
105	307.8396282	305.78963	300.861665	299.1014204	287.834019	286.881147
106.5	307.7500313	305.67466	300.723911	298.9458882	287.763538	286.807625
108	307.6610423	305.56033	300.587772	298.7920715	287.695866	286.736976
109.5	307.5726584	305.44663	300.453231	298.6399513	287.630894	286.669089
111	307.4848763	305.33355	300.320269	298.4895089	287.568516	286.603855
112.5	307.3976931	305.22111	300.188869	298.3407258	287.508631	286.541171
114	307.3111056	305.10928	300.059014	298.1935838	287.451142	286.480936
115.5	307.2251109	304.99808	299.930688	298.0480646	287.395957	286.423056
117	307.1397057	304.88749	299.803873	297.9041505	287.342984	286.367438
118.5	307.0548869	304.77751	299.678553	297.7618236	287.292137	286.313993
120	306.9706516	304.66814	299.554711	297.6210666	287.243335	286.262638
121.5	306.8869965	304.55937	299.432331	297.481862	287.196497	286.213289
123	306.8039186	304.45121	299.311396	297.3441928	287.151546	286.16587

124.5	306.7214147	304.34364	299.191892	297.2080421	287.108409	286.120303
126	306.6394818	304.23667	299.073801	297.073393	287.067016	286.076518
127.5	306.5581166	304.13029	298.957109	296.940229	287.027298	286.034444
129	306.4773163	304.0245	298.8418	296.8085338	286.98919	285.994014
130.5	306.3970776	303.91929	298.727858	296.6782911	286.95263	285.955164
132	306.3173975	303.81467	298.615269	296.5494849	286.917557	285.917833
133.5	306.2382728	303.71062	298.504017	296.4220994	286.883912	285.881961
135	306.1597007	303.60715	298.394087	296.2961189	286.851642	285.847491
136.5	306.0816779	303.50425	298.285466	296.1715279	286.820692	285.814368
138	306.0042015	303.40192	298.178138	296.0483111	286.79101	285.782539
139.5	305.9272685	303.30016	298.072089	295.9264533	286.762547	285.751955
141	305.8508758	303.19896	297.967305	295.8059396	286.735256	285.722566
142.5	305.7750205	303.09832	297.863771	295.686755	286.709092	285.694325
144	305.6996995	302.99823	297.761475	295.568885	286.684009	285.667189
145.5	305.6249099	302.8987	297.660401	295.4523151	286.659967	285.641112
147	305.5506488	302.79972	297.560538	295.3370309	286.636925	285.616056
148.5	305.4769133	302.70129	297.46187	295.2230182	286.614843	285.591978
150	305.4037003	302.6034	297.364386	295.110263	286.593685	285.568841
151.5	305.3310071	302.50605	297.268071	294.9987514	286.573415	285.546609
153	305.2588308	302.40924	297.172913	294.8884698	286.553997	285.525246
154.5	305.1871684	302.31296	297.0789	294.7794045	286.5354	285.504717
156	305.1160172	302.21722	296.986017	294.6715422	286.51759	285.484991
157.5	305.0453744	302.12201	296.894253	294.5648696	286.500538	285.466036
159	304.9752371	302.02732	296.803596	294.4593734	286.484214	285.447821
160.5	304.9056025	301.93316	296.714033	294.3550409	286.468589	285.430319
162	304.836468	301.83952	296.625552	294.2518591	286.453638	285.413501
163.5	304.7678306	301.7464	296.53814	294.1498154	286.439332	285.39734
165	304.6996878	301.65379	296.451787	294.0488971	286.425648	285.38181
166.5	304.6320369	301.56169	296.366481	293.9490919	286.412562	285.366888
168	304.564875	301.47011	296.282209	293.8503876	286.400049	285.352548
169.5	304.4981996	301.37902	296.198961	293.7527719	286.388089	285.33877
171	304.4320081	301.28845	296.116725	293.6562328	286.376658	285.325529
172.5	304.3662978	301.19837	296.03549	293.5607586	286.365738	285.312806
174	304.301066	301.10879	295.955245	293.4663373	286.355308	285.300581
175.5	304.2363103	301.01971	295.875979	293.3729575	286.34535	285.288833
177	304.172028	300.93112	295.797681	293.2806077	286.335844	285.277544
178.5	304.1082166	300.84302	295.720341	293.1892764	286.326774	285.266697
180	304.0448735	300.75541	295.643947	293.0989524	286.318122	285.256274
181.5	303.9819964	300.66828	295.56849	293.0096247	286.309873	285.246258
183	303.9195826	300.58163	295.49396	292.9212822	286.302011	285.236633
184.5	303.8576297	300.49547	295.420345	292.8339141	286.294522	285.227385
186	303.7961353	300.40978	295.347637	292.7475097	286.287389	285.218498
187.5	303.7350969	300.32456	295.275824	292.6620582	286.280601	285.209958
189	303.6745121	300.23981	295.204898	292.5775492	286.274144	285.201752
190.5	303.6143786	300.15554	295.134848	292.4939723	286.268004	285.193867

192	303.5546939	300.07172	295.065665	292.4113173	286.26217	285.18629
193.5	303.4954557	299.98838	294.997339	292.3295739	286.256631	285.179009
195	303.4366617	299.90549	294.929861	292.248732	286.251374	285.172013
196.5	303.3783096	299.82306	294.863222	292.1687818	286.246388	285.16529
198	303.320397	299.74109	294.797412	292.0897135	286.241665	285.15883
199.5	303.2629217	299.65957	294.732423	292.0115172	286.237193	285.152622
201	303.2058815	299.5785	294.668245	291.9341834	286.232962	285.146657
202.5	303.149274	299.49788	294.60487	291.8577025	286.228964	285.140925
204	303.0930971	299.41771	294.542289	291.7820652	286.22519	285.135418
205.5	303.0373485	299.33798	294.480492	291.7072622	286.221632	285.130125
207	302.9820261	299.25869	294.419473	291.6332842	286.21828	285.125039
208.5	302.9271277	299.17984	294.359221	291.5601221	286.215127	285.120152
210	302.8726512	299.10142	294.29973	291.487767	286.212166	285.115456
211.5	302.8185943	299.02344	294.24099	291.4162099	286.209389	285.110944
213	302.7649551	298.94589	294.182993	291.345442	286.20679	285.106608
214.5	302.7117314	298.86877	294.125732	291.2754547	286.204361	285.102441
216	302.658921	298.79207	294.069198	291.2062394	286.202096	285.098438
217.5	302.606522	298.7158	294.013383	291.1377874	286.19999	285.09459
219	302.5545324	298.63995	293.95828	291.0700904	286.198035	285.090893
220.5	302.5029499	298.56452	293.903881	291.0031401	286.196227	285.087341
222	302.4517728	298.48951	293.850178	290.9369282	286.194559	285.083927
223.5	302.4009988	298.41491	293.797164	290.8714467	286.193028	285.080647
225	302.3506262	298.34073	293.744832	290.8066873	286.191626	285.077495
226.5	302.3006528	298.26695	293.693174	290.7426422	286.19035	285.074467
228	302.2510768	298.19358	293.642182	290.6793035	286.189196	285.071556
229.5	302.2018961	298.12062	293.59185	290.6166634	286.188157	285.06876
231	302.153109	298.04806	293.54217	290.5547142	286.187231	285.066072
232.5	302.1047135	297.97591	293.493136	290.4934483	286.186413	285.06349
234	302.0567076	297.90415	293.44474	290.4328581	286.185699	285.061009
235.5	302.0090896	297.83279	293.396976	290.3729361	286.185085	285.058624
237	301.9618575	297.76182	293.349837	290.3136751	286.184568	285.056333
238.5	301.9150096	297.69125	293.303317	290.2550677	286.184143	285.054131
240	301.8685439	297.62107	293.257407	290.1971067	286.183808	285.052016
241.5	301.8224587	297.55127	293.212103	290.139785	286.18356	285.049983
243	301.7767522	297.48186	293.167398	290.0830956	286.183395	285.048029
244.5	301.7314226	297.41284	293.123284	290.0270314	286.18331	285.046152
246	301.6864681	297.34419	293.079757	289.9715855	286.183302	285.044348
247.5	301.641887	297.27593	293.036809	289.9167512	286.183369	285.042615
249	301.5976775	297.20804	292.994435	289.8625217	286.183508	285.04095
250.5	301.5538379	297.14053	292.952628	289.8088904	286.183716	285.039349
252	301.5103665	297.07339	292.911382	289.7558505	286.183991	285.037811
253.5	301.4672616	297.00663	292.870692	289.7033957	286.184331	285.036334
255	301.4245214	296.94023	292.830551	289.6515194	286.184733	285.034914
256.5	301.3821445	296.8742	292.790954	289.6002153	286.185195	285.033549
258	301.3401289	296.80853	292.751895	289.549477	286.185715	285.032238

259.5	301.2984732	296.74323	292.713369	289.4992984	286.186292	285.030978
261	301.2571757	296.67829	292.675368	289.4496732	286.186922	285.029767
262.5	301.2162348	296.61371	292.637889	289.4005953	286.187604	285.028604
264	301.1756489	296.54948	292.600926	289.3520588	286.188337	285.027486
265.5	301.1354163	296.48562	292.564473	289.3040576	286.189119	285.026412
267	301.0955355	296.4221	292.528524	289.2565858	286.189948	285.02538
268.5	301.056005	296.35893	292.493076	289.2096376	286.190823	285.024388
270	301.0168232	296.29612	292.458121	289.1632073	286.191741	285.023435
271.5	300.9779885	296.23365	292.423656	289.117289	286.192702	285.022519
273	300.9394994	296.17153	292.389674	289.0718772	286.193705	285.021639
274.5	300.9013545	296.10975	292.356172	289.0269663	286.194747	285.020793
276	300.8635521	296.04831	292.323144	288.9825507	286.195828	285.01998
277.5	300.8260908	295.98721	292.290584	288.938625	286.196946	285.019199
279	300.7889692	295.92645	292.258489	288.8951838	286.198101	285.018449
280.5	300.7521858	295.86603	292.226853	288.8522217	286.19929	285.017728
282	300.7157391	295.80594	292.195672	288.8097334	286.200514	285.017035
283.5	300.6796276	295.74618	292.16494	288.7677138	286.20177	285.016369
285	300.64385	295.68676	292.134654	288.7261577	286.203059	285.01573
286.5	300.6084049	295.62766	292.104808	288.6850599	286.204379	285.015115
288	300.5732908	295.56889	292.075399	288.6444154	286.205728	285.014524
289.5	300.5385063	295.51044	292.046421	288.6042191	286.207107	285.013957
291	300.50405	295.45232	292.01787	288.5644663	286.208514	285.013411
292.5	300.4699207	295.39451	291.989742	288.5251518	286.209949	285.012887
294	300.4361169	295.33703	291.962032	288.486271	286.21141	285.012383
295.5	300.4026372	295.27987	291.934736	288.4478191	286.212898	285.0119
297	300.3694804	295.22302	291.907851	288.4097912	286.214411	285.011434
298.5	300.3366452	295.16648	291.881371	288.3721828	286.215948	285.010988
300	300.3041301	295.11026	291.855292	288.3349892	286.21751	285.010558

Note: because of the huge number of data, the other results of this calculation of Case 5-scenario 2 are in the CD.

- **Scenario 1:** Trip of the gas supply
  - Flow rate behaviour in the gas pipeline of the Western Libya Gas Project (Fig. 6.5)

Time (hr)	m_{1in} (kg/s)	m_{1out} (kg/s)	m_{2in} (kg/s)	m_{2out} (kg/s)	m_{3in} (kg/s)	m_{3out} (kg/s)
0	80.365	80.251	38.565	39.151	47.486	51.191
0.251306	80.37	80.256	38.57	39.151	47.485	51.191
0.502111	80.375	80.258	38.574	39.151	47.484	51.191
0.75075	80.384	80.262	38.578	39.151	47.483	51.191
1.001556	80.388	80.264	38.584	39.151	47.482	51.191
1.300361	80.395	80.267	38.586	39.151	47.482	51.191
1.601333	80.401	80.271	38.59	39.151	47.48	51.191
1.900111	80.41	80.274	38.596	39.151	47.479	51.191
2.201083	0	80.278	38.6	39.151	47.478	51.191
2.502083	0	80.28	38.604	39.151	47.477	51.191
2.800861	0	80.27	38.594	39.151	47.475	51.191
3.101833	0	80.122	38.453	39.151	47.468	51.191
3.400639	0	79.673	38.025	39.151	47.448	51.191
3.701611	0	78.862	37.243	39.151	47.418	51.191
4.000417	0	77.739	36.162	39.151	47.378	51.191
4.301389	0	76.373	34.844	39.151	47.329	51.191
4.600194	0	74.867	33.395	39.151	47.272	51.191
4.901167	0	73.281	31.872	39.151	47.209	51.191
5.202139	0	71.677	30.339	39.151	47.139	51.19
5.500944	0	70.115	28.853	39.151	47.062	51.19
5.801917	0	68.598	27.418	39.15	46.979	51.19
6.100389	0	67.168	26.078	39.15	46.891	51.19
6.401	0	65.815	24.82	39.15	46.794	51.19
6.701611	0	64.553	23.661	39.15	46.692	51.19
7.000028	0	63.391	22.609	39.15	46.583	51.19
7.400833	0	61.97	21.344	39.15	46.426	51.19
7.801639	0	60.699	20.243	39.15	46.257	51.19
8.204611	0	59.559	19.286	39.15	46.073	51.19
8.600583	0	58.557	18.479	39.15	45.878	51.19
9.000889	0	57.652	17.785	39.15	45.667	51.19
9.401194	0	56.84	17.199	39.15	45.441	51.19
9.8015	0	56.109	16.711	39.15	45.199	51.19
10.2105	0	55.432	16.298	39.15	44.935	51.19
10.61081	0	54.829	15.97	39.15	44.659	51.19
11.06103	0	54.205	15.677	39.15	44.328	51.19
11.40175	0	53.765	15.504	39.15	44.061	51.19
11.80756	0	53.269	15.345	39.15	43.724	51.19
12.20469	0	52.809	15.234	39.15	43.375	51.19
12.61486	0	52.354	15.159	39.15	42.994	51.19
13.00114	0	51.937	15.122	39.15	42.615	51.19

13.40044	0	51.516	15.113	39.15	42.203	51.19
13.80408	0	51.096	15.132	39.15	41.764	51.19
14.20122	0	50.686	15.173	39.15	41.312	51.19
14.60053	0	50.273	15.236	39.15	40.836	51.19
15.01286	0	49.844	15.321	39.15	40.323	51.19
15.40256	0	49.435	15.418	39.15	39.817	51.19
15.81603	0	48.995	15.534	39.15	39.26	51.19
16.2035	0	48.576	15.657	39.15	38.72	51.19
16.60181	0	48.141	15.792	39.15	38.148	51.19
17.00011	0	47.697	15.938	39.15	37.559	51.19
17.40275	0	47.241	16.092	39.15	36.949	51.19
17.82056	0	46.761	16.259	39.15	36.302	51.19
18.20153	0	46.315	16.415	39.15	35.699	51.19
18.55525	0	45.897	16.564	39.15	35.133	51.19
19.00231	0	45.36	16.754	39.15	34.407	51.19
19.19753	0	45.123	16.837	39.15	34.087	51.19
19.502	0	44.75	16.967	39.15	33.582	51.19
19.80214	0	44.377	17.097	39.15	33.081	51.19
20.11092	0	43.99	17.229	39.15	32.562	51.19
20.43481	0	43.582	17.368	39.15	32.014	51.19
20.71767	0	43.223	17.489	39.15	31.534	51.19
21.04372	0	42.805	17.626	39.15	30.979	51.19
21.28772	0	42.49	17.728	39.15	30.562	51.19
21.62456	0	42.053	17.867	39.149	29.986	51.19
22.002	0	41.562	18.02	39.149	29.342	51.19
22.30364	0	41.167	18.141	39.149	28.826	51.19
22.64003	0	40.724	18.273	39.149	28.251	51.19
23.51419	0	40.219	17.653	39.149	28.366	51.189
23.69369	0	39.991	17.723	39.149	28.068	51.19
24	0	39.604	17.839	39.149	27.565	51.19

- Pressure history in the gas pipeline of the Western Libya Gas Project during the gas supply trip (Fig. 6.6)

Time (hr)	P_1in (bar)	P_1out (bar)	P_2in (bar)	P_2out (bar)	P_3in (bar)	P_3out (bar)
0	63.9	42.993	42.993	40.509	42.993	37.695
0.251306	63.9	42.989	42.989	40.504	42.989	37.69
0.502111	63.9	42.985	42.985	40.5	42.985	37.686
0.75075	63.9	42.981	42.981	40.496	42.981	37.682
1.001556	63.9	42.978	42.978	40.491	42.978	37.678
1.300361	63.9	42.973	42.973	40.486	42.973	37.673
1.601333	63.9	42.969	42.969	40.481	42.969	37.668
1.900111	63.9	42.965	42.965	40.477	42.965	37.663
2.201083	60.68	42.96	42.96	40.472	42.96	37.659
2.502083	58.529	42.956	42.956	40.467	42.956	37.654
2.800861	57.013	42.952	42.952	40.463	42.952	37.65
3.101833	55.754	42.943	42.943	40.458	42.943	37.64
3.400639	54.662	42.919	42.919	40.452	42.919	37.615
3.701611	53.672	42.87	42.87	40.442	42.87	37.564
4.000417	52.768	42.792	42.792	40.421	42.792	37.479
4.301389	51.922	42.681	42.681	40.383	42.681	37.358
4.600194	51.131	42.539	42.539	40.325	42.539	37.204
4.901167	50.377	42.367	42.367	40.239	42.367	37.015
5.202139	49.66	42.167	42.167	40.126	42.167	36.796
5.500944	48.978	41.944	41.944	39.984	41.944	36.55
5.801917	48.319	41.697	41.697	39.812	41.697	36.277
6.100389	47.689	41.43	41.43	39.613	41.43	35.982
6.401	47.077	41.142	41.142	39.385	41.142	35.664
6.701611	46.485	40.837	40.837	39.132	40.837	35.326
7.000028	45.915	40.518	40.518	38.858	40.518	34.972
7.400833	45.175	40.068	40.068	38.458	40.068	34.473
7.801639	44.461	39.596	39.596	38.023	39.596	33.948
8.204611	43.767	39.101	39.101	37.557	39.101	33.398
8.600583	43.104	38.598	38.598	37.074	38.598	32.839
9.000889	42.451	38.076	38.076	36.564	38.076	32.257
9.401194	41.814	37.543	37.543	36.036	37.543	31.663
9.8015	41.192	36.999	36.999	35.492	36.999	31.059
10.2105	40.568	36.436	36.436	34.923	36.436	30.432
10.61081	39.969	35.879	35.879	34.356	35.879	29.813
11.06103	39.306	35.247	35.247	33.706	35.247	29.112
11.40175	38.811	34.765	34.765	33.208	34.765	28.578
11.80756	38.229	34.189	34.189	32.61	34.189	27.942
12.20469	37.666	33.624	33.624	32.019	33.624	27.32
12.61486	37.092	33.04	33.04	31.406	33.04	26.681
13.00114	36.557	32.491	32.491	30.827	32.491	26.082
13.40044	36.009	31.924	31.924	30.227	31.924	25.469
13.80408	35.461	31.354	31.354	29.619	31.354	24.855
14.20122	34.927	30.796	30.796	29.022	30.796	24.26

14.60053	34.395	30.237	30.237	28.422	30.237	23.67
15.01286	33.85	29.665	29.665	27.803	29.665	23.071
15.40256	33.339	29.126	29.126	27.218	29.126	22.515
15.81603	32.801	28.559	28.559	26.6	28.559	21.937
16.2035	32.301	28.033	28.033	26.023	28.033	21.408
16.60181	31.792	27.497	27.497	25.433	27.497	20.878
17.00011	31.287	26.966	26.966	24.845	26.966	20.362
17.40275	30.781	26.435	26.435	24.254	26.435	19.854
17.82056	30.261	25.89	25.89	23.644	25.89	19.344
18.20153	29.79	25.399	25.399	23.091	25.399	18.893
18.55525	29.359	24.949	24.949	22.582	24.949	18.487
19.00231	28.818	24.387	24.387	21.943	24.387	17.991
19.19753	28.584	24.145	24.145	21.665	24.145	17.78
19.502	28.218	23.767	23.767	21.231	23.767	17.456
19.80214	27.861	23.398	23.398	20.805	23.398	17.145
20.11092	27.496	23.023	23.023	20.37	23.023	16.833
20.43481	27.117	22.633	22.633	19.915	22.633	16.515
20.71767	26.787	22.296	22.296	19.52	22.296	16.244
21.04372	26.411	21.912	21.912	19.066	21.912	15.94
21.28772	26.132	21.627	21.627	18.728	21.627	15.717
21.62456	25.749	21.238	21.238	18.264	21.238	15.418
22.002	25.325	20.81	20.81	17.749	20.81	15.094
22.30364	24.991	20.472	20.472	17.339	20.472	14.842
22.64003	24.62	20.099	20.099	16.885	20.099	14.568
23.51419	23.672	19.074	19.074	15.699	19.074	13.045
23.69369	23.48	18.867	18.867	15.45	18.867	12.882
24	23.154	18.522	18.522	15.024	18.522	12.612

- **Scenario 2:** gas delivery stops at the Mellitah Complex after one hour.
    - Flow rate behavior in the gas pipeline of the Western Libya Gas Project Fig. (6.7).

Time (hr)	m_{1in} (kg/s)	m_{1out} (kg/s)	m_{2in} (kg/s)	m_{2out} (kg/s)	m_{3in} (kg/s)	m_{3out} (kg/s)
0	78.122	78.128	38.644	39.151	45.494	51.191
0.049472	78.123	78.13	38.646	39.151	45.494	51.191
0.102833	78.124	78.13	38.646	39.151	45.493	51.191
0.149083	78.125	78.13	38.647	39.151	45.493	51.191
0.202472	78.127	78.13	38.648	39.151	45.493	51.191
0.252278	78.127	78.132	38.649	39.151	45.493	51.191
0.298556	78.128	78.131	38.649	39.151	45.492	51.191
0.351917	78.129	78.132	38.649	39.151	45.492	51.191
0.40175	78.131	78.132	38.65	39.151	45.492	51.191
0.451556	78.131	78.132	38.651	39.151	45.492	51.191
0.501361	78.132	78.133	38.651	39.151	45.492	51.191
0.551194	78.132	78.133	38.651	39.151	45.491	51.191
0.601	78.135	78.133	38.652	39.151	45.491	51.191
0.700639	78.135	78.135	38.655	39.151	45.491	51.191
0.800278	78.138	78.135	38.656	39.151	45.491	51.191
0.903472	78.139	78.136	38.656	39.151	45.49	51.191
1.003111	78.14	78.136	38.656	0	45.49	51.191
1.102722	78.142	78.137	38.657	0	45.489	51.191
1.202361	78.144	77.428	37.854	0	45.584	51.191
1.302	78.145	75.749	36.013	0	45.747	51.192
1.401639	78.147	73.927	34.056	0	45.882	51.192
1.501278	78.149	72.269	32.294	0	45.985	51.192
1.600917	78.15	70.83	30.773	0	46.067	51.192
1.700528	78.152	69.594	29.466	0	46.138	51.192
1.800167	78.153	68.524	28.334	0	46.201	51.192
1.910472	78.155	67.494	27.239	0	46.266	51.192
2.003	78.154	66.734	26.427	0	46.317	51.192
2.202278	78.156	65.329	24.919	0	46.419	51.192
2.4015	78.152	64.166	23.662	0	46.516	51.192
2.60075	78.137	63.182	22.586	0	46.605	51.192
2.803528	78.109	62.314	21.633	0	46.692	51.192
3.00275	78.062	61.568	20.806	0	46.772	51.192
3.202	77.996	60.904	20.065	0	46.848	51.192
3.301667	77.954	60.599	19.724	0	46.885	51.192
3.401306	77.907	60.309	19.398	0	46.921	51.192
3.600611	77.798	59.77	18.79	0	46.991	51.192
3.803472	77.662	59.275	18.227	0	47.058	51.192
3.999222	77.513	58.834	17.723	0	47.12	51.192
4.202083	77.34	58.415	17.243	0	47.181	51.192
4.401389	77.148	58.034	16.804	0	47.24	51.192
4.600694	76.943	57.679	16.394	0	47.296	51.192
4.8	76.72	57.349	16.011	0	47.35	51.192
5.002861	76.482	57.035	15.645	0	47.402	51.192

5.202167	76.234	56.744	15.302	0	47.452	51.192
5.401472	75.975	56.471	14.981	0	47.5	51.192
5.600778	75.707	56.212	14.676	0	47.546	51.192
5.800083	75.431	55.965	14.384	0	47.591	51.192
5.999389	75.149	55.73	14.106	0	47.634	51.192
6.20225	74.854	55.503	13.836	0	47.676	51.192
6.401556	74.56	55.287	13.581	0	47.717	51.192
6.600861	74.26	55.081	13.335	0	47.756	51.192
6.800167	73.958	54.882	13.099	0	47.794	51.192
7.003056	73.645	54.686	12.865	0	47.831	51.192
7.202361	73.338	54.5	12.645	0	47.866	51.192
7.401667	73.028	54.318	12.427	0	47.901	51.192
7.600972	72.717	54.143	12.219	0	47.934	51.192
7.800278	72.403	53.972	12.016	0	47.966	51.192
8.003139	72.086	53.801	11.812	0	47.998	51.192
8.305889	71.612	53.555	11.521	0	48.044	51.192
8.601528	71.15	53.321	11.244	0	48.087	51.192
8.9185	70.656	53.077	10.957	0	48.131	51.192
9.199806	70.219	52.869	10.711	0	48.167	51.192
9.498778	69.758	52.648	10.452	0	48.206	51.191
9.779944	69.329	52.449	10.219	0	48.24	51.191
10.10025	68.842	52.222	9.955	0	48.278	51.191
10.39564	68.399	52.021	9.722	0	48.311	51.191
10.69842	67.95	51.817	9.484	0	48.343	51.191
11.00139	67.507	51.616	9.253	0	48.374	51.191
11.27231	67.114	51.442	9.052	0	48.401	51.191
11.54319	66.726	51.27	8.854	0	48.426	51.191
11.84975	66.294	51.077	8.632	0	48.455	51.191
12	66.083	50.984	8.526	0	48.468	51.191

- Pressure history behaviour in the gas pipeline of the Western Libya Gas Project during the trip of gas delivery to the Mellitah Complex (Fig. 6.8)

Time (hr)	P_1in (bar)	P_1out (bar)	P_2in (bar)	P_2out (bar)	P_3in (bar)	P_3out (bar)
0	63.9	44.478	44.478	42.089	44.478	39.732
0.049472	63.9	44.477	44.477	42.088	44.477	39.731
0.102833	63.9	44.477	44.477	42.088	44.477	39.73
0.149083	63.9	44.476	44.476	42.087	44.476	39.73
0.202472	63.9	44.476	44.476	42.086	44.476	39.729
0.252278	63.9	44.475	44.475	42.086	44.475	39.729
0.298556	63.9	44.475	44.475	42.085	44.475	39.728
0.351917	63.9	44.474	44.474	42.085	44.474	39.728
0.40175	63.9	44.474	44.474	42.084	44.474	39.727
0.451556	63.9	44.473	44.473	42.084	44.473	39.727
0.501361	63.9	44.473	44.473	42.083	44.473	39.726
0.551194	63.9	44.472	44.472	42.083	44.472	39.726
0.601	63.9	44.472	44.472	42.082	44.472	39.725
0.700639	63.9	44.471	44.471	42.081	44.471	39.724
0.800278	63.9	44.47	44.47	42.08	44.47	39.723
0.903472	63.9	44.469	44.469	42.079	44.469	39.722
1.003111	63.9	44.468	44.468	42.375	44.468	39.721
1.102722	63.9	44.467	44.467	43.118	44.467	39.72
1.202361	63.9	44.483	44.483	43.524	44.483	39.728
1.302	63.9	44.551	44.551	43.837	44.551	39.784
1.401639	63.9	44.656	44.656	44.102	44.656	39.886
1.501278	63.9	44.784	44.784	44.336	44.784	40.016
1.600917	63.9	44.922	44.922	44.551	44.922	40.159
1.700528	63.9	45.065	45.065	44.751	45.065	40.31
1.800167	63.9	45.21	45.21	44.941	45.21	40.462
1.910472	63.9	45.369	45.369	45.14	45.369	40.631
2.003	63.9	45.501	45.501	45.301	45.501	40.772
2.202278	63.9	45.78	45.78	45.629	45.78	41.069
2.4015	63.9	46.051	46.051	45.938	46.051	41.358
2.60075	63.9	46.313	46.313	46.23	46.313	41.638
2.803528	63.9	46.571	46.571	46.514	46.571	41.913
3.00275	63.9	46.817	46.817	46.781	46.817	42.176
3.202	63.9	47.055	47.055	47.038	47.055	42.431
3.301667	63.9	47.172	47.172	47.163	47.172	42.555
3.401306	63.9	47.287	47.287	47.286	47.287	42.678
3.600611	63.9	47.512	47.512	47.525	47.512	42.919
3.803472	63.9	47.735	47.735	47.761	47.735	43.158
3.999222	63.9	47.946	47.946	47.983	47.946	43.382
4.202083	63.9	48.158	48.158	48.205	48.158	43.61
4.401389	63.9	48.362	48.362	48.418	48.362	43.827
4.600694	63.9	48.561	48.561	48.626	48.561	44.04
4.8	63.9	48.756	48.756	48.828	48.756	44.249
5.002861	63.9	48.95	48.95	49.03	48.95	44.456
5.202167	63.9	49.137	49.137	49.223	49.137	44.656
5.401472	63.9	49.32	49.32	49.412	49.32	44.852

5.600778	63.9	49.5	49.5	49.598	49.5	45.044
5.800083	63.9	49.676	49.676	49.779	49.676	45.232
5.999389	63.9	49.849	49.849	49.957	49.849	45.417
6.20225	63.9	50.022	50.022	50.135	50.022	45.602
6.401556	63.9	50.189	50.189	50.306	50.189	45.78
6.600861	63.9	50.352	50.352	50.474	50.352	45.956
6.800167	63.9	50.514	50.514	50.639	50.514	46.128
7.003056	63.9	50.675	50.675	50.804	50.675	46.3
7.202361	63.9	50.83	50.83	50.963	50.83	46.467
7.401667	63.9	50.984	50.984	51.12	50.984	46.63
7.600972	63.9	51.134	51.134	51.274	51.134	46.791
7.800278	63.9	51.282	51.282	51.425	51.282	46.95
8.003139	63.9	51.431	51.431	51.577	51.431	47.108
8.305889	63.9	51.648	51.648	51.798	51.648	47.34
8.601528	63.9	51.854	51.854	52.009	51.854	47.561
8.9185	63.9	52.071	52.071	52.229	52.071	47.792
9.199806	63.9	52.258	52.258	52.42	52.258	47.992
9.498778	63.9	52.453	52.453	52.619	52.453	48.2
9.779944	63.9	52.632	52.632	52.801	52.632	48.391
10.10025	63.9	52.831	52.831	53.003	52.831	48.604
10.39564	63.9	53.01	53.01	53.186	53.01	48.795
10.69842	63.9	53.19	53.19	53.368	53.19	48.986
11.00139	63.9	53.365	53.365	53.546	53.365	49.173
11.27231	63.9	53.518	53.518	53.701	53.518	49.336
11.54319	63.9	53.667	53.667	53.853	53.667	49.496
11.84975	63.9	53.833	53.833	54.021	53.833	49.672
12	63.9	53.912	53.912	54.102	53.912	49.757

- **Scenario 3:** trip of gas delivery both in the Mellitah Complex and in the TPP.
  - Flow rate behaviour in the gas pipeline of the Western Libya Gas Project

Time (hr)	m_{1in} (kg/s)	m_{1out} (kg/s)	m_{2in} (kg/s)	m_{2out} (kg/s)	m_{3in} (kg/s)	m_{3out} (kg/s)
0	78.122	78.118	38.644	39.151	45.494	45.191
0.20247	78.127	78.12	38.648	39.151	45.493	45.191
0.40175	78.131	78.122	38.65	39.151	45.492	45.191
0.601	78.135	78.123	38.652	39.151	45.491	45.191
0.80028	78.138	78.125	38.656	39.151	45.491	45.191
1.00667	78.141	74.814	42.156	0	38.679	0
1.21661	78.144	63.586	63.154	0	0.432	0
1.41231	78.147	61.035	60.648	0	0.387	0
1.60092	78.149	58.505	58.135	0	0.37	0
1.80372	78.15	55.957	55.597	0	0.359	0
2.003	78.136	53.632	53.279	0	0.353	0
2.20583	78.094	51.445	51.099	0	0.345	0
2.4015	78.017	49.497	49.157	0	0.339	0
2.59725	77.895	47.699	47.366	0	0.333	0
2.80367	77.713	45.95	45.624	0	0.326	0
3.00653	77.476	44.368	44.048	0	0.319	0
3.20583	77.187	42.93	42.617	0	0.312	0
3.40514	76.842	41.597	41.291	0	0.305	0
3.60444	76.442	40.357	40.058	0	0.299	0
3.80019	75.994	39.222	38.929	0	0.293	0
4.00661	75.469	38.104	37.819	0	0.287	0
4.20592	74.91	37.096	36.814	0	0.282	0
4.40167	74.314	36.162	35.886	0	0.275	0
4.601	73.661	35.264	34.996	0	0.27	0
4.82167	72.891	34.33	34.066	0	0.264	0
5.00319	72.218	33.599	33.342	0	0.259	0
5.20975	71.416	32.808	32.554	0	0.254	0
5.427	70.532	32.013	31.764	0	0.249	0
5.60508	69.778	31.388	31.145	0	0.244	0
5.81167	68.871	30.69	30.452	0	0.239	0
6.00044	68.017	30.073	29.838	0	0.235	0
6.20347	67.07	29.432	29.201	0	0.231	0
6.4065	66.1	28.808	28.581	0	0.226	0
6.61664	65.069	28.178	27.957	0	0.222	0
6.80542	64.125	27.628	27.411	0	0.218	0
7.00147	63.125	27.063	26.849	0	0.213	0
7.21178	62.036	26.474	26.264	0	0.209	0
7.40425	61.021	25.938	25.733	0	0.205	0
7.611	59.915	25.373	25.173	0	0.201	0
7.80703	58.853	24.841	24.645	0	0.196	0

8.03517	57.6	24.231	24.039	0	0.191	0
8.19914	56.69	23.795	23.604	0	0.189	0
8.406	55.53	23.249	23.064	0	0.184	0
8.60575	54.4	22.724	22.543	0	0.18	0
8.80194	53.278	22.211	22.034	0	0.177	0
9.00528	52.107	21.681	21.51	0	0.172	0
9.20156	50.969	21.173	21.003	0	0.168	0
9.40144	49.8	20.653	20.489	0	0.164	0
9.60136	48.624	20.135	19.975	0	0.161	0
9.80486	47.416	19.61	19.453	0	0.156	0
10.0226	46.116	19.045	18.894	0	0.152	0
10.2154	44.96	18.548	18.401	0	0.148	0
10.401	43.837	18.067	17.923	0	0.143	0
10.6009	42.623	17.551	17.41	0	0.14	0
10.808	41.36	17.013	16.878	0	0.137	0
11.0043	40.156	16.503	16.37	0	0.132	0
11.2078	38.902	15.976	15.85	0	0.128	0
11.4006	37.708	15.476	15.353	0	0.124	0
11.6042	36.442	14.946	14.826	0	0.12	0
11.8008	35.216	14.433	14.317	0	0.115	0
12	33.982	13.922	13.811	0	0.111	0

- Pressure behaviour in the gas pipeline of the Western Libya Gas Project during the trip of total gas delivery

Time (hr)	P_1in (bar)	P_1out (bar)	P_2in (bar)	P_2out (bar)	P_3in (bar)	P_3out (bar)
0	63.9	43.478	43.478	41.089	43.478	38.732
0.20247	63.9	43.476	43.476	41.086	43.476	38.729
0.40175	63.9	43.474	43.474	41.084	43.474	38.727
0.601	63.9	43.472	43.472	41.082	43.472	38.725
0.80028	63.9	43.47	43.47	41.08	43.47	38.723
1.00667	63.9	43.493	43.493	41.422	43.493	42.535
1.21661	63.9	44.704	44.704	42.609	44.704	44.704
1.41231	63.9	45.296	45.296	43.39	45.296	45.296
1.60092	63.9	45.83	45.83	44.117	45.83	45.83
1.80372	63.9	46.385	46.385	44.867	46.385	46.385
2.003	63.9	46.918	46.918	45.57	46.918	46.918
2.20583	63.9	47.449	47.449	46.254	47.449	47.449
2.4015	63.9	47.952	47.952	46.885	47.952	47.952
2.59725	63.9	48.446	48.446	47.49	48.446	48.446
2.80367	63.9	48.956	48.956	48.102	48.956	48.956
3.00653	63.9	49.447	49.447	48.681	49.447	49.447
3.20583	63.9	49.919	49.919	49.229	49.919	49.919
3.40514	63.9	50.381	50.381	49.758	50.381	50.381
3.60444	63.9	50.833	50.833	50.271	50.833	50.833
3.80019	63.9	51.268	51.268	50.759	51.268	51.268
4.00661	63.9	51.717	51.717	51.258	51.717	51.717
4.20592	63.9	52.142	52.142	51.726	52.142	52.142
4.40167	63.9	52.551	52.551	52.174	52.551	52.551
4.601	63.9	52.959	52.959	52.618	52.959	52.959
4.82167	63.9	53.401	53.401	53.097	53.401	53.401
5.00319	63.9	53.757	53.757	53.481	53.757	53.757
5.20975	63.9	54.155	54.155	53.908	54.155	54.155
5.427	63.9	54.565	54.565	54.346	54.565	54.565
5.60508	63.9	54.895	54.895	54.697	54.895	54.895
5.81167	63.9	55.27	55.27	55.095	55.27	55.27
6.00044	63.9	55.606	55.606	55.452	55.606	55.606
6.20347	63.9	55.961	55.961	55.828	55.961	55.961
6.4065	63.9	56.31	56.31	56.195	56.31	56.31
6.61664	63.9	56.663	56.663	56.567	56.663	56.663
6.80542	63.9	56.975	56.975	56.895	56.975	56.974
7.00147	63.9	57.292	57.292	57.228	57.292	57.292
7.21178	63.9	57.625	57.625	57.578	57.625	57.625
7.40425	63.9	57.924	57.924	57.891	57.924	57.924
7.611	63.9	58.24	58.24	58.221	58.24	58.239
7.80703	63.9	58.532	58.532	58.527	58.532	58.532
8.03517	63.9	58.865	58.865	58.875	58.865	58.865

8.19914	63.9	59.1	59.1	59.12	59.1	59.1
8.406	63.9	59.39	59.39	59.423	59.39	59.39
8.60575	63.9	59.664	59.664	59.709	59.664	59.664
8.80194	63.9	59.927	59.927	59.983	59.927	59.927
9.00528	63.9	60.193	60.193	60.261	60.193	60.193
9.20156	63.9	60.445	60.445	60.522	60.445	60.445
9.40144	63.9	60.694	60.694	60.782	60.694	60.694
9.60136	63.9	60.938	60.938	61.036	60.938	60.938
9.80486	63.9	61.18	61.18	61.288	61.18	61.18
10.0226	63.9	61.432	61.432	61.55	61.432	61.432
10.2154	63.9	61.649	61.649	61.776	61.649	61.649
10.401	63.9	61.853	61.853	61.988	61.853	61.853
10.6009	63.9	62.067	62.067	62.21	62.067	62.067
10.808	63.9	62.282	62.282	62.433	62.282	62.282
11.0043	63.9	62.479	62.479	62.638	62.479	62.479
11.2078	63.9	62.678	62.678	62.844	62.678	62.678
11.4006	63.9	62.86	62.86	63.034	62.86	62.86
11.6042	63.9	63.046	63.046	63.227	63.046	63.046
11.8008	63.9	63.22	63.22	63.407	63.22	63.22
12	63.9	63.387	63.387	63.581	63.387	63.387

AUTHOR BIOGRAPHY

Abdo-almonaim S. M. Alghlam was born on April 12, 1973 in Tripoli, Libya. He attended primary, secondary, and high school in Libya between 1980 and 1992. At the Faculty of Engineering of 7^{th} of April University he enrolled in the academic year 1992/1993. Years at the same University he graduated in July 1997 from the department of Mechanical Engineering where he got his Bachelor of sciences (BSc). In 2000 he started to work as a teaching assistant at the same faculty as a part time job, also from 2000 to 2006 Mr Alghlam worked at the General Electricity Company of Libya (GECOL) as an Operation Engineer of Gas Turbine Power Plant (Tripoli South Power Plant). As an engineer of the Gecol he sent to India for training in 2004 where he got certificate in Gas Turbine Power Plant operation and control (BHEL and SIEMENS) companies.

Mr Alghlam enrolled for postgraduate studying at the School of Engineering - Liverpool John Moores University, UK in 2006 and got the master of sciences (MSc) in Mechanical Engineering in 2007. The title of project was "Study, Evaluation, and Improvement of Tripoli South Power Plant Performance". In 2008, he started to study at the University of Technology Malaysia UTM for a master of engineering ME at the Faculty of Mechanical Engineering in Thermo-fluid Engineering Department where he graduated in 2012. The research topic was "Numerical Scheme for modeling Natural Gas Flow in Cross-Border Pipelines.

From 2012 to 2014, Mr Alghlam worked as a lecture at the Faculty of Engineering of 7th of April University, and he was the organizer of the education quality brunch at the mechanical engineering department.

Прилог 1.

Изјава о ауторству

Потписани Abdoalmonaim S.M. Alghlam

број индекса Д27-2014

Изјављујем

да је докторска дисертација под насловом

Нумеричка симулација прелазних процеса у гасоводима

(„Numerical simulation of natural gas pipeline transients“)

- резултат сопственог истраживачког рада,
- да предложена дисертација у целини ни у деловима није била предложена за добијање било које дипломе према студијским програмима других високошколских установа,
- да су резултати коректно наведени и
- да нисам кршио/ла ауторска права и користио интелектуалну својину других лица.

Потпис докторанда

У Београду, 15.01.2020.

Прилог 2.

Изјава о истоветности штампане и електронске верзије докторског рада

Име и презиме аутора Abdoalmonaim S.M. Alghlam

Број индекса Д27-2014

Студијски програм Докторске студије

Наслов рада Нумеричка симулација прелазних процеса у гасоводима

(„Numerical simulation of natural gas pipeline transients“)

Ментор проф. др Владимир Д. Стевановић

Потписани Abdoalmonaim S.M. Alghlam

Изјављујем да је штампана верзија мог докторског рада истоветна електронској верзији коју сам предао/ла за објављивање на порталу **Дигиталног репозиторијума Универзитета у Београду.**

Дозвољавам да се објаве моји лични подаци везани за добијање академског звања доктора наука, као што су име и презиме, година и место рођења и датум одбране рада.

Ови лични подаци могу се објавити на мрежним страницама дигиталне библиотеке, у електронском каталогу и у публикацијама Универзитета у Београду.

Потпис докторанда

У Београду, 06.02.2020.

Прилог 3.

Изјава о коришћењу

Овлашћујем Универзитетску библиотеку „Светозар Марковић“ да у Дигитални репозиторијум Универзитета у Београду унесе моју докторску дисертацију под насловом:

Нумеричка симулација прелазних процеса у гасоводима

(„Numerical simulation of natural gas pipeline transients“)

која је моје ауторско дело.

Дисертацију са свим прилозима предао/ла сам у електронском формату погодном за трајно архивирање.

Моју докторску дисертацију похрањену у Дигитални репозиторијум Универзитета у Београду могу да користе сви који поштују одредбе садржане у одабраном типу лиценце Креативне заједнице (Creative Commons) за коју сам се одлучио/ла.

1. Ауторство

2. Ауторство - некомерцијално

3. Ауторство – некомерцијално – без прераде

4. Ауторство – некомерцијално – делити под истим условима

5. Ауторство – без прераде

6. Ауторство – делити под истим условима

(Молимо да заокружите само једну од шест понуђених лиценци, кратак опис лиценци дат је на полеђини листа).

Потпис докторанда

У Београду, 15.01.2020.

1. Ауторство - Дозвољавате умножавање, дистрибуцију и јавно саопштавање дела, и прераде, ако се наведе име аутора на начин одређен од стране аутора или даваоца лиценце, чак и у комерцијалне сврхе. Ово је најслободнија од свих лиценци.

2. Ауторство – некомерцијално. Дозвољавате умножавање, дистрибуцију и јавно саопштавање дела, и прераде, ако се наведе име аутора на начин одређен од стране аутора или даваоца лиценце. Ова лиценца не дозвољава комерцијалну употребу дела.

3. Ауторство - некомерцијално – без прераде. Дозвољавате умножавање, дистрибуцију и јавно саопштавање дела, без промена, преобликовања или употребе дела у свом делу, ако се наведе име аутора на начин одређен од стране аутора или даваоца лиценце. Ова лиценца не дозвољава комерцијалну употребу дела. У односу на све остале лиценце, овом лиценцом се ограничава највећи обим права коришћења дела.

4. Ауторство - некомерцијално – делити под истим условима. Дозвољавате умножавање, дистрибуцију и јавно саопштавање дела, и прераде, ако се наведе име аутора на начин одређен од стране аутора или даваоца лиценце и ако се прерада дистрибуира под истом или сличном лиценцом. Ова лиценца не дозвољава комерцијалну употребу дела и прерада.

5. Ауторство – без прераде. Дозвољавате умножавање, дистрибуцију и јавно саопштавање дела, без промена, преобликовања или употребе дела у свом делу, ако се наведе име аутора на начин одређен од стране аутора или даваоца лиценце. Ова лиценца дозвољава комерцијалну употребу дела.

6. Ауторство - делити под истим условима. Дозвољавате умножавање, дистрибуцију и јавно саопштавање дела, и прераде, ако се наведе име аутора на начин одређен од стране аутора или даваоца лиценце и ако се прерада дистрибуира под истом или сличном лиценцом. Ова лиценца дозвољава комерцијалну употребу дела и прерада. Слична је софтверским лиценцама, односно лиценцама отвореног кода.